Copyright Warning & Restrictions

The copyright law of the United States (Title 17, United States Code) governs the making of photocopies or other reproductions of copyrighted material.

Under certain conditions specified in the law, libraries and archives are authorized to furnish a photocopy or other reproduction. One of these specified conditions is that the photocopy or reproduction is not to be "used for any purpose other than private study, scholarship, or research." If a, user makes a request for, or later uses, a photocopy or reproduction for purposes in excess of "fair use" that user may be liable for copyright infringement,

This institution reserves the right to refuse to accept a copying order if, in its judgment, fulfillment of the order would involve violation of copyright law.

Please Note: The author retains the copyright while the New Jersey Institute of Technology reserves the right to distribute this thesis or dissertation

Printing note: If you do not wish to print this page, then select "Pages from: first page # to: last page #" on the print dialog screen

ABSTRACT

MODELING SUBCONCUSSIVE AND CUMULATIVE SUBCONCUSSIVE IMPACTS USING A LATERAL FLUID PERCUSION INJURY DEVICE

by
Mathew Todd Long

Repetitive mTBI and concussion are a major risk factor for developing long-term cognitive and behavioral impairments. Curiously, cumulative head injuries sustained over an individuals' career, involving contact activities (e.g. athletes and military personnel), are beginning to be implicated in long-term consequences, such as dementia. Recently, chronic traumatic encephalopathy (CTE) has gained momentum in the science and medical community as a neurodegenerative disease of repetitive head injuries. CTE was observed at autopsy of former athletes that did not closely correlate with a clinical history of concussion. Thus, suggesting cumulative subconcussive insults may induce long-term damage.

Investigating the etiology of subconcussive and cumulative subconcussive insults clinically is not feasible; however, understanding what correlation exists between cumulative effects of repetitive subconcussive insults is crucial for the medical and scientific community. This study used a lateral fluid percussion injury (lFPI) to model a subconcussive insult; specifically, to test the hypothesis that an initial subconcussive insult will not lead to any significant detectable levels of behavioral or cellular damage, yet cumulative intra-day subconcussive insults will manifest into detectable changes in neuropathology and behavior.

This study developed a novel animal model of subconcussive brain injury (scTBI) paradigm and the effects of cumulative intra-day scTBI utilizing a digitally controlled fluid percussion injury device (dcFPI). Acute behavioral effects of cumulative 5x scTBI resulted in longer duration in latency of righting reflex compared to 5x SHAM group. Neuronal degeneration was assessed at 24 h using Fluoro – Jade C, with sparse neuronal degeneration in the granule cell layer of the hippocampus and all 5x scTBI subjects exhibit hemorrhage. Neurobehavior assessment revealed transient suppression of ASR on PID1, returning to SHAM levels by PID4. The presence of immunoreactive microglia and reactive astrocytes was observed in cumulative 5x scTBI at 24 h and 1 w when compared to 5x SHAM group. These findings indicate one scTBI does not result in acute behavior deficits or neuronal degeneration, however cumulative scTBI results transient brainstem dysfunction, blood brain barrier disruption and prolonged neuroinflammation.

MODELING SUBCONCUSSIVE AND CUMULATIVE SUBCONCUSSIVE IMPACTS USING A LATERAL FLUID PERCUSION INJURY DEVICE

by
Mathew Todd Long

A Dissertation
Submitted to the Faculty of
New Jersey Institute of Technology
and Rutgers University Biomedical and Health Sciences
in Partial Fulfillment of the Requirements for the Degree of
Doctor of Philosophy in Biomedical Engineering

Department of Biomedical Engineering

August 2017

APPROVAL PAGE

MODELING SUBCONCUSSIVE AND CUMULATIVE SUBCONCUSSIVE IMPACTS USING A LATERAL FLUID PERCUSION INJURY DEVICE

Mathew Todd Long

Dr. Bryan Pfister, Dissertation Advisor — Date
Professor of Biomedical Engineering, NJIT

Dr. Namas Chandra, Committee Member — Date
Distinguished Professor of Biomedical Engineering, NJIT

Dr. James Haorah, Committee Member — Date
Associate Professor of Biomedical Engineering, NJIT

Dr. Vijayalakshmi Santhakumar, Committee Member — Date
Associate Professor of Pharmacology, Physiology and Neuroscience, Rutgers University

---

Dr. Kevin Pang, Committee Member — Date
Professor of Pharmacology, Physiology and Neuroscience, Rutgers University

BIOGRAPHICAL SKETCH

Author: *Mathew Todd Long*

Degree: Doctor of Philosophy

Date: August 2017

Undergraduate and Graduate Education:

- Doctor of Philosophy in Biomedical Engineering,
  New Jersey Institute of Technology, Newark, NJ, 2017

- Doctor of Philosophy in Biomedical Sciences
  Rutgers University Biomedical and Health Sciences, Newark NJ 2017

- Master of Science in Biomedical Engineering,
  New Jersey Institute of Technology, Newark, NJ, 2011

- Bachelor of Science in Information Management and Technology,
  Syracuse University, Syracuse, NY 1999

Major: Biomedical Engineering

Presentations and Publications:

Abdul-Muneer, P. M., M. Long, A. Conte, V. Santhakumar, B. Pfister (2017). "Traumatic brain injury induced matrix metalloproteinase2 cleaves CXCL12α (stromal cell derived factor 1α) and causes neurodegeneration." Brain, behavior, and immunity 59: 190-199.

Abdul-Muneer, P. M., Long, M., A. Conte V. Santhakumar, B. Pfister (2017)."High Ca2+ influx during traumatic brain injury leads to caspase-1-dependent neuroinflammation and cell death." Molecular neurobiology 54.6: 3964-3975.

Pang, K. C., S. Sinha, P. Avcu, J. J. Roland, N. Nadpara, B. Pfister, M. Long, V. Santhakumar and R. J. Servatius (2015). "Long-lasting suppression of acoustic startle response after mild traumatic brain injury." Journal of neurotrauma 32(11): 801-810.

Long, M., A. Aravind, A. Fitzsimmons, V. Santhakumar, K. Pang and B. Pfister. "Characterization of Cumulative Subconcussive Exposures of Blunt and Blast Injury." Proc. of Neurotrauma, Kentucky, Lexington. 2016

Long, M., A. Fitzsimmons, V. Santhakumar, K. Pang and B. Pfister. "Establishment and Characterization of a Rodent Model of Repetitive Subconcussive Traumatic Brain Injury." Proc. of Neuroscience, Illinois, Chicago. 2015

Long, M., S. Sinha, V. Santhakumar, K. Pang and B. Pfister. "Digitally Controlling the Biomechanics of Fluid Percussion Injury to Better Understand the Range of Mild TBI." Proc. of Neuroscience, District of Columbia, Washington. 2014

Long, M. and B. Pfister. "Digitally Controlling the Biomechanics of Fluid Percussion Injury." Proc. of Biomedical Engineering Society, Texas, San Antonio. 2014

I would like to dedicate this work to my parents, Tom and Mary Ann, and my sister, Meredith, for never letting me give up on my dreams. Their constant encouragement, love, and support has been the backbone of my success.

AKNOWLEDGMENT

This work could not have been accomplished without the continued support and dedication of Dr. Bryan Pfister. His guidance, creativity and enthusiasm have been indispensable towards my success. I would like to thank him for the opportunity to work in his lab. Very special thanks are given to Dr. Viji Santhakumar and Dr. Kevin Pang. This work would not have been possible without their expertise, insight and support. I would like to acknowledge Dr. Namas Chandra, Dr. James Haorah and Dr. Bharat Biswal for serving on my committee and continued support. Special thanks to John Hoinowski for his creativity, time and insight. Without him, my concepts could not have come to fruition.

I would love to thank my colleagues, Aswati Aravind, Millie Swietek, Ashley Fitzsimmons in Dr. Pfister's Lab; Eric Neuberger and Akshata Korgaonkar in Dr. Santhakumar's Lab; Swamini Sinha, Kevin Spiegler and Ian Smith in Dr. Pang's Lab. I would also like to thank former lab members, George Magou, Joseph Loverde and Mevan Siriwardane for their encouragement, insight and continued support. It has been a pleasure working alongside each of them.

I would like to thank the New Jersey Commission on Brain Injury for providing me the funding to do this research.

Lastly, I would like to thank my parents, Tom and Mary Ann, my sister, Meredith who have always been an amazing source of encouragement.

TABLE OF CONTENTS

TABLE OF CONTENTS
(Continued)

TABLE OF CONTENTS
(Continued)

TABLE OF CONTENTS
(Continued)

Chapter **Page**

LIST OF TABLES

LIST OF FIGURES

LIST OF FIGURES
(Continued)

LIST OF FIGURES
(Continued)

CHAPTER 1

INTRODUCTION AND BACKGROUND

1.1 Introduction

It is estimated at 1.7 million traumatic brain injuries (TBI) a year occur in the U.S. annually, of which almost 80% are classified as mild (mTBI) (Langlois, Rutland-Brown et al. 2006). The American Congress of Rehabilitation Medicine define mTBI in individuals that have a physiological disruption of brain function that includes at least one of the following: 1. Loss of consciousness (less than 30 minutes), 2. Loss of memory for events immediately before or after the accident (less than 24 hours), 3. Any alteration of mental state at the time of the accident, and 4. Develop focal neurological deficit, which may or may not be come transient, 5. Glasgow Coma Scale (GCS) range of 13-15. Concussion is often used as a synonym for mTBI. While there is no single definition of concussion universally acknowledged (Blennow, Hardy et al. 2012, Khurana and Kaye 2012), it is regarded as a subset under the umbrella of mTBI towards the less severe end of brain injury. Concussion - defined herein as traumatically induced transient disturbance of brain function, involving a complex pathophysiologic process with symptoms typically observed in the absence of significant structural damage (McCrory, Meeuwisse et al. 2009, Harmon, Dre zner et al. 2013). Immediate consequences of concussion may affect cognition or motor functions, such as dizziness, headaches, confusion, and loss of coordination, mobility and memory. A concussed individual could experience one symptom or several of those referenced above. Therefore, translating the relationship between head impact and brain injury is not well defined. While a majority of research has been focused on the etiology of a multiple mTBI and

concussions, little is known about repetitive subconcussive impacts, often referred to as repetitive subconcussions.

Athletes and military personnel that engage in contact activities are already at an increased risk of sustaining an mTBI or concussion. In addition, these activities make individuals more susceptible to repetitive subconcussive injuries. A single subconcussive insult may not produce a detectable injury to the brain or diminish brain function, however repeated subconcussive insults may manifest into an injury at later time points (McKee, Cantu et al. 2009, Gavett, Stern et al. 2011, Stern, Riley et al. 2011, Spiotta, Bartsch et al. 2012, Talavage, Nauman et al. 2013). Some of the important parameters to consider of repetitive injury include the peak amplitude of the injury, number of injuries and the time between injuries (Laurer, Bareyre et al. 2001, Longhi, Saatman et al. 2005, Weber 2007, Prins, Hales et al. 2010, Meehan III, Zhang et al. 2012). Indeed, repetitive injuries could have long-term consequences. Dementia pugilistica, coined by Millspaugh (Millspaugh 1937), is a syndrome of progressive neurodegeneration, which shares clinicopathological features with Alzheimer disease (Allsop, Haga et al. 1990, Hof, Bouras et al. 1992, Areza-Fegyveres, Rosemberg et al. 2007). Initially described in retired boxers whom experienced repetitive sublethal impacts over their career whom experience dementia. This concept is now referred as chronic traumatic encephalopathy (CTE). The symptoms of CTE are insidious. Individuals with CTE have reported dizziness, headaches and confusion, changes in mood (depression, anxiety, apathy), degradation in cognition (memory loss, attention), behavior (impulse control problems (e.g., short-fuse), aggression)), motor and impeded speech problems. (Parkinsonism, Dysarthria, Dysphagia). The pathology that accompanies CTE involves tau-

immunoreactive neurofibrillary tangle deposition and brain atrophy (McKee, Cantu et al. 2009, Gavett, Stern et al. 2011). This neuropathology has also been observed in animal models following fluid percussion injury (Hoshino, Tamaoka et al. 1998, Hawkins, Krishnamurthy et al. 2013).

Professional English soccer player Jeffrey Astle, noted for repetitive heading in soccer throughout his career, died at an early age of 59. He had a five-year history of accelerated deterioration of cognitive capacity before his death (Spiotta, Bartsch et al. 2012). At autopsy, degenerative brain disease and tauopathy consistent with CTE pathology were discovered. Minor repetitive trauma was declared as the origin of death. Mckee et al. noted on observations of autopsies of former athletes, individuals with long-term neurodegeneration did not specifically correlate with a clinical history of concussion. Alluding to a possible undiagnosed head injury further exacerbated by a mechanism of neurodegeneration as a result of multiple subconcussive insults. Interestingly, Talavage et al. using functional magnetic resonance imaging (fMRI) showed that high school football players, without observable signs of concussion, exhibited significant neurocognitive and neurophysiological changes comparable to teammates who were diagnosed as concussed. Additionally, a preliminary diffuse tensor imaging (DTI) study by Brazen et al. showed that multiple subconcussive head impacts resulted in white matter alterations, and that the extent of these changes approached that of a subject whom experienced a concussion. Subsequently, these changes were 3x that of the controls, suggesting repetitive subconcussive impacts have an effect on neurophysiology. Clarifying the effects of these changes warrants further studies. Additionally, VA- BU CLF Brain Bank has shown individuals with CTE without a

recognized concussion. These individuals experienced many thousands of subconcussive insults over their career, believed to have had a cumulated effect, resulting in the manifestation of CTE (Montenigro, Bernick et al. 2015). Present observations as ones referenced above and studies on animal models of repetitive mTBI(Laurer, Bareyre et al. 2001, DeFord, Wilson et al. 2002, Longhi, Saatman et al. 2005, Prins, Hales et al. 2010, Spain, Daumas et al. 2010, Shitaka, Tran et al. 2011, Fujita, Wei et al. 2012, Meehan III, Zhang et al. 2012, Mouzon, Chaytow et al. 2012, Shultz, MacFabe et al. 2012, Hawkins, Krishnamurthy et al. 2013) has caused a paradigm shift in view of brain injury for the potential long-term detrimental effects of accumulated subconcussive impacts over an athlete's career.

1.2 Objectives

This study encompasses complementary objectives. The first was to develop a fluid percussion injury device capable of delivering pressure waveforms analogous to short temporal durations reported in the literature from football collisions. The second objective was to establish the foundation for a subconcussive brain injury paradigm using the lateral fluid percussion injury (LFPI) model. Finally, cumulative effects of intra-day subconcussive brain injury were examined.

1.3 Hypothesis

There is growing evidence that cumulative mTBI results in behavioral symptoms, neuropathological changes and neurodegeneration. However, subconcussion is different from mTBI. Little is known about subconcussion and cumulative subconcussive insults. Initial subconcussive insult will not lead to any detectable levels of damage, yet

cumulative intra-day subconcussive insults, will manifest into detectable changes in neuropathology and neurobehavior.

1.4 Experimental Design

1.4.1 Aim 1

Current pendulum fluid percussion injury (pFPI) models are limited to only adjusting the peak pressure and therefore cannot be used to explore both the magnitude and temporal scale of subconcussive brain injury. Therefore, we sought to develop and characterize a digital controlled fluid percussion injury device dcFPI. To produce fluid percussions that accurately mimic subconcussive biomechanics, we sought to:

a. Determine if dcFPI device is capable of accurate and reproducible output waveforms in a closed system (i.e. without animal attached).
b. Examine if the output waveform is altered under different mechanical loads (i.e., with the animal attached).
c. Determine if placement of pressure sensor effects the measurement of the peak amplitude of waveform delivered to the animal.
d. Determine if pressure measurements differ between extra and intra-cranial measurements after TBI.

1.4.2 Aim 2

Test the hypothesis that a single subconcussive brain insult will not lead to detectable outcomes as defined by the absence of acute behavioral measures and neuronal degeneration.

a. Determine whether subconcussive brain injury results in significant changes of acute behavioral measures including apnea, righting time, toe-pinch reflex, presence of hyperextension of the limbs and seizures.
b. Determine if subconcussive brain injury results in neurodegeneration at 24 h as measured by Fluoro – Jade C.

1.4.3 Aim 3

Test the hypothesis that a cumulative subconcussive brain injury results in changes in acute neurobehavior and neurodegeneration.

a. Determine if cumulative subconcussive brain injury results in significant differences of acute behavioral measures.
b. Examine if cumulative subconcussive brain injury results in neurodegeneration at 24 h.

1.4.4 Aim 4

Test the hypothesis that cumulative subconcussive brain injury results in behavioral deficits and changes in neuropathophysiology.

a. Determine if cumulative subconcussive brain injury results in memory impairments as assessed with the Morris Water Maze task at 24 h and 1 week.

b. Examine whether cumulative subconcussive brain injury leads to reduction of acoustic startle response at 24 h, 4 and 7 days' post injury.
c. Determine if cumulative subconcussive brain injury develop neuroinflammation and immune activation 24 h and 7 days' post injury.

Together these experiments will advance unique insights into the sequela of cumulative intra-day subconcussive brain injury phenomena.

1.5 Background

1.5.1 Fluid Percussion Injury Device

The mechanical forces and temporal events of TBI are multifaceted, which can add to the variability of TBI outcome and complication in linking the resulting pathophysiology. However, experimental models that can recreate the forces and temporal window of mild or concussive level events could prove useful in diagnosing the underlying pathophysiology of these epidemics. Several experimental techniques to study mTBI exist today that have included a compressed-air gun, weight drop method, controlled cortical impact, linear and rotational acceleration models and pendulum fluid percussion models (Cernak 2005). In particular, the pendulum fluid percussion injury device (pFPI) is one of the most frequently used and established injury models (Thompson, Lifshitz et al. 2005) that can produce focal and diffuse pathological characteristics of TBI as reported in humans.

Figure 1.1 shows the pendulum model consists of a metal hammer, which drops from a predetermined height, impacting a large fluid-filled cylinder with a male Luer-lok

fitting attached at the opposite end. This percussion propagates a fluid pressure waveform into the cranial cavity of the animal.

Figure 1.1 Pendulum fluid percussion model.

While this model is replete in the literature, it has several mechanical limitations to studying TBI in a very mild range. Amplitude (or severity) of injury in the pFPI model is determined by the height of the pendulum which affects the amplitude, rise time and duration of the percussion. The pFPI model does not have independent control over rise time (Wahab 2009) or duration of the pressure wave. Early impact studies on cadavers have suggested approximately 20 - 40 ms duration of the insult, however recent data suggests the temporal window of head impacts in athletic collisions range in duration from 7 – 16 ms, with mean duration of ~10 ms (Broglio, Sosnoff et al. 2009). pFPI has been capable to produce 10 ms duration, however only under severe head injury settings (55.1-58.7 psi) (D'Ambrosio, Fairbanks et al. 2004). Mild to moderate TBI has been suggested at far lower threshold (15-30 psi) with impact durations ranging from 20 – 29 ms (Alder, Fujioka et al. 2011, Nakadate, Inuzuka et al. 2014). Indeed,

subconcussive thresholds may require even lower pressure amplitude levels which are difficult to reproduce in the pFPI system. Understanding the pathologies associated with repetitive mild to subconcussive head insults due to low magnitude, short temporal durations could prove beneficial towards solutions for neuroprotective equipment, therapies and recovery methods.

1.5.2 Subconcussive Phenomena

Subconcussive phenomena is relatively new concept that has gained traction in medical research. Kamins and Giza have suggested a working definition of subconcussion as "a proposed construct of biomechanical force causing subclinical injury in the absence of overt signs or symptoms" (Kamins and Giza 2016). Therefore, establishing what the threshold for a subconcussion is in the clinical setting is difficult to obtain. However, research using animal models provides a medium from which we can explore behaviorally and histologically, the neural substrates affected from an insult.

To date, only two studies have been reported on assessment of subconcussive injury in animal models. Fujita et al. (Fujita, Wei et al. 2012) used an Impact Acceleration Injury (IAI) device to deliver repetitive subthreshold injuries to adult rats. They quantified axonal damage using an antibody targeting for amyloid precursor protein (APP) in the brainstem regions and examined for vasculature dysfunction, whereby injecting acetylcholine over the left parietal lobe. Dysfunction of cerebrovasculature has been implicated in second-impact syndrome (SIS). SIS is associated when athlete sustains a head trauma and experiences another head trauma before the symptoms associated with the first trauma have cleared. APP is a marker of impaired axonal

transport and acetylcholine elicits vasodilation. Earlier studies using IAI, dropping a weight from a height of 2m elicited axonal injury in the brainstem and vascular responsiveness within the brain microcirculation. Fujita adjusted this IAI model for a repetitive subconcussive measurement, using a weight drop from a height of 0.5m with injury spaced out twice at three-hour and thrice at 1.5 hour intervals, 0.75m injured twice at 3-hour interval and 1.0m single injuries. The single and repetitive subconcussive insults resulted in no detectable signs of axonal injury in the medulla, pons and midbrain or vascular dysfunction in the parietal lobe. However, these measures for assessing subconcussive injury may not be sensitive enough. Indeed, Shitaka et al., demonstrated argyrophilic abnormalities indicative of multifocal axonal injury in mice from repetitive TBI could be seen via the use of silver salts that was not seen to the same degree when using APP (Shitaka, Tran et al. 2011).

pFPI studies conducted with a force greater than 1.0 atm (14.695 psi) can induce behavioral and pathological changes in rodents common to those in the human condition when exposed to a single fluid percussion (Thompson, Lifshitz et al. 2005, Anderson, Heitger et al. 2006, Shultz, MacFabe et al. 2011). Thus, Shultz et al. (Shultz, MacFabe et al. 2012) suggested a subconcussive threshold injury range 0.50-0.99 atm. The results of the study demonstrated one single pFPI injury produced no significant axonal pathology via APP staining and absence of behavioral impairments; however, they did observe an increase in neuroinflammation evident by immunoreactive microglia/macrophages. Thus, APP may be a less sensitive marker to establish additional pathological changes that occur from a subconcussive insult.

Here, this study used a novel dcFPI device to determine a subconcussive threshold as defined by absence of acute behavioral measures, such as apnea, righting time, toe-pinch reflex and presence of hyperextension of the limbs and seizures (Longhi, Saatman et al. 2005, Gurkoff, Giza et al. 2006), and cellular damage. pFPI devices are one of the most frequently used and well-established injury models in rodents (Thompson, Lifshitz et al. 2005); specifically acknowledged for the ability to produce focal and diffuse injury characteristics. While the pendulum method of FPI is extensive in literature, the design permits ease of control of peak amplitude, but does not allow independent control of rise time or duration of injury; resulting in minimal allowance for accurate adjustment in the subconcussive range. The dcFPI digitally delivers a well-controlled percussion with control over, the magnitude, rate, duration and impulse of the pressure wave (Abdul-Wahab, Swietek et al. 2011).

Detecting subconcussive events in humans is also difficult owing to its asymptomatic nature. Several on-field or post concussive measures exist to assess the initial degree of a concussive injury (e.g., Glasgow Coma Scale (GCS) Post-Concussive Symptom Scale (PCSS), Standardize Assessment of Concussion (SAC), Balance Error Scoring System (BESS), Immediate Post-Concussion and Cognitive Testing (ImPACT)) in addition to off-field assessment via structural imaging (e.g., computed tomography or magnetic resonance imaging) of gross brain anatomy (Khurana and Kaye 2012). However, these protocols may not detect subtleties that occur from a subconcussive insult. Indeed, in absence of any overt damage, the first insult may predispose the brain to further susceptibility, with repetitive insults compounding the injury (Weber 2007, Friess, Ichord et al. 2009).

Work now is attempting to also associate concussive and subconcussive events with the kinematics of head trauma. The Head Impact Telemetry System (HITs) has been used in numerous studies for head impact analysis (Broglio, Sosnoff et al. 2009, Crisco, Fiore et al. 2010, Crisco, Wilcox et al. 2011, McAllister, Flashman et al. 2012). HITs system provides multiple metrics such as linear and rotational acceleration, impact duration, location, force, impulse and frequency. Zhang et al., compiled information on National Football League (NFL) players who experienced concussions and recreated these events in the laboratory. They modeled the impacts and determined the brainstem and thalamus were brain structures that received the greatest shearing forces (Zhang, Yang et al. 2004). The shearing of axons is a result of accelerating/decelerating forces within the brain which is known to initiate the pathology of diffuse axonal injury (DAI) (Pfister and Bao , Povlishock 1992, Smith, Meaney et al. 2003, Blennow, Hardy et al. 2012). With importance to this study, individuals using HITs have reported the number of subconcussion exposures over a single season ranging from 226-2154 for football and hockey at high school and collegiate levels, while heading in soccer has ranged from 32-5400. The average number of impacts per game ranged from 13-15.87 while heading a soccer ball during games was 6-12 (Broglio, Sosnoff et al. 2009, Crisco, Fiore et al. 2010, Crisco, Wilcox et al. 2011, McAllister, Flashman et al. 2012, Lipton, Kim et al. 2013, Talavage, Nauman et al. 2013). Often at the high school level in football, players participate both in offense and defense increasing their exposure to repetitive insults in a shorter time frame. The occurrence of head impacts led to the design of a repetitive intra-day study to explore the effects of cumulative subconcussions.

1.5.3 Neurobehavior and Pathophysiology

It has been reported that individuals exposed to subconcussive and repetitive subconcussive insults may experience symptoms such as disorientation, light-headedness, headaches and fatigue (Guterman and Smith 1987, Janda, Bir et al. 2002, McKee, Cantu et al. 2009). These symptoms are partially mediated by the brainstem. One neural circuit regulated by the brainstem is acoustic startle response (ASR). The neural mechanisms of ASR are well documented and conserved between rodents and humans (Davis, Gendelman et al. 1982, Lee, Lapez et al. 1996), therefore providing translational study on the functional outcome. A previous study exploring the effects of mTBI on ASR observed significant suppression to both sensitivity (threshold of response) and responsivity (amplitude of response) of the ASR (Pang, Sinha et al. 2015). The findings on reduction to both sensitivity and responsivity suggest a novel indicator for mTBI to assess brainstem dysfunction. Thus, a benefit of ASR is that it may be a more sensitive measure to indicate alteration of basal cellular function outside of neuronal death.

Individuals that have suffered mTBI or repetitive mTBI often demonstrate cognitive deficits (Martindale et al. Makdissi et al. Boll et al.). A majority of these cognitive deficits resolve within a year, however a 1.0 - 20% of the population remain effected with post concussive symptoms (Bergersen, Halvorsen et al. 2017). A common cognitive deficit is working memory impairment. Working memory is the ability to incorporate the acquisition and spatial localization of relevant sensory cues that are processed, consolidated, retained and then retrieved in order to execute complex cognitive tasks. Here, the study examines the effects of repetitive subconcussive impacts on working memory impairment utilizing Morris Water Maze (MWM) task. MWM has

been used extensively in rodent models to assess working memory deficits (Creeley 2004, Pang, Jiao et al. 2011).

Growing evidence in animal studies has indicated inflammation and immune activation can worsen existing brain pathology (Frank-Cannon, Alto et al. 2009, Blaylock and Maroon 2011, Das, Mohapatra et al. 2012). Trauma to the brain can result in acute neuroinflammation and activation of the innate immune system within the central nervous system (CNS), however repetitive trauma within a vulnerable period may exacerbate the response (Allen, Gerami et al. 2000, Longhi, Saatman et al. 2005, Frank-Cannon, Alto et al. 2009). Additionally, studies have shown single and repetitive mTBI in animal models results in blood brain barrier (BBB) permeability (Laurer, Bareyre et al. 2001, Cernak, Vink et al. 2004), further activating the immune system in the CNS. Inflammation and immune activation can have a cyclic effect on each other, which has been shown to be detrimental to the CNS over time (Frank-Cannon, Alto et al. 2009, Blaylock and Maroon 2011, Das, Mohapatra et al. 2012). In animal studies, neuroinflammation and immune activation have been identified by activated microglia and astrocytes. Shultz et al. demonstrated a single subconcussive insult can result in acute neuroinflammation (Shultz, MacFabe et al. 2011). These are important identifiers, as continued activation may predispose an individual to further complications after additional insults at later time points.

CHAPTER 2

CHARACTERIZATION OF dcFPI DEVICE

2.1 Materials and Methods

2.1.1 dcFPI System Overview

Figure 2.1 shows the schematic design and dcFPI device, of which, was based on an earlier prototype (Abdul-Wahab, Swietek et al. 2011). Here a new system was carefully constructed to achieve percussion waveforms that are able to produce varying severities of TBI with gaining tighter control of the biomechanical aspects of the fluid percussion, enabling us to study TBI in very mild range. The dcFPI system consists of a housed linear voice coil actuator (BEI Kimco, LAH28-52-000A-12I) with a stroke length of 12.5 mm, coil mass of .74 kg, peak force of 266.9 N and peak power of 416 w. The actuator is connected to a shaft with a piston at the end. The fluid-fill chamber of the prototype consisted of a 10 ml syringe; here, the piston is housed in a 33 ml acrylic fluid-filled chamber ((22 mm diameter (Figure 2.2)). The inner cylinder wall was polished to minimize friction between the piston and wall for smooth fluid motions. In addition to minimizing friction of the walls of the fluid-fill chamber, the piston was lubricated with silicone grease to reduce inertia of the motion profile. The increase in size of the chamber and piston were designed to gain better control of the motion profile under shorter displacement. With the new design of the chamber, removing unwanted air bubbles was accomplished effortlessly. The chamber is 75% filled with degassed water, followed by one or two 180° rotations of the chamber to remove air bubbles surround the piston. Once removed, manually injecting degassed water from the reservoir (located on the top of the fluid-filled chamber) till the system was completely filled. Afterwards, the chamber and piston are placed over the encoder and piston mounts, and piston shaft

attached to the linear voice coil actuator. The piston mounts were designed to streamline and maintain position of the piston shaft over the encoder for accurate feedback, while also having the ability to adjust to other chamber designs of different sizes. A male-nozzle fitting (2.6 mm inner diameter), similar to the pFPI device, at the opposite end of the chamber was designed to tailor Luer-lok design commonly used in animal craniectomy.

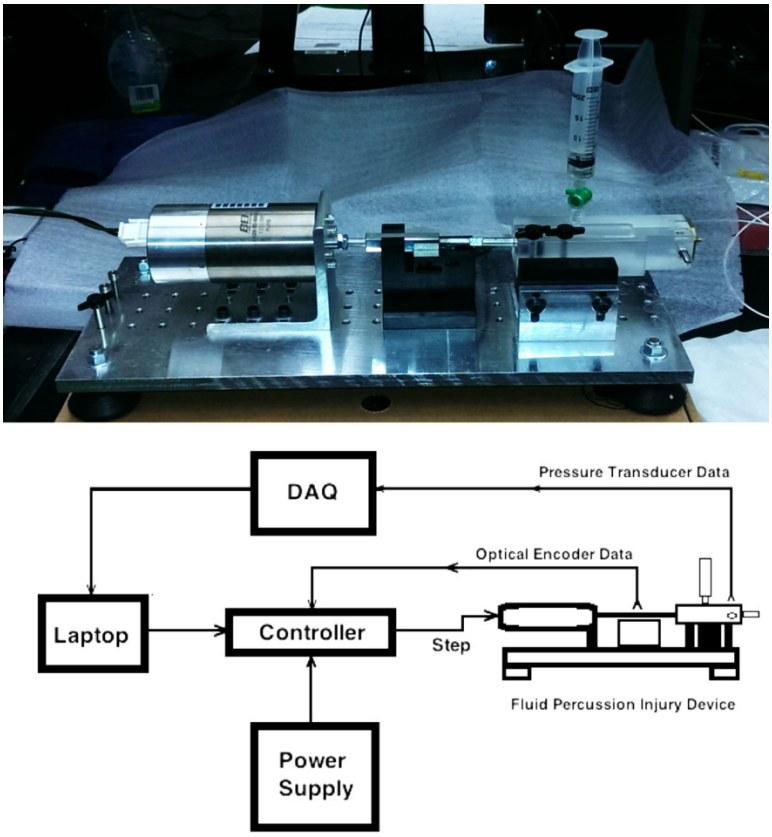

Figure 2.1 dcFPI schematic and physical device.

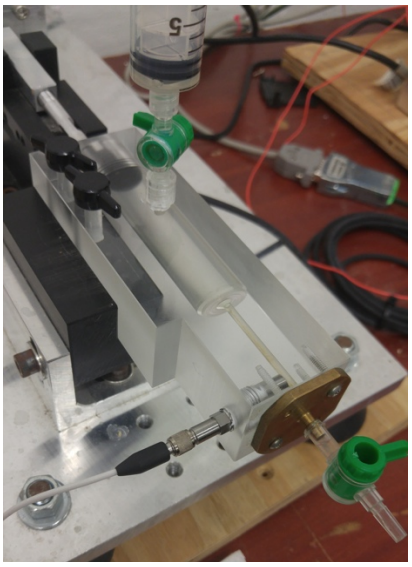

Figure 2.2 dcFPI fluid-filled chamber, sensor and release valve.

2.1.2 Motion Control

The voice coil motion is generated by a servo drive, SilverSterling S3 ((QCI-S3-IG), QuickSilver Controls, Inc.)) controller. The S3 trajectory generator software uses a Position Velocity Feedback/Feed Forward, Integral, Acceleration Feedback/Feed Forward (PVIA™) algorithm (See Appendix A). The algorithm comprises a series of data points with each servo cycle (120 μs) using position information from the feedback system. The feedback system from the prototype vFPI had a resolution of 1 μm. Here, a linear encoder ((Renishaw Tonic T1100A30A linear encoder) with 500 nm resolution was installed into custom encoder mount to improve the overall response of the motion profile. (Figure 2.3)). The stability of the feedback system is critical for reproducible and accurate performance; thus, a custom encoder mount was designed to protect the encoder from damage and stabilize the position for accurate feedback response. Enhancements

like the chamber design, piston mounts and feedback system all contributed to optimal performance of the system.

Figure 2.3 Linear encoder.

This information along with actual velocity and acceleration (determined from temporal history data of position) is feed in real-time to the PVIA™ servo algorithm. The algorithm uses the differences of those data points between the target and actual parameters to generate the torque required to move the piston forward/backwards accurately. The controller is powered by a 48 V power supply (Mean Well SE-1000-48 (Figure 2.4)).

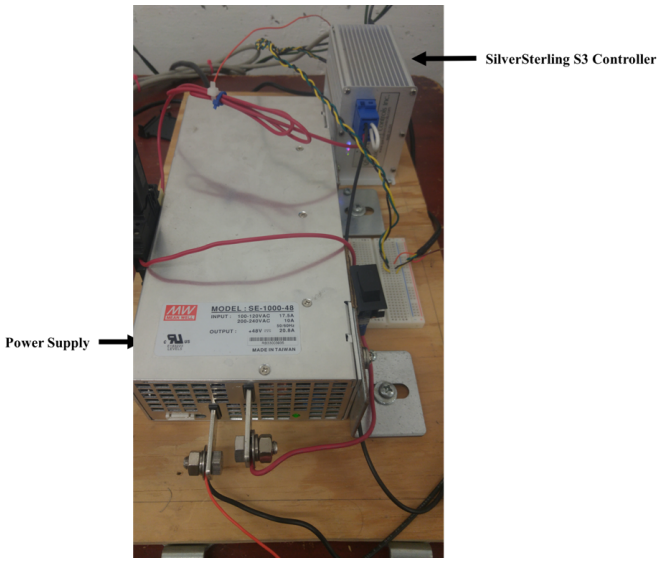

Figure 2.4 Controller and power supply.

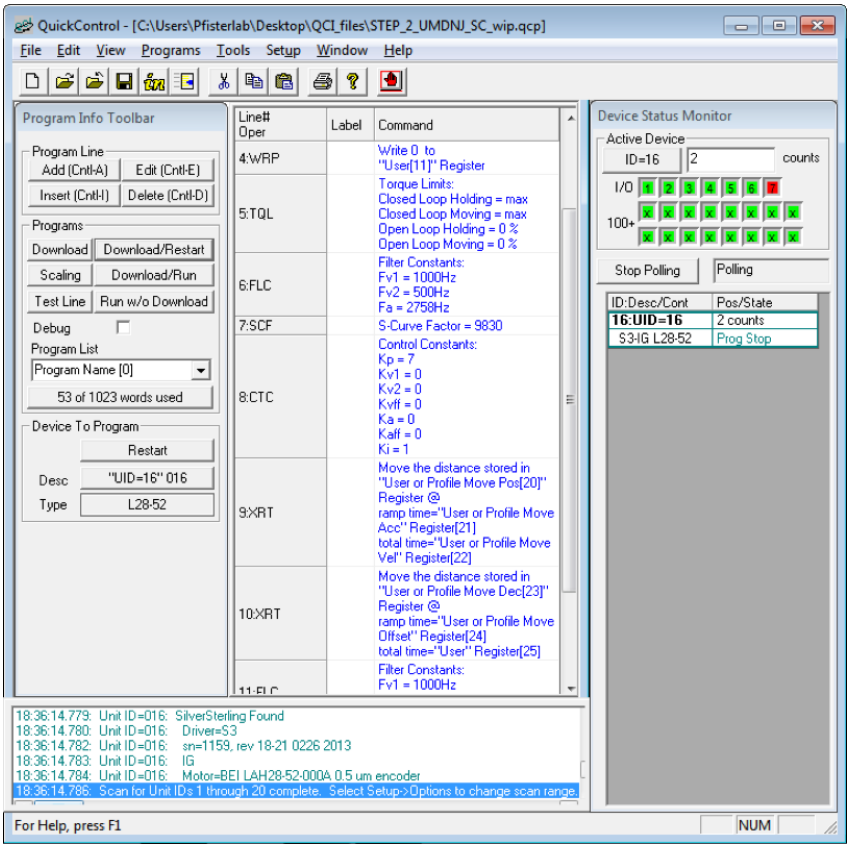

Figure 2.5 QuickControl programming interface.

Figure 2.5 shows QuickControl® programming software that was used to develop the motion protocol. The software allows developers to easily create an array of programs to control motion(s). The motion algorithm created entailed utilizing three main parameters: position (counts), acceleration (servo tick) and duration (milliseconds) to deliver the amplitude, rise time and duration of injury, respectively (Figure 2.6). Briefly, the user input three register values; desired displacement, acceleration and duration of motion.

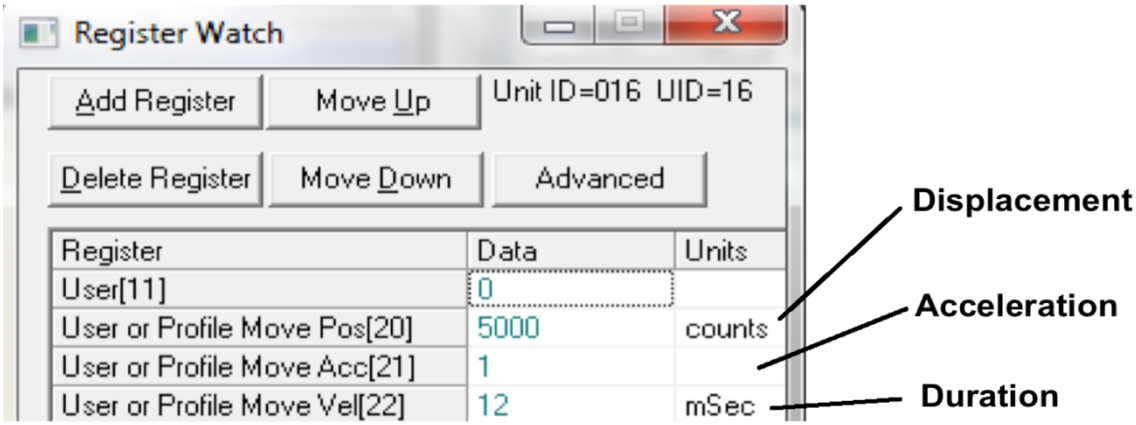

Figure 2.6 Motion profile parameters.

To prevent unwanted motions, the "Engage" key on the laptop is disabled until an additional field (Register: User[11]) in the software is supplied with an alphanumeric character, to enable it. Programs were composed to utilize motion control in both directions or emulate the percussion of the pFPI. (e.g., After the controller produces the forward motion, the last step in the program kills current to the motor, enabling the shaft to reverse direction from any reflected wave that may propagate from the initial impact.)

The parameters input by the user result in a specific current to produce the necessary torque to drive the target motion of the piston.

2.1.3 Waveform Measurements of dcFPI Device

The prototype device used a static strain gauge pressure sensor (PX61V0-100GV, Omegadyne, Figure 2.7 A). Strain gauges are often bulky and response times suited to static applications (i.e., loading for several minutes). Piezoelectronic sensors are dynamic and relative small size are ideal for instantaneous changes in pressure that are common in pFPI models, while suited for tight installation space. Measuring peak amplitude of the pressure wave was accomplished using a high rate pressure sensor (PCB Piezotronics, High resolution ICP pressure model 112A22 (Figure 2.7 B)). The prototype, Omegadyne sensor, had a 10.7 mm diameter and housed in 19 mm diameter compartment. The Piezoelectronic sensor has 5.5 mm diameter and housed in a 6.5 mm diameter compartment enabling the placement of the sensor to be mounted in the acrylic fluid-filled chamber 16.5 mm away from the end of the nozzle.

Figure 2.7 A. Omegadyne strain gauge B. PCB piezoelectric sensor.

The sensor acquires samples, at a rate of 10,000 Hz, is coupled to a battery powered signal conditioner (PCB Piezoelectronics model 480C02). The signal conditioner acts as a low pass filter on signal from the pressure sensor, sending 10K sampling rate filtered data directly into NI-DAQ USB 6211. The data points are then feed into a custom LabVIEW program to view (Figure 2.8) and recorded for on and off-line analysis. Most TBI literature is based off peak amplitude of injury, while recent evidence is suggesting the brain's response to mechanical insult is sensitive to both rate and magnitude (Morrison III, Cater et al. 2003, Magou, Guo et al. 2011, Neuberger, Abdul Wahab et al. 2014). The data collected with LabVIEW enables us to examine additional biomechanical measures outside of peak amplitude of pressure wave, such as rise-time (also referred to as rate), duration and impulse of the wave-form.

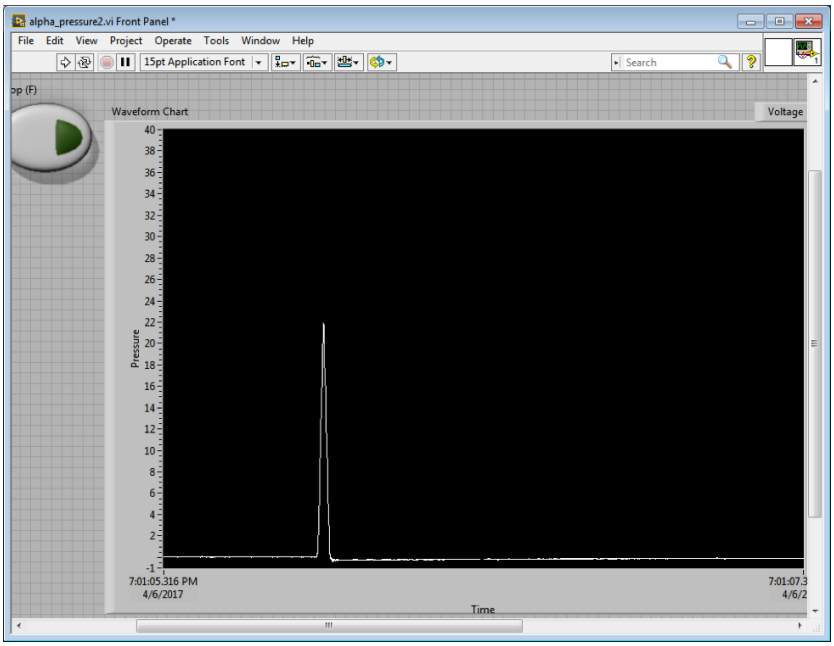

Figure 2.8 LabVIEW pressure display and recording software.

2.2 Statistical Analysis

Data was analyzed using SPSS software (Version 20, Chicago, IL). Data for peak pressure amplitudes, rise-time, duration and impulse were expressed as mean ± standard deviation.

2.3 dcFPI Motion-Pressure Waveform Characterization

Motion control is effected by its interrelated and independent components as well as the dynamic operations of the system. This includes overcoming mass and friction of the system and importantly the varying load on the system (i.e., the cranium of the rat). To ensure the mechanical system could produce a reproducible, controlled fluid percussion waveform, a rigid closed-system (e.g., nothing attached) is used. This configuration was useful for adjusting and optimizing the gain settings of the PVIA controller software. A rigid closed system consisted of a Luer-Lok valve in the closed position (Figure 2.9). The rigid closed system cancels out potential variability introduced from loads coupled to the outside of the system (e.g., mouse, rat, cat).

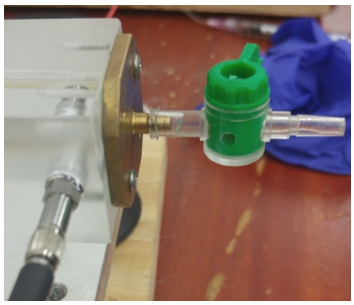

Figure 2.9 Rigid closed system Luer-Lok valve.

2.4 Digitally Controlled Motion Profiles Assessed

To assess the capability of the dcFPI device to produce accurate and reproducible pressure waveforms over different iterations, several motion profiles adjusting spatial and temporal characteristics were performed with the closed system. Recent data from head impact telemetry studies suggest impact durations range from 6 – 16 ms with a mean duration ~ 10 ms (Figure 2.10), while many pFPI studies report 20 ms and higher (Figure 2.11). For this study, two different displacement motion profiles were developed to simulate the temporal profiles or HITS data and pFPI studies. The different temporal durations 10 ms (Short Duration - SD) and 20 ms (Long Duration - LD) over 15 trials were used. To create these motions, the controller was programmed for 1200 and 1500 counts (counts refers to quadrature data used by the linear encoder. 2000 counts = 1 mm displacement), Each trial consisted of one impact.

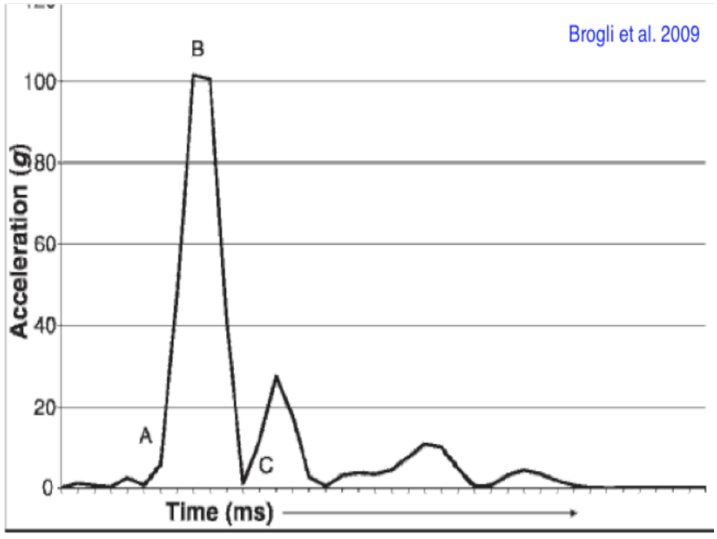

Figure 2.10 Impact durations reported by head impact telemetry systems.

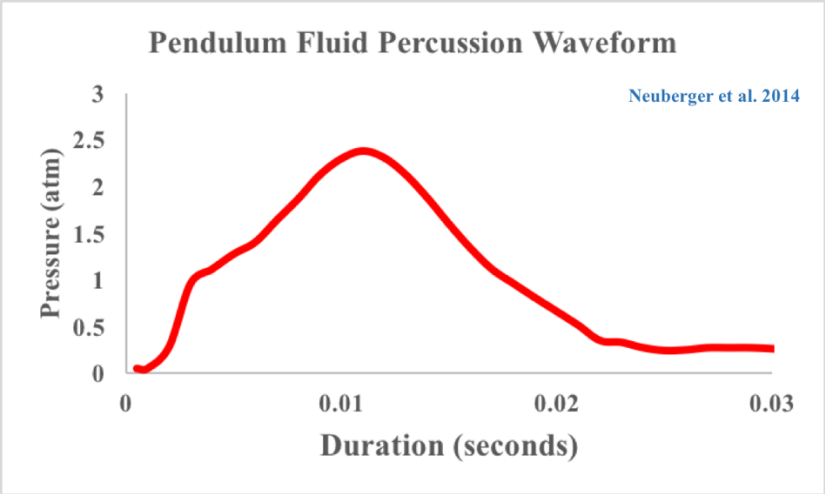

Figure 2.11 Impact amplitude and duration with pFPI model.

Rise-time was calculated at a linear fit of the pressure slope from a 10% increase to 90% of peak amplitude of pressure wave. Duration was calculated as the fluid pulse width where the pressure amplitude exceeded 4x the standard deviation of the baseline activity. 4x the standard deviation was chosen based on Gaussian distribution of data that indicates ~ 99% of data lies within three standard deviations of the mean. The 4th SD implies the data points are different from the baseline data points and representative of the significant change from the baseline. In this study, that was the beginning of the pressure waveform. The area under the pressure-time curve was used to calculate the impulse of the pressure waveform using the following formula:

$$Impulse = \int_{t=s}^{t=e} P(t)dt$$

Where “I” is the Impulse (Pa.s), P(t) is the function of pressure waveform, “t=s” is the start of the pressure waveform and “t=e” is the end of the waveform. Data was recorded in LabVIEW and analyzed off-line.

2.5 Location of Pressure Sensor Effects Pressure Amplitude

The pressure generated by the fluid piston is dynamic and traverses as a pressure wave from the piston to the animal. Additionally, the dynamic pressure will change as it moves through the orifice and connection fitting at the end. Therefore, the pressure measured by the sensor within the piston should also be different to the actual pressure pulse the subject receives. Here we investigated the effect the sensor’s location in the chamber had on the measured output. A fluid-filled chamber was designed to house two sensors, recording at different locations. Figure 2.12 schematic illustrates the location of the PCB Piezoelectric sensors, mounted at a proximal (16.5 mm) and distal (50.8 mm) positions from the male jet stream nozzle.

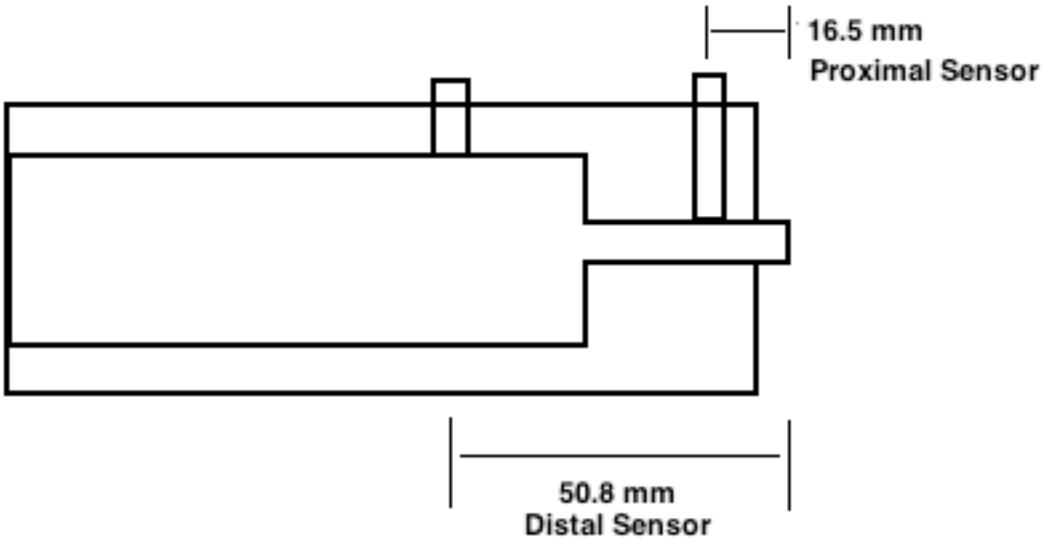

Figure 2.12 Schematic of dual pressure sensors.

Two motion profiles, simulating a low-end peak pressure amplitude and moderate peak pressure amplitude were used to test the placement of sensor location. 25 impact motions were performed for each motion profile. Data was recorded in LabVIEW and analyzed off-line.

Next, the effect of sensor placement in the left ventricle of the rodent is compared to the measurements of the sensor in proximal location (i.e., 16.5 mm away from nozzle end) of dcFPI device. Adult Sprague Dawley rats were used (n = 2). Six hours prior to injury, rats are anesthetized with ketamine (80 mg/kg) /xylazine (10 mg/kg) mixture and surgically implanted with a Luer-Lok syringe hub to the skull. This hub surrounds a craniectomy of the same size; positioned -6.0 mm from Bregma and 1.5 mm lateral from midline suture. Two screws are implanted on the contralateral side of the skull for increased support. A 1 mm burr hole is created for the insertion of the ICP probe (Millar SP-407); positioned -1.0 from Bregma and 1.5 mm lateral from midline suture. A

modified syringe needle tip was used to house the probe. An additional cap that surrounds the syringe hub and probe insert is applied. Dental cement is applied around the syringe hub and probe insert and between the cap to ensure fluid transmission and support. Insertion of ICP probe was completed 30 min prior to injury. ICP probe was inserted to the ipsilateral ventricle 3.5 mm below the dura. Prior to implantation, ketamine (80 mg/kg) /xylazine (10 mg/kg) mixture was used to anesthetized the animal. The subject is connected to the dcFPI and injury is induced. Immediately after, the animal is removed and set up for probe extraction. Pressure waveforms are recorded with the dcFPI device, while simultaneously measuring pressure amplitude in the ipsilateral ventricle of the rat brain. Pressure pulse data was recorded in LabVIEW and analyzed to determine peak amplitude of the pressure wave, rise-time and duration. Rise-time was calculated at a linear fit of the pressure slope from 10% increase to 90% of the peak pressure. Duration was calculated such that, when the pressure amplitude exceeded 4x the standard deviation of the baseline activity.

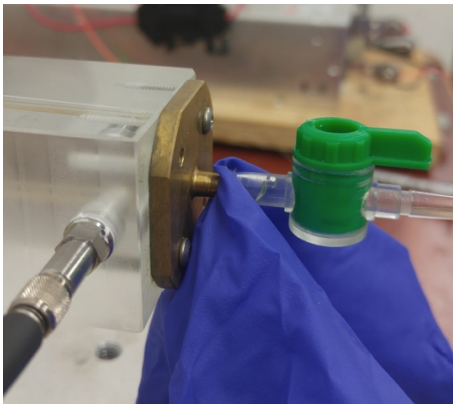

Figure 2.13 Elastic membrane load.

2.6 Mechanical Load Conditions of Peak Pressure Amplitude

System performance was examined in the presence of a non-compliant load, rigid closed system referred to earlier in Section 2.4 to that of several loads that introduce increasing compliance into the system. Motion profile used above (1500 counts, 20 ms duration) was executed on rigid closed system and compliant loads and the resulting pressure waveforms were recorded. The compliant loads included an elastic nitrile membrane (Figure 2.13), a surrogate model of the rat head developed in our lab (Figure 2.14) and a rat connected to the system. Briefly the surrogate model was designed as a cylinder with an elastic nitrile membrane fitted on one end and PCB piezoelectric sensor placed on the opposite end of the surrogate. The surrogate was cylindrical with an inner diameter (ID) of 9.8 mm, an outer diameter (OD) of 13.9 mm and a height of 40 mm. Creo's analysis tools were used to determine the volume of the surrogate to be 3.067 ml. with PTC Creo Parametric 3.0 M020. Cura software was used to prepare for printing on Ultimaker 3 Extended printer. The material used for printing was Polylactic Acid (PLA) filament with an extruder temperature of 200°C and build plate temperature of 60°C. Layer thickness was .100 mm. Supports were printed on the build plate and on the interior of the second, smaller cylinder as an interface to connect to the dcFPI device**.** The luer-lock-type interface ID was 4.15 mm and OD of 5.32 mm. A small razor blade was used to remove supports from the build plate. The surrogate was filled with distilled water and attached to the dcFPI device.

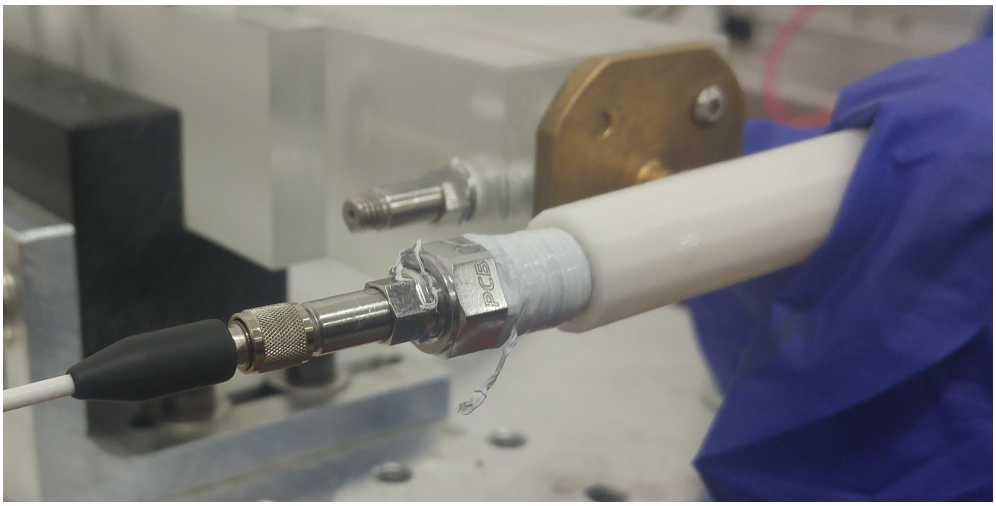

Figure 2.14 Surrogate model.

2.7 Results

2.7.1 Consistent and Reproducible Waveforms

Table 2.1 summarizes the mechanical characteristic of the pressure waveform in the rigid closed configuration (without a load attached) from short duration (SD) and long duration (LD) motion profiles. The low standard deviation in the data indicate accurate and reproducible capabilities of dcFPI device to deliver consistent pressure waveforms in closed-system (± Standard Deviation).

Table 2.1 Mechanical Characteristics of Closed System

	Mean Pressure (psi)	Rise Time (ms)	Duration (ms)	Impulse (Pa-s)
1200 Closed System SD	18.11 ± 0.053	2.97 ± 0.025	7.96 ± 0.143	63.94 ± 0.61
1200 Closed System LD	18.47 ± 0.072	5.41 ± 0.079	19.98 ± 0.503	149.91 ± 1.96
1500 Closed System SD	24.27 ± 0.039	2.90 ± 0.052	8.22 ± 0.114	87.843 ± 0.46
1500 Closed System LD	24.71 ± 0.090	5.58 ± 0.033	19.52 ± 0.412	203.67 ± 1.24

The mechanical characteristics reported in Table 2.1 were calculated from n=15 replicates of the example pressure waveforms illustrated in Figure 2.15. With minimal variation in amplitudes, rise-time and durations, Figures 2.16 and 2.17 depict consistent and reproducible peak pressure amplitudes, while motion profiles of short duration (< 10 ms) and long duration (< 20 ms) were applied.

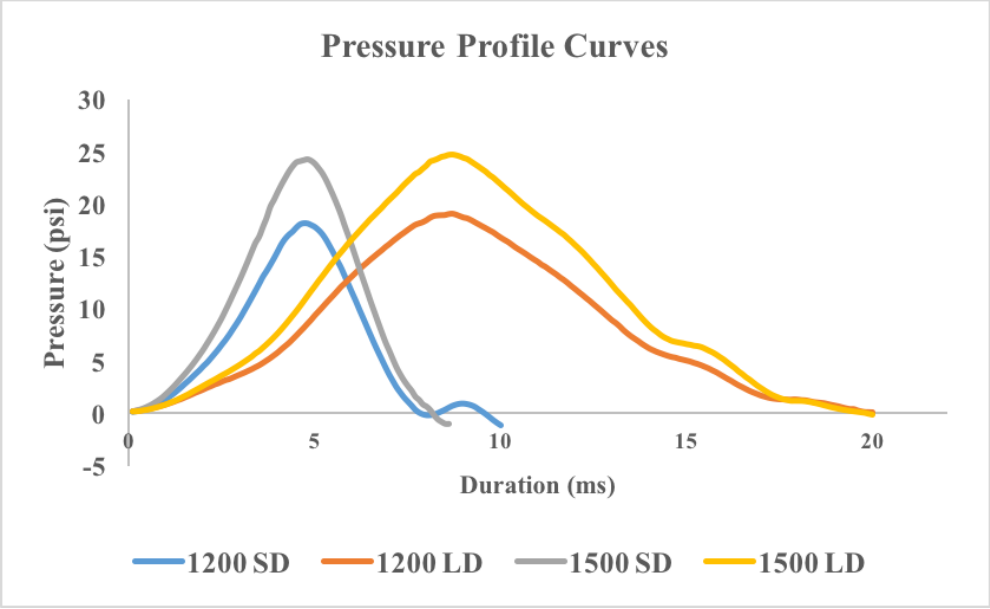

Figure 2.15 Pressure waveforms from rigid closed system in table 2.1.

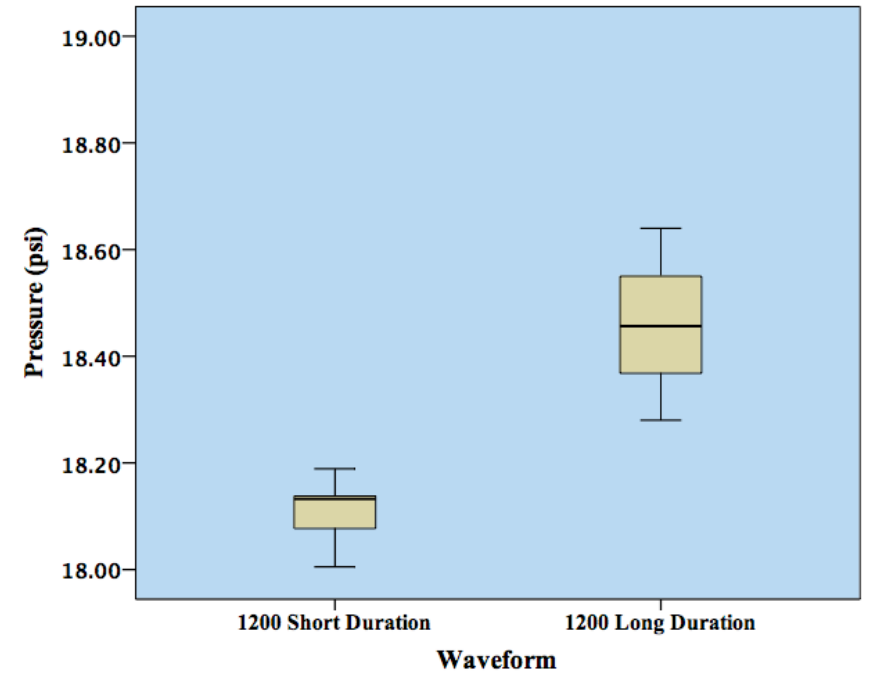

Figure 2.16 Accurate and reproducible 1200 SD and 1200 LD peak amplitude of pressure waveforms

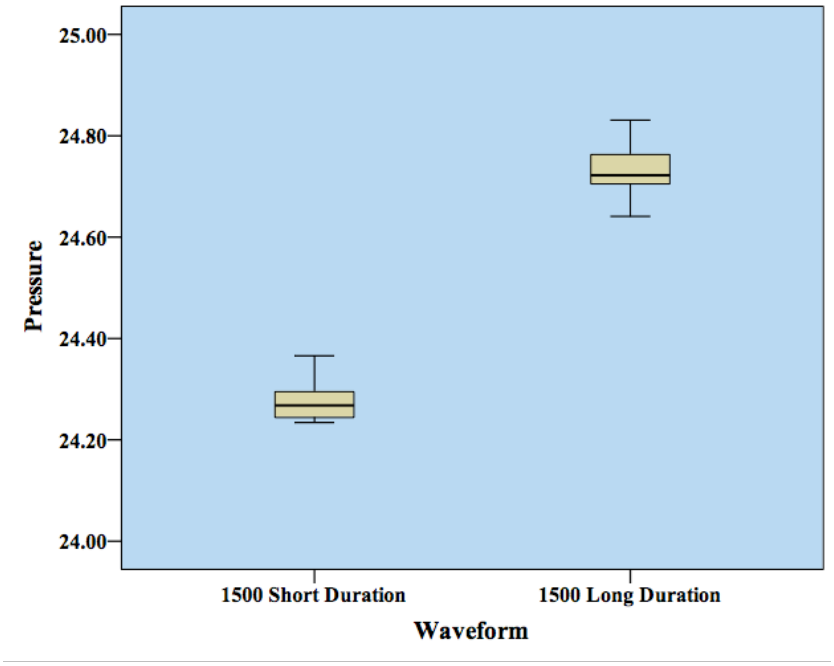

Figure 2.17 Accurate and reproducible 1500 SD and 1500 LD waveforms.

2.7.2 Mechanical Load Conditions Effect Peak Pressure Amplitude

Table 2.2 presents the mechanical characteristics of the closed system compared to the compliant loads. The compliance of the loads, as expected, dampens the response of the waveform characteristics, in this case reducing the peak amplitude of the pressure waveform, in addition with the surrogate model, increasing the rise-time. Figure 2.20 represents the waveform results of one motion profile applied to three different loading conditions. A One-way ANOVA found a significant statistical difference between all three loads in peak pressure, rise-time and duration ($p < 0.001$).

Table 2.2 Mechanical characteristics of a closed system and compliant systems

	Mean Pressure (psi)	Rise Time (ms)	Duration (ms)	Impulse (Pa-s)
Closed System	24.71 ± 0.09	5.58 ± 0.03	19.52 ± 0.41	203.67 ± 1.24
Elastic Membrane	19.09 ± 0.52	5.331 ± 0.07	20.36 ± 0.57	162.3 ± 8.26
Surrogate	6.83 ± 0.88	6.503 ± 0.50	17.68 ± 1.73	47.3 ± 6.74

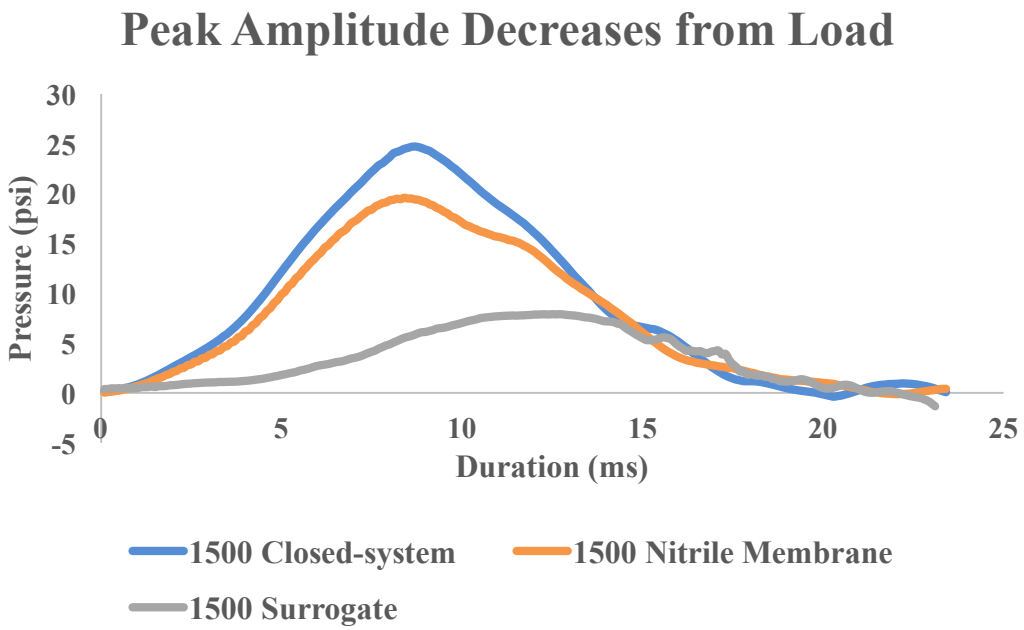

Figure 2.18 Peak pressure amplitudes decrease as compliances changes.

2.7.3 Sensor Location

The placement of the sensor location in the fluid-filled chamber at the proximal location (16.5 mm from the connector) was different measurement compared to the measurements at distal placed sensor (50.8 mm from the connector). Figure 2.19 shows the results of a

low-end peak pressure amplitude. The mean pressure for the proximal sensor (9.66 psi ± 0.38, 0.624 atm ± 0.03) was significantly decreased when compared to that of the distal sensor (10.75psi ± 0.44, 0.732 atm ±0.03) (independent-samples t-test, t(48) =8.912, p <0.001, two-tailed). In Figure 2.20, the results show similar trend for a moderate peak pressure amplitude. As referenced above, the mean pressure for the proximal sensor (31.37 psi ± 0.68, 2.13 atm ± 0.03) was significantly decreased than that for the distal sensor (35.54 psi ± 0.92, 2.41 atm ± 0.04) (independent-samples t-test, t(48) =8.318, p <0.001, two-tailed).

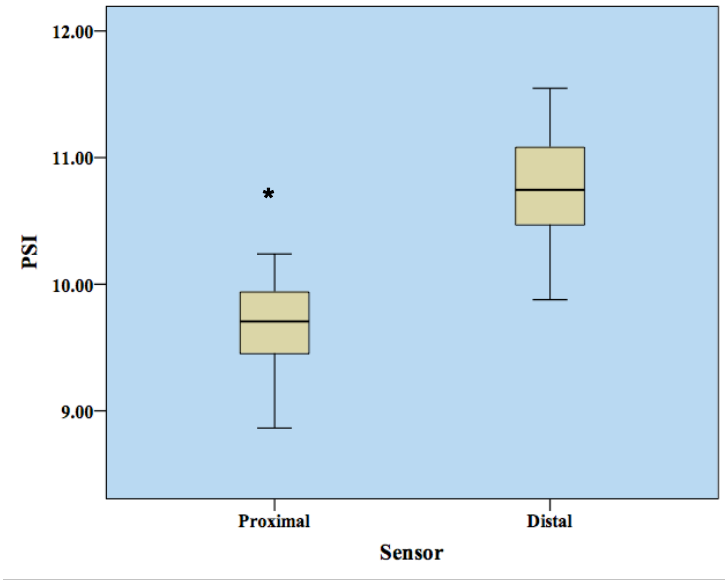

Figure 2.19 Proximal location of sensor results in lower peak amplitude of pressure wave.

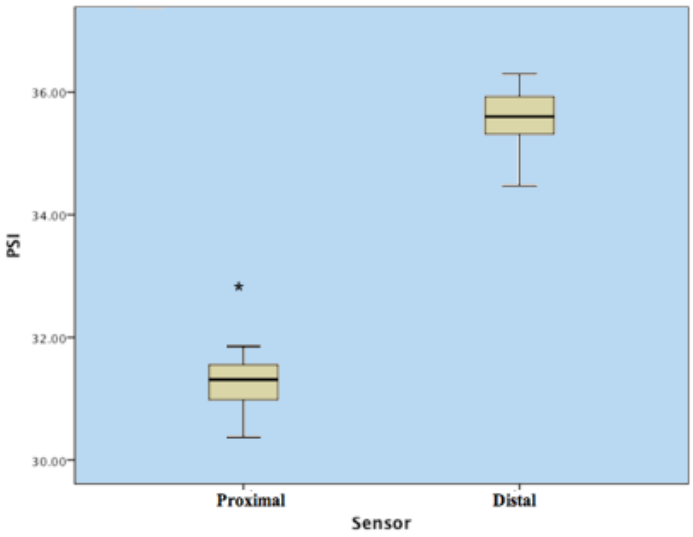

Figure 2.20 Proximal location of sensor results in lower peak amplitude of pressure wave than distal location.

Table 2.3 Biomechanical Characteristics of Intracranial and Extracranial Brain Injury

	Mean Pressure (psi)	Rise-time	Duration (ms)
FPI Probe	27.93 ± 0.25	5.08 ± 0.54	26.7 ± 3.5
ICP Probe	25.88 ± 0.31	5.075 ± 0.35	26.25 ± 0.55

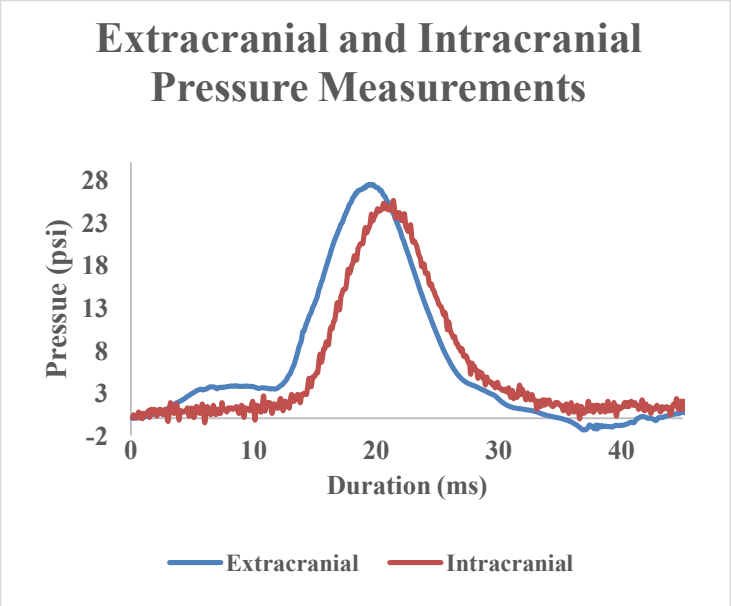

Figure 2.21 Extracranial and intracranial pressure measurements in rodents.

The extracranial (i.e.,proximal location on dcFPI device) sensor provides a close estimation of the intracranial (i.e., sensor location in the rat's ventricle) pressure pulse, Table 2.3. With only a n of two, we don't know the standard deviation with any accuracy. Based off an independent t-test, with a df=1, to get a 95% confidence interval, a multiplicative factor of 12.71 needs to be applied to the current standard deviation numbers, resulting in larger error bars (not shown). A higher N would make this more powerful. There was an expected time lag between the extracranial and intracranial sensor reflecting the proximity of the extracranial sensor to the source of the pressure pulse. The time lag to the sensor located in the ipsilateral ventricle was 8.5 ± 0.8 ms. Figure 2.21 illustrates the delay in the pressure waveform.

The difference in intracranial pressure peak (i.e., distal sensor) was not statistically significant from that of the extracranial pressure peak (i.e., proximal sensor)

(independent samples t-test, $t(2) = 3.34$, $p = 0.072$, two-tailed). Similar, rise times (independent samples t-test, $t(2) = 0.011$, $p = 0.992$, two-tailed) and duration of the waveforms were not found statistically significant (independent samples t-test, $t(2) = 3.830$, $p = 0.062$, two-tailed (Table 2.2)).

2.8 Discussion

2.8.1 General

Fluid percussion injury is one of the most frequently used and established injury models of TBI (Thompson, Lifshitz et al. 2005). This study characterized a redesigned and improved version of preceding VC-FPI device (Abdul-Wahab, Swietek et al. 2011). The digitally controlled fluid percussion injury device (dcFPI) was successful at producing consistent and reproducible pressure waveforms in a closed system. The initial results show smooth invariable motion profiles, however the introduction of different loads (e.g., nitrile membrane, surrogate model and adult rat) resulted in differences of output pressure waveforms. In addition, the location of the pressure sensor plays an important role in accurate measurements. Overall, the ability to independently control additional biomechanical parameters of the pressure waveform, such as rise-time, duration, and impulse to produce different spatial and temporal profiles analogous to that of which current athletes may experience participating in daily contact sports may prove useful in diagnosing the underlying pathophysiologies.

2.8.2 The Design

To reproduce the biomechanical parameters of different brain injury severities, the dcFPI was engineered and built around a voice-coil actuator and QuickSilver S3 Controller. A voice coil actuator was based on the electromagnetic (EM) coil design. An electromagnetic (EM) coil design has several advantages: 1. EM coils are recognized to produce high velocities with nearly all-compact devices. 2. EM coils use a stationary magnet to propel a wire coil. This coil is typically lighter than iron cores used in solenoids, resulting in quicker accelerations over shorter spatial displacements. 3. Motion direction is accomplished by reversing the polarity of the current. This is critical when precise position control is necessary. Precise position control works in tandem with encoder data feed back to the controller. A 0.5 μm encoder resolution was used for rigorous discrete motion control.

Traditional motion control involves Proportional, Integral, and Derivative position loop (PID) controllers to address disturbance rejection characteristics of the system (e.g. torque disturbances of motor shaft). Briefly, the proportional term affects the overall response of the system to position error, the integral term is required to force a steady state position error to zero for constant position command and derivative term is required to provide damping response. A limitation to PID controller is all three parameters are interdependent, adjusting one parameter will affect any of the previous parameter adjustments. For example, overshoot and rise times are tightly coupled, making gain adjustments difficult with PID control (Parker). Thus, tuning a system can be difficult for optimum performance.

We chose the QuickSilver Sterling S3 controller for its' novel Proportional Velocity Feedforward/Feedback, Integral, Acceleration Feedfoward/Feedback algorithm (PVIA™). The PVIA™ algorithm provides a method to reduce settling times and minimize overshoot by reducing the tracking error that accompany overshoot and rise-time issues of PID. In the PVIA™ system, the velocity error, position error and acceleration error are integrated together, allowing large manipulations of integral term without causing oscillations issues to the system to better predict the system response. This is important in generating desired pressure waveforms that take into account different compliances (e.g. adult vs juvenile rat).

Although the pFPI model is replete in literature, its size may present issues for labs that are limited on space (e.g., city schools and universities). The pFPI model is large in scale (1.23 x 0.46 x 1.16 m) with a mass > than 40 Kg. It can be cumbersome to set-up and calibration can tricky, discouraging moving the device to new locations once installed. Alternatively, the dcFPI device is minimal in scale in comparison, compact (0.46 x 0.25 x 0.15 m) and a mass of < 4.5 Kg, making the device readily portable from lab-to-lab.

2.8.3 Producing Fluid Percussions via Digital Motion Control

Biomechanical studies on closed head impact have shown the temporal duration of head impacts are often at a shorter time-frame then currently assessed in most animal models. The ability to recreate pressure waveform pulses analogous to those in involved in contact sports or military related service is important characteristic for animal injury models. Here, accurate and reproducible control of the independent biomechanical

parameters, peak amplitude, rise time, duration and impulse, are demonstrated by dcFPI motion profiles in the closed system. It was possible to vary duration of impact independently of the peak amplitude of the pressure wave similar to pendulum model studies in addition demonstration on shorter durations similar to those reported by the HIT system.

Here we identify the importance of the location of the pressure sensor effects the accuracy of the measurement the subject receives. Sensor location in pFPI models may vary from the point of injury depending on the nozzle-end configuration (e.g., elbow vs straight nozzle). These configurations result in sensor placement away from the point of injury between ~100 - 150 mm. This experiment compared (Figures 2.18, 2.19) the results of dual sensors embedded in the fluid filled chamber, demonstrating ~10% reduction in pressure amplitude measured at the proximal location of the sensor on dcFPI device (16.5 mm away from impact location) and is a better estimate of the peak pressure amplitude the animal receives during impact, when compared to the sensor that was placed in the distal location (50.8 mm away). Additionally, we found the measurement between the extracranial sensor (proximal sensor on dcFPI) and intracranial sensor (i.e., implanted in left ventricle of the rat) showed a ~10% reduction in pressure amplitude further validating the proximal sensor is a better measure. Thus, the location of the pFPI sensor may not provide an accurate measurement of impact pressure amplitude the brain receives. This experiment led to the next generation chamber design to position the PCB sensor 16.5 mm away from site of impact for optimal performance measurements.

Waveform characteristics are dependent on the load. An earlier study by Wahab et al. demonstrated different waveform profiles in adolescents compared to adult rats

when subjected to the moderate injury profile. In that study, they suggested the adolescent brain was more compliant to that of the adult rat brain resulting in different deformation of the brain. Here, introducing loads with different compliances resulted in different waveform outputs. Clearly, compliance of the system affects the output of the dcFPI model. This is expected, as the displacement of the piston will generate less pressure if the load is compliant. Whereas, in a rigid closed system, the fluid cannot move and will behave more like an incompressible system. Variation in the loads mostly lead to a decrease in measured pressure, while maintaining minimal variation duration. The trend in decreasing pressure continues with the surrogate model, while a longer rise-time was observed, Table 2.2. A longer rise time was an interesting observation. This makes sense as an additional volume of water is required to move into the surrogate to increase the pressure, and the location pressure sensor attached to distal end of the surrogate, may have an integrated effect on diminishing the pressure waveform characteristics. The peak amplitude measurement in the surrogate are similar to that of the intracranial sensor placed in the animal.

External pressure measurements are sufficient in animal models of FPI. Clausen et al. performed a study on extra – intracranial pressures from pFPI in a rodent model (Clausen and Hillered 2005). There, they applied a severe injury paradigm and observed no significant difference between extra and intracranial peak pressure measurements. Similarly, to this study, there was not a statistical significant difference between the two sensor measurements, however we did see a consistent trend of ~ 10% decrease in peak pressure amplitude between dcFPI sensor and the intracranial sensor placed in the left ventricle of the rodent (n = 4). Importantly, Clausen et al. also showed a time lag between

the extracranial and intracranial pressure measurements. In that study, the time lag reported was 16 ± 3 ms, where this study showed a time lag of 8.5 ± 0.8 ms. The smaller difference in measurement from the current study would be due to the extracranial sensor placement proximal (16.5 mm) away from site of impact, while the pFPI sensor placement they may have used was > than 100 mm away from site of impact. It should also be noted that our sample of two animals is small and might not give an accurate representation of a larger data set.

CHAPTER 3

SUBCONCUSSIVE BRAIN INJURY

3.1 Intro

To establish our subconcussive brain injury model, animals were divided into three groups subjected to small peak amplitude and short temporal impact profiles compared to SHAM. The criteria for the subconcussive brain injury model included the absence of acute behavioral measures and neuronal degeneration from one subconcussive impact.

3.2 Materials and Methods

3.2.1 Injury Groups

Wistar rats (21- 28 day old, 44-60 g, Charles River Laboratories) were divided into three brain injury groups below 1 atm and one SHAM group to examine if a threshold peak amplitude existed for a subconcussive brain injury: SHAM group (n=20), subconcussive high-range (SC-HI) (> 0.88 – 0.99 atm, n= 12), subconcussive mid-range (SC-MI) (> 0.68 - 0.88 atm, n=15) , subconcussive low-range (SC-LO) (> 0.50 – 0.68, n = 20)) (Table 3.1). A range from 0.50 > 0.99 atm was selected based on previous FPI experiments demonstrating peak amplitude of pressure waveforms 1.0 > 1.5 atm resulted in axonal injury and cognitive deficits (Shultz, MacFabe et al. 2011).

3.2.2 Fluid Percussion Injury

Injury is performed using the dcFPI device. The novel device permits independent control over key variables defining the waveform characteristics. Specifically controlling

the magnitude, rise time and duration of the waveform to produce the injury. This device uses a BEI Kimco actuator, which generates a precise linear motion under the function of Quick Silver motion controller and optical encoder with 500 nm resolution. The voice-coil is coupled to a piston shaft, housed in a fluid (degassed water) filled chamber that delivers a defined fluid percussion waveform into the cranial cavity of the animal. 24 hours prior to injury, rats were anesthetized with ketamine (80 mg/kg) /xylazine (10 mg/kg) mixture and surgically implanted with a Luer-Lok syringe hub to the skull. This hub surrounds a craniectomy of the same size; positioned 3.0mm posterior from Bregma and 3.5mm lateral from Sagittal suture. An additional cap that surrounds the syringe hub is applied. One screw is implanted on the contralateral side of the skull for increased support. Dental cement is applied around the syringe hub and between the cap to ensure fluid transmission and support. Immediately prior to injury, subjects were anesthetized with 5% isoflurane for 1 minute until foot-pinch reflex is absent. The subject was connected to the dcFPI. Once when toe pinch response is observed, injury is induced and the subject was observed for acute signs. Rats may exhibit 1) Apnea, 2) Loss of consciousness (LOC), and/or 3) Hyperextension of the tail and hind limbs. LOC is measured from the time of injury until the rat is in prone position. Sham subjects receive the same surgery as injured, anesthetized and connected to the dcFPI without the injury. Finally, biomechanics of the pressure wave were recorded. These included peak amplitude (atm), rise time (ms) and duration of injury (ms).

3.2.3 Histology

All rats were euthanized for histology 24 h after last injury/sham injury. Rats were anesthetized with pentobarbital and perfused with 4% paraformaldehyde; afterwards,

brains were post-fixed in a solution of 4% paraformaldehyde for 24 h, followed by solution of sucrose until ready to be analyzed. Tissue was coronally sectioned on a freezing microtome at 40 μm thickness, with every 6th and 12th sections to be stained. Neuronal degeneration was assessed with Fluoro-Jade C.

3.2.3.1 Fluoro – Jade C staining. Sections were mounted on gelatinized slides and air-dried. Sections were hydrated and incubated in 0.06% potassium permanganate before being stained with 0.001% Fluoro-Jade C in 0.1% acetic acid in complete darkness for 30 m. After staining, sections were rinsed three 1 min changes of distilled water. After final rinsing, slides were dehydrated, cleared and cover slips laid over. Cell counts were performed using the optical fractionator of Stereo Investigator V.10.02 **(MBF Bioscience, Williston, VT)** on an Olympus BX51 microscope with a 60X objective. 10 sections per animal. In each section, the cortex was outlined by a contour traced using a 10X objective. Sampling parameters were set at 60X: counting frame=200 μm by 200 μm, dissector height = 25 μm, and top guard zone = 5 μm. Approximately 125 sites per contour were selected using randomized systematic sampling protocols in Stereo Investigator (West, Slomianka et al. 1991, Yu, Proddutur et al. 2013).

3.3 Statistical Analysis

Statistical analysis was performed with SPSS 20. Chi-Square test was used for categorical variables. All independent samples were tested for normality and homogeneity of variance in SPSS. For comparison of neuronal degeneration, results from sham administered 1x and 5x experiments were pooled. One-way analysis of variance (ANOVA) was applied to biomechanical parameters and latency of righting

reflex. When appropriate, Bonferroni post-hoc test was used to assess statistical significance of between-group differences. Significance was set to $p < 0.05$. Data shown are mean ± standard error of mean (sem).

3.4 Results

3.4.1 Effects of a Subconcussive Impact on Acute Behavioral Measures and Neuronal Degeneration

Injury characteristics are summarized in Table 3.1. The SHAM group and SC-LO displayed no observable hyperextension of limbs, however the SC-HI and SC-MI groups, each had a subject display hyperextension of limbs, however these did not reach significance (chi-squared test for independence, $\chi^2 = 2.99$, df =3, n=67, p =0.243).

Table 3.1 Injury characteristics of the three subconcussive impact groups

Group	Peak Magnitude (atm) ±SEM	Rise Time (ms)	Duration (ms)	Apnea		Neuronal Degeneration	Hyper-extension	Latency of Righting Reflex (s) ±SEM
SHAM n = 20	0	0	0	0		2	0 of 20 subjects	139.1 ± 14.9
SC-HI > 0.88 - 0.99 atm n = 12	0.937 ± 0.02*	4.7 ± 0.56	11.64 ± 1.2	6 of 12 subjects *	2.3 (s)*	0	1 of 12 subjects	143.2 ± 22.6
SC-MI > 0.68 - 0.88 atm n = 15	0.757 ± 0.01*	4.9 ± 0.34	11.08 ± 0.45	0		2	1 of 15 subjects	134.3 ± 20.5
SC-LO 0.50 - 0.68 atm n = 20	0.599 ± 0.01*	5.1 ± 0.39	10.33 ± 0.29	0		0	0 of 20 subjects	123.5 ± 16.1

The frequency of apnea present in SC-HI group was found statistically significant compared to the animals that did have it (chi-squared test for independence, $\chi^2 = 18.4$, df=3, n=67, $p < 0.001$). In contrast, when examining righting time, neither of the injured groups differed significantly in latency to return to prone position compared to the SHAM group (One-way ANOVA ($F(3,64) = 0.641$, $p=0.592$)) as shown in Figure 3.1.

Levene's test for homogeneity of variance revealed no significant differences in variances between groups, p=0.701.

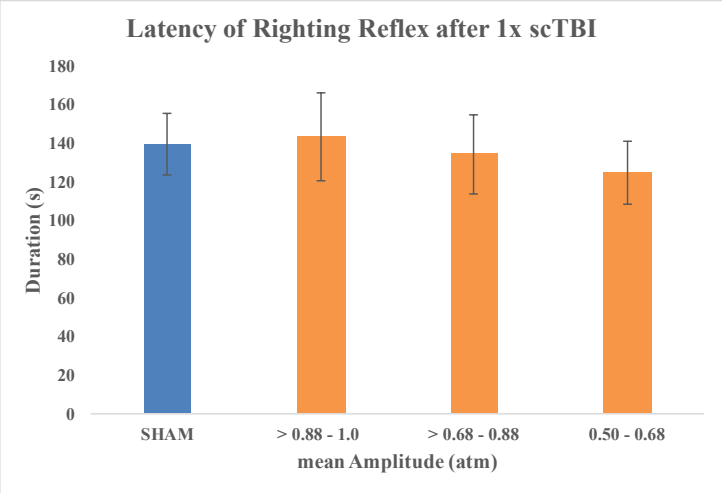

Figure 3.1 Latency of righting reflex was not significantly different from SHAM or scTBI groups.

The presence of apnea is a concern when evaluating a subconcussive impact. Apnea involves temporary brainstem dysfunction which would suggest the impact severity in the mTBI or higher range of traumatic brain injury. Therefore, only the SHAM, SC-MI and SC-LO were analyzed for neuronal degeneration.

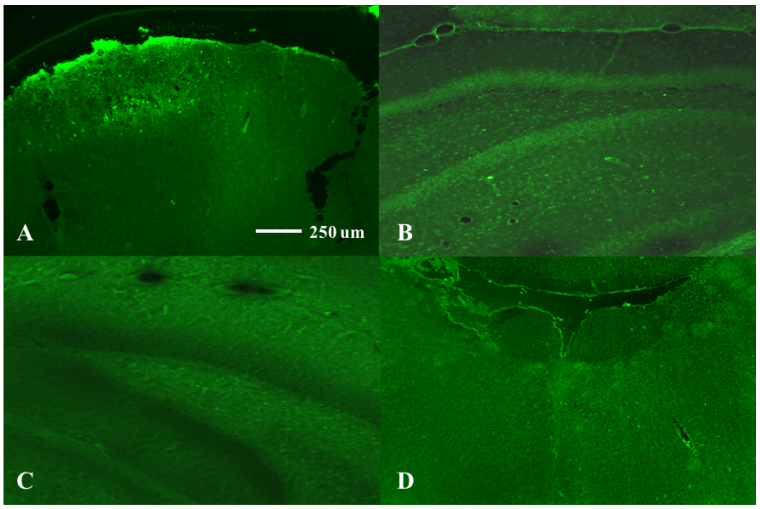

Figure 3.2 Neuronal degeneration. A. Sparse positive Fluoro-Jade C labeling in cortex, B. & C. No evidence of Fluoro Jade labeled cells in the hippocampus, nor D. Caudal pontine reticular nucleus.

Fluoro-Jade C labeling conducted at 24 h revealed no evidence of neuronal degeneration in the hippocampus or caudal pontine reticular nucleus (PnC) of SC-MI and SC-LO or SHAM-injured groups (SHAM n=12, SC-MI n=15, SC-LO n=20). Two of 15 subjects in SC-MI group that had observable positive Fluoro-Jade C labeling in the cortex, shown in Figure 3.2, however it was not found statistically significant when analyzed with the two SHAM animals that had similar positive Fluoro-Jade C labeling in the cortex (independent samples t-test, $t(2) = -0.588$, $p= 0.616$, two-tailed) shown in Figure 3.3.

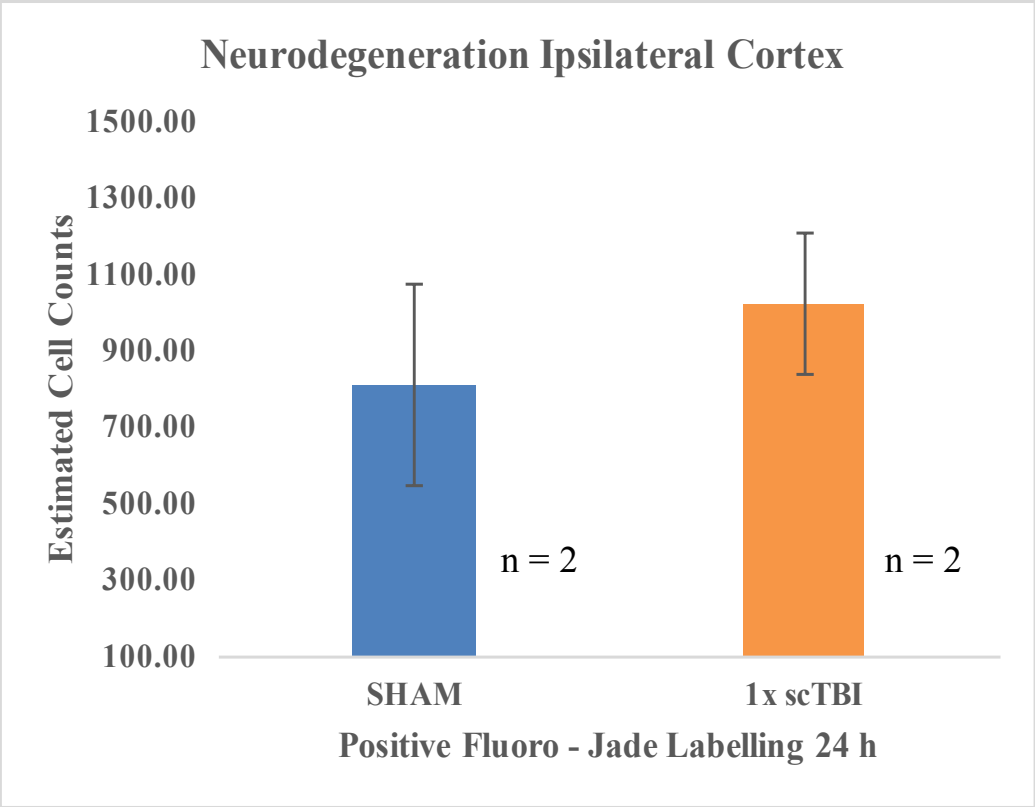

Figure 3.3 Estimated cell counts of neuronal degeneration in SHAM and 1x scTBI groups.

The data from the acute neurobehavioral measures and absence of Fluoro-Jade positive labeling, suggest a subconcussive impact amplitudes in the SC-MI and SC-LO groups (0.50 > 0.88 atm) to explore subconcussive phenomena. This range is similar to an earlier LFP subconcussive study by Shultz et al. utilizing a mean pressure amplitude of 0.80 atm in the range of their LFP subconcussive paradigm.

3.5 Discussion

3.5.1 General

Animal models are a powerful means to explore cause-and-effect relationships between

brain trauma and resulting pathophysiology and behavior. The majority of TBI research reports on impairments in cognition and behavior, cellular and molecular dysfunction and neuronal degeneration and death (Schmued, Albertson et al. 1997, Santhakumar, Ratzliff et al. 2001, DeRoss, Adams et al. 2002, Lovell, Collins et al. 2003, Crisco, Fiore et al. 2010, Blaylock and Maroon 2011, Crisco, Wilcox et al. 2011, McAllister, Flashman et al. 2012) from mild to severe injury spectrum. However, reports on the effects of subconcussion are scant in comparison. This study incorporates a novel animal model of subconcussive brain injury and the acute effects a scTBI utilizing a digitally controlled fluid percussion injury device (dcFPI). The dcFPI device was successful at generating peak pressure amplitude and impact durations reported in the literature. Results from biomechanical parameters analysis of three subconcussive groups demonstrate no significant difference in rise time and duration between the groups, however peak amplitude and impulse were statistically different. Acute behavioral effects of a scTBI resulted in no significant differences in latency of righting reflex. Examination for neuronal degeneration was not found significant in the SC-LO and SC-MI groups. In this study, the absence of neuronal degeneration and acute behavioral deficits, suggest peak pressure amplitudes between $0.50 > 0.88$ atm are optimal to study subconcussive brain injury.

The temporal and spatial patterns of a subconcussive brain injury are different than those that have been previously researched under the umbrella of traumatic brain injury. Literature from animal models of LFPI have reported mTBI peak amplitudes range from 1.0 to 1.5 atm (Pang, Sinha et al. 2015), while moderate and severe injuries have often been reported hovering around 2.0 and 3.0 and higher atm, respectively (Smith

et al.). Conversely, a pFPI study on subconcussive brain injury explored the effects of one subconcussive brain injury over a range of peak amplitudes from 0.50 - 0.99 atm, with a mean peak pressure amplitude of 0.80 atm. In this study, the dcFPI was successfully used as a similar technique to probe peak amplitudes of a subconcussive range used above.

Although a majority of literature reports peak amplitude as one of the main criteria to assess injury, improvement on brain injury models should encompass other biomechanical parameters, such as duration. Earlier pFPI studies on mTBI have reported waveform duration of 20 ms (Prins, Hales et al. 2010, Li, Korgaonkar et al. 2015), conversely in a different animal model of mTBI, a controlled cortical impact (CCI) performs dwell times of 100 ms or longer (Brody, Mac Donald et al. 2007, Kim, Fu et al. 2017). These impact durations model mild brain trauma, however the temporal duration of a subconcussion are different than a mild injury. Indeed, recent data from head impact telemetry studies (HITs) on high school and collegiate football players suggest durations referenced above may not mimic a similar impact. The data from HITs reported mean subconcussive impact durations ~10 ms (7 – 16 ms range) (Broglio, Sosnoff et al. 2009). Earlier, we developed and characterized the dcFPI device to produce pressure waveforms that aligned with the biomechanics of subconcussive brain impacts. This included reduced temporal waveform durations as reported from the HITs data and peak amplitude of pressure waveforms less than 1.0 atm as reported in animal studies. The results on duration together with peak amplitude suggest the dcFPI model as an ideal animal model to replicate subconcussive brain injury.

In addition to biomechanical parameters reported on injury severity, acute behavioral effects have been used to assess the level of injury. One behavioral measure commonly reported in literature is latency of righting reflex. Righting reflex is considered an analog to loss of consciousness experience in the clinical setting, thus it has been suggested as a surrogate indicator of experimental brain injury. Shultz et al. used LFP to investigate acute behavioral effects of one subconcussive mean impact force of 0.80 atm in adult rats. In that study, they did not see any statistical difference in latency of righting reflex. This current study produced similar results, showing no statistical significant difference in latency of righting reflex in any of the groups compared to sham-injured. However, unlike Shultz et al. whom observed no signs of apnea, this study had a few subjects in SC-HI group that exhibited apnea. This difference could be attributed to the use adolescent rats in the current study compared to adult rats used by Shultz et al. An earlier study by Prins et al., explored pFPI in the developing and adult rat. The study did not explore subconcussive brain injury range, however it did look examine mild, moderate and severe impacts. Of which, they observed in the mild range, P28 (juvenile rats) subjects exhibited more than twice as long duration of apnea, as compared to the adult, (24.5 s and 10.4 s, respectively) suggesting the younger animals may be more prone to brainstem damage. Age may be one of the factor that needs to be considered for the discrepancy in apnea. In addition to age, the presence of apnea may also be due to the use of the dcFPI to that of a traditional pendulum FPI (pFPI) model. The dcFPI device allows precise control over the biomechanics of the wave-form parameters, such as duration, rise-time and amplitude. Although the study by Shultz et al. did not reference all of the biomechanics of the waveform, the subconcussive pressure waveforms modeled

here, were mirrored on metrics reported from head impact telemetry system on athletes (Broglio, Sosnoff et al. 2009). Factors such as shorter temporal duration, young age of the adolescent rats and higher peak amplitude of the pressure wave may account for the reported observations of apnea.

Multiple studies of mTBI have shown positive Fluoro-jade labeling after mTBI delivered via FPI (Frank-Cannon, Alto et al. 2009, Blaylock and Maroon 2011, Das, Mohapatra et al. 2012, Neuberger, Abdul Wahab et al. 2014, Li, Korgaonkar et al. 2015) in the cortex and hippocampal regions, while less have reported on neuronal degeneration in the PnC (Hallam, Floyd et al. 2004). In the absence of acute behavioral changes, we examined the ipsilateral cortex, ipsilateral hippocampal region and PnC regions for any signs of neurodegeneration from peak amplitude of impacts. While a few subjects in the SHAM group and SC-MI had a few positive labeled Fluoro-jade cells in the ipsilateral cortex, it was not found significant. Neurodegeneration may be the result of the synaptic pruning process that occurs in the developing brain. Elimination of infrequently used synaptic connections could be the result of glia processes degrading cells, while strengthen more efficient synaptic connections. An earlier study by Cole et al. demonstrated that the craniotomy performed on the SHAM animals, intact dura, resulted in brain lesions around the site of the surgery and an increase in several pro-inflammatory cytokines compared to naïve animals (Cole, Yarnell et al. 2011). Suggesting that secondary cascades result from the initial craniotomy. Although this study didn't look histologically at cell death, it is plausible that the craniectomy procedure performed resulted in minimal neurodegeneration at the cortex level. Furthermore, additional FPI studies of mTBI have reported SHAM positive labeled Fluoro – Jade cells in the cortex

(Neuberger, Abdul Wahab et al. 2014, Pang, Sinha et al. 2015) collectively supporting the notion that the craniectomy procedure may result in neurodegenerative cells. Together with the acute behavioral data and absence of significant neurodegeneration this study suggests a range of SC-LO and SC-MI (0.50 – 0.88 atm) groups for peak pressure amplitude of scTBI. Furthermore, these findings suggest the dcFPI scTBI model is a suitable paradigm to continue investigating the underpinnings of what subconcussive brain injury encompasses.

CHAPTER 4

EFFECTS OF CUMULATIVE INTRA-DAY REPETITIVE SUBCONCUSSIVE BRIAN INJURY

4.1 Intro

Chapter 3 focused on establishing what subconcussive brain injury conditions could be examined in the fluid percussion injury paradigm. While no detrimental consequences from a single subconcussive impact are believed to be problematic, repetitive subconcussive trauma has been shown to result in neurophysiological, cognitive and structural changes as demonstrated by several imaging modality studies (Marchi, Bazarian et al. 2013, Talavage, Nauman et al. 2014). Here the cumulative effects from repetitive intra-day subconcussive impacts are examined for changes in acute behavioral measures, neuronal degeneration, behavioral deficits and changes in neuropathophysiology.

4.2 Materials and Methods

4.2.1 Fluid Percussion Injury

Animals were injured as explained in Section 3.1.1, with the addition of a cumulative injury paradigm. The cumulative paradigm encompassed one scTBI at five minute intervals repeated for five trials. Similar to Section 3.1.1, immediately prior to injury, rats were anesthetized with 5% isoflurane for 1 min. until foot-pinch reflex is absent. The animal was then connected to the dcFPI, once toe pinch response is observed, subconcussive brain injury is induced. The animal is removed from dcFPI device and kept under 2.5% isoflurane until the next scTBI. The scTBI interval between impacts was set at 5 min. The average duration of high school football games is around 2 h

including stoppage and half-time. Offensive and defensive linemen experience subconcussive insults every few minutes while other positions experience subconcussive insults further apart. A five-minute interval was chosen based on that logic. A mTBI results in a cellular energy crisis, of which can include, an imbalance of decreased cerebral blood flow, ionic fluctuations , and the increased hyperglycolysis occurs during and beyond this five-minute time interval (Giza and Hovda 2001). Additionally, in-vitro work from our laboratory has shown the degradation of III-IV intra-axonal loop of the NaCh α-subunit at a 20 minute time point from stretch-induce injury, resulting in persistent elevations in Ca^{2+} intracellularly. (Iwata, Stys et al. 2004). After the last impact, the animal is laid supine and latency of righting reflex is recorded.

4.2.2 Acoustic Startle Response

The acoustic startle reflex (ASR) in rodents is a whole-body response to a brief, yet sharp white noise. ASR was performed as previously described (Servatius, Beck et al. 2005). Rats were weighed and then with minimal restrainment and placed on a platform with a built-in accelerometer that is designed to transduce motion (Coulbourn Instruments, Langhorne, PA). In a single testing session, 24 acoustic stimuli of white noise were randomly presented at three loudness levels 84, 94 and 102dB with 100ms duration with 8 trials/intensity. Startle responses were analyzed offline. Startle response was scored if motion exceeded the threshold amplitude during a 250ms window starting at the onset of the stimulus. The criteria for response is any activity from onset of stimulus that exceeds four times the standard deviation of activity occurring in a 250ms stimulus-free baseline period. At which, it is determined if the subject responds (sensitivity) and to what level

of amplitude (responsivity) of the whole body is measured. The test chamber was cleaned with a detergent between the testing of each rat.

4.2.3 Spatial Working Memory Test

To analyze spatial working memory deficits following cumulative subconcussive impacts, delayed match to sample experiments were conducted using the Morris water maze (Pang, Jiao et al. 2011). The training phase consisted of rats learning to locate an escape platform (10 · 10 cm) located above the water surface in a pool (1.5 m diameter). This included a 2-day regiment; day 1 pre-training, each subject was placed on the platform for 20 s, immediately after placed in the pool ~ 4 inches away from platform and manually led to platform if it did not attempt to get back on the platform immediately. The subject is left on the platform for 20s. The subject is then placed ~12-15 inches away from the platform, given a minute to find the platform. If the subject did not find the platform, it was manually guided to it. The subject is removed for 60 s. Next the subject is given one trial consisting of sample and choice phase (explained in detail below). Day 2 pre-training consisted of the subjects going through sample and choice phase until it would find the platform in the choice phase. This typically included two to three iterations. With the escape platform submerged below water, baseline testing for spatial working memory performance was assessed at 24 h before cumulative scTBI paradigm, to match and assign into SHAM and injured groups. Working memory performance was assessed post injury day 1 (PID1), day 7 and day 14. Each subject under went one session per day. A session consisted of 6 trials. Each trial had two phases: a sample phase and choice phase. During the sample phase, the escape platform was placed

randomly in the pool. Rats began from a predetermined location within a zone and given 60 s to locate the platform. If the rat did not find the platform within 60 s, it was manually led to the platform. There, the rat was left on the platform for 20 s. The choice phase started after a retention interval of 60 s. The start location, the escape platform location, and time allotted to find the escape platform were identical to the sample phase. In between trials (i.e. escape platform location and starting quadrant were changed) the rat was put in a holding cage for a minimum of 30 minutes before the beginning of the next trial. For each session, the locations of the start and escape platform were distributed such that neither were located in the same zone. Swim paths were recorded for offline analysis of path efficiency (defined as the straight-line distance between start and escape platform location/total distance traveled by a rat; a value of 1 indicates the most efficient path) using ANYmaze software.

4.2.4 Histology

Rats were euthanized at 24 h and after last injury/sham injury for acute behavior and Fluoro – Jade stain, rats from the MWM experiment were euthanized at one week for Fluoro – Jade stain and the rats from the ASR experiment were euthanized at 24 h and 1 week after last cumulative scTBI for mRNA analysis. A subset of animals at day 18 and 30 were euthanized and stored in the brain bank for post analysis if required. Rats were anesthetized with pentobarbital and perfused with 4% paraformaldehyde; afterwards, brains were post-fixed in a solution of 4% paraformaldehyde for 24 h, followed by solution of sucrose until ready to be analyzed. Tissue was coronally sectioned on a freezing microtome at 40 μm thickness, with every 6^{th} and 12th sections to be stained.

Neuronal degeneration was assessed with Fluoro-Jade C, activated microglia was assessed for ionized calcium-binding adaptor molecule (IBA-1) and immunoreactive astrocytes with glial fibrillary acid protein (GFAP).

4.2.4.1 GFAP. Sections were blocked with 10% normal donkey serum in PBS for one hour. Afterwards, sections were incubated with mouse anti-GFAP antibody (1:500, Mouse monoclonal antibody MAB360, Millipore) in 4° for 24 h. The following day, sections were rinsed three 5-minute changes of PBS. A fluorescent secondary donkey anti-mouse antibody (1:500) is applied for 24 h. Finally, sections were rinsed three 5-minute changes of PBS. After final rinsing, slides were mounted, cleared and cover slips laid over.

4.2.4.2 IBA-1. Sections were blocked with 10% normal donkey serum in PBS for one hour. Afterwards, sections were incubated with goat anti-rat IBA-1 (1:500, Goat polyclonal to Iba1 AB5076, Abcam) overnight at 4° C. The following day, sections are rinsed three 5-minute changes of PBS and a secondary donkey anti-goat fluorescent antibody (1:500) were added and stored in 4° C for 24 h. Finally, slides sections were rinsed three 5-minute changes of PBS. After final rinsing, sections were mounted, cleared and cover slips for protection.

4.2.5 Reverse Transcription Polymerase Chain Reaction

Following the last behavioral tests at 24 h or 1 w, rats were euthanized by decapitation. Brain tissue was immediately dissected and stored in DNAse/RNAas free tubes and

stored in -80° C until assayed. Dissected regions included ipsilateral cortex and hippocampus and the PnC. RNA extraction was completed by homogenizing the tissue with 400 µl of Trizol reagent (Life Technologies) for 30 min, vortexed for additional 10 min and spun in centrifuge for 2 min at 12200 rpm. The supernatant was transferred to a new tube and added equal volume of ethanol (~350 µl), vortex for 15-30 s, loaded into a column and spun down for 1 min. Next, 5 µl of DNase, 8 µl of 10x DNase reaction buffer, 3 µl of DNase/RNase free water and 64 µl RNA wash buffer was added to the each sample and incubated for 30 min at room temperature, then spun down for 30 s. 400 µl of RNA prewash was added, spun for 1 min, discarded flow through, then repeated one more time. 700 µl of wash buffer is added, spun for 1 min, discarded flow through. Spun again for 2 min discarded any additional flow through. The column was then transferred to RNAse free-tube. Finally, DNAse/RNAse free water was added, spun for 1 min. RNA concentration samples were measured using spectrophotometry (BioTek, Take3).

Reverse Transcription reaction was accomplished by adding 18 µl of RNA diluted to 1 µg/µl into a new tube. One µl of RT primers was added to the samples and incubated in 65° C for 5 min, then immediately transferred to ice for 5 min. Next, 6 µl of 5x Superscript Buffer, 1.5 ul of 0.1 M DTT, 1.5 µl of 10 mM dNTPs, 1 µl of RNase out and 1 µl of Superscript III were added to the samples and incubated at room temperature for 10 min. followed by 2 h at 45° C. The reverse transcription reaction was terminated by heating at 70° C for 15 min. cDNA was then stored at -80° C or continued to RT-PCR.

RT-PCR was achieved using Roche LightCycler. Briefly, a master mix for each probe was created. The master mix contained 3 ul cDNA, 10 µl of Taq polymerase, 6 µl

of PCR H_2O and 1 μl of Taq probe (IL-1α Taqman Probe, IL-1β Taqman Probe and TNF-α Taqman Probe, Life Technologies) were distributed into each well. Tissue was assayed in triplicate for each target gene. Means of the triplicate were used as target values and normalized to the mean of beta-actin. Fold changes for each gene were calculated as previously described (Janke et al. 2015).

4.2.6 Image Intensity Analysis

Images were captured with Leica Aperio Versa 200 scanner. Aperio ImageScope software, Area Quantification FL, was used to assess regions of interest. The algorithm calculates the contribution of each dye at every image pixel as either a single dye or dye combination, if more than one dye was used. Dye intensity for minimum and maximum intensity thresholds (0 – 1) are set for each dye. Output used for analysis was total area of analysis (mm^2) and total area of specified dye(s) (mm^2). Intensity is determined by (area specified dye / total area of analysis).

4.3 Statistical Analysis

Statistical analysis was performed with SPSS 20. Both ASR sensitivity and amplitude were analyzed in a mixed-design, repeated measures analysis of variance (rmANOVA), with between-subjects factor of injury (2 levels: 5x SHAM or 5x scTBI) and day of sacrifice (3 levels: Pre-Injury, PID1, and PID7) and within-subject factor of stimulus intensity (3 levels: 84, 94 and 102 dB). Independent samples t-test was applied to analyze latency of righting reflex, immunocytochemistry and each gene/cellular marker. Normality and homogeneity of variance was tested in SPSS. Several

immunocytochemistry image intensity data did not have normal distribution and were positively skewed. A $\log_{(10)}$ transform was applied and geometric mean data presented. Significance was set to $p < 0.05$. Data shown are mean ± standard error of mean (sem).

4.4 Results

4.4.1 General Characteristics

Table 4.1 Type of Experiment, Subject Grouping, Timeline and Method of Tissue Analysis (Neurodegeneration: Fluoro – Jade staining; IHC: Immunohistochemistry; PCR: Polymerase chain reaction)

			Neurodegeneration		IHC		PCR	
Experiment	**No. of Animals**	**Groups**	**PID1**	**PID7**	**PID1**	**PID7**	**PID1**	**PID7**
Acute Behavior	7 SHAM 8 scTBI		X (n =7,8)		X (n =7,8)			
Spatial Memory	15 SHAM 15 scTBI	1. PID 1 (n=4)* 2. PID 7 (n=6) 3. PID 30 (n=5)		X (n = 3)		X (n = 3)		
Acoustic Startle Response	15 SHAM 15 scTBI	1. PID 1 (n=4)* 2. PID 7 (n=4) 3. PID 18 (n=7)					X (n = 4)	X (n = 4)

Table 4.2 Biomechanical Characteristics from Cumulative scTBI

Acute Behavior	Amplitude (atm)	Rise Time (ms)	Duration (ms)	Impulse (Pa-s)	Righting Reflex (s)
5x scTBI	0.504 ± 0.03	5.01 ± 0.18	12.34 ± 0.34	497.5 ± 40.3	1501.1 ± 26.9
5x SHAM	0	0	0	0	1479.6 ± 42.3
MWM					
5x scTBI	0.571 ± 0.03	6.14 ± 0.21	15.44 ± 0.31	638.8 ± 37.1	1538.7 ± 23.2*
5x SHAM	0	0	0	0	1482.7 ± 11.5
ASR					
5x scTBI	0.627 ± 0.03	5.84 ± 0.13	16.4 ± 0.43	699.3 ± 38.1	1542.8 ± 24.2*
5x SHAM	0	0	0	0	1455.2 ± 14.1

4.4.2 Acute Behavior and Neuronal Degeneration from Cumulative scTBI

Rats were divided into two groups, 5x SHAM and 5x scTBI (n = 7 and n = 8). Table 4.2 summarizes the biomechanical characteristics of the pressure waveforms. There was no significant difference in latency of righting reflex of 5x scTBI to 5x SHAM group (Independent samples t-test, t(13)=-1.126, p =0.281, two-tailed). Figure 4.1 illustrates the individual waveforms of a subject.

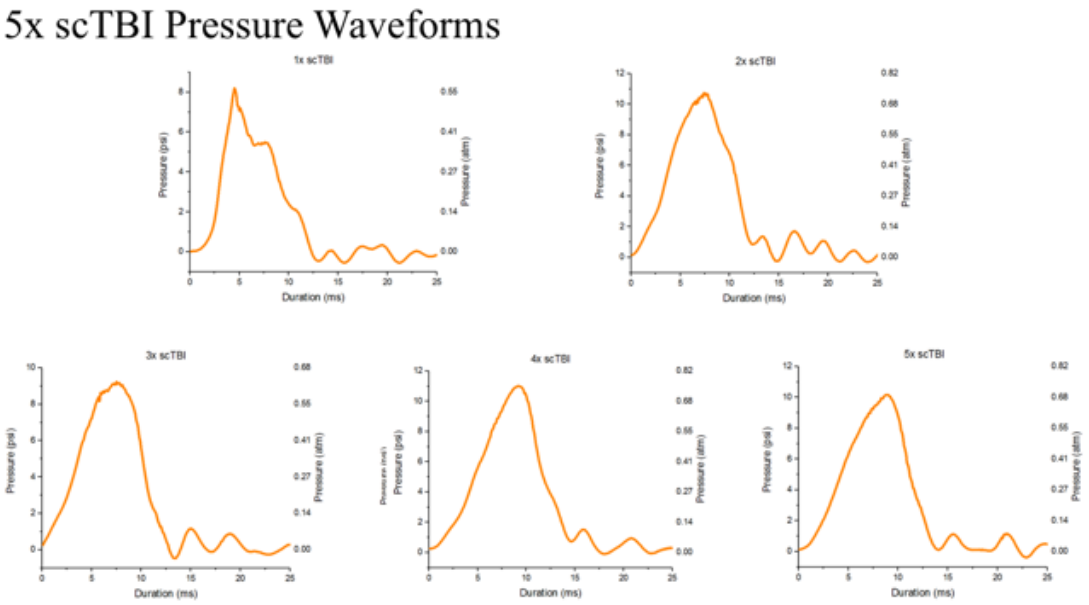

Figure 4.1 Pressure waveforms from 5x scTBI.

Neuronal degeneration was assessed 24 h after the last scTBI (Figure 4.2). Positive Fluoro – Jade C labeling was observed in the cortex of 50% of scTBI animals and 14.3% of 5x SHAM animals, however cell counts for positive labeled Fluoro – Jade C, did not reach statistical significance (independent samples t-test, $t(13)=-1.65$, $p = 0.102$, two-tailed). Neuronal degeneration was found in the granule cell layer of 50% of scTBI animals, while the 5x SHAM animals had no apparent neuronal degeneration in the granule cell layer. The 5x scTBI animals with Positive Fluoro – Jade C cell counts in the granule cell layer did not reach statistical significance (Independent samples t-test, $t(7.00) = -2.829$, $p = 0.055$, two-tailed) when analyzed with the 5x scTBI animals that did not present positive Fluoro – Jade staining in the granule cell layer. Neither groups had any apparent neuronal degeneration in the PnC. One 5x SHAM rat was removed from analysis due to higher Fluoro – Jade positive cell counts than any 5x scTBI subjects. A surprising result we did not expect to see was evidence of disruption of the blood brain

barrier (BBB-D) in all of 5x scTBI animals, above the hippocampus fissure (Figure 4.3) while 5x SHAM animals did not demonstrate BBB-D.

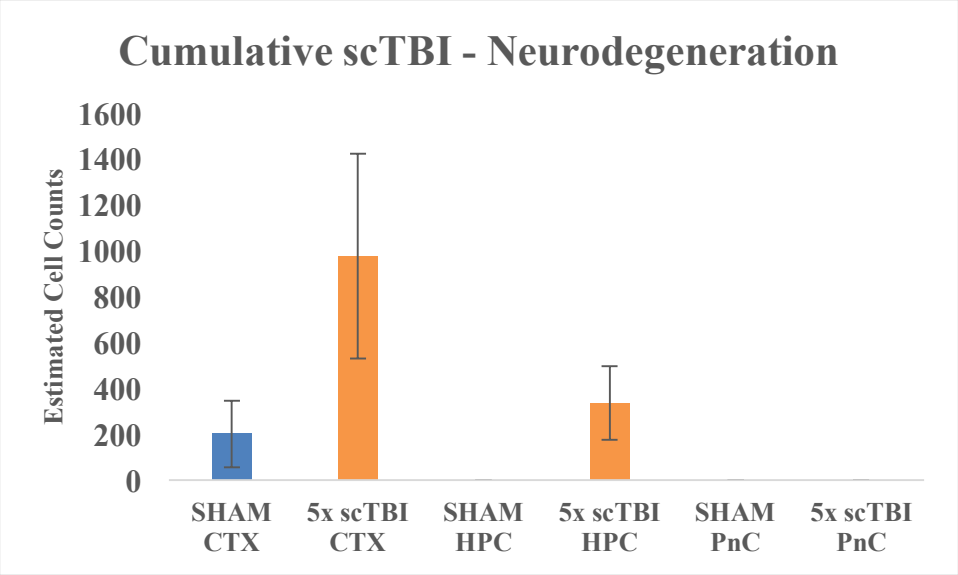

Figure 4.2 Estimated neurodegenerative cell counts after cumulative scTBI.

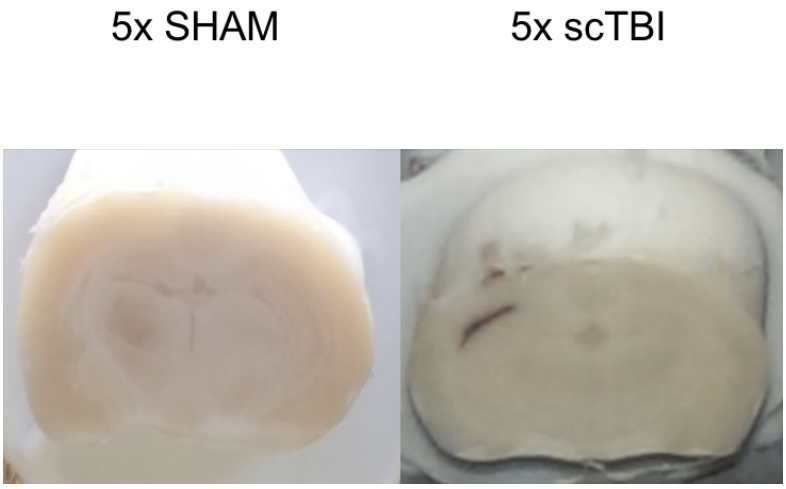

Figure 4.3 Blood brain barrier disruption in the hippocampus fissure.

4.4.3 Cumulative Effects of scTBI on Acoustic Startle Response

4.4.3.1 Startle Sensitivity and Amplitude. Figure 4.4 illustrates the acoustic startle response circuit. Cumulative scTBI resulted in a temporary suppression of ASR. ASR is well defined in literature and can be applied translational to clinical setting to that of eye-blink. Table 4.2 lists the biomechanical characteristics ASR experiment.

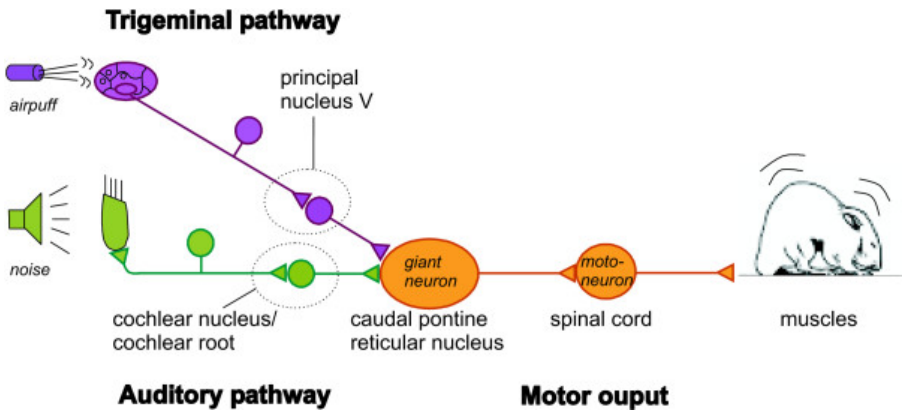

Figure 4.4 Acoustic Startle Response circuit. (Simons-Weidenmair et al. 2006)

Rats in the 5x scTBI nor 5x SHAM group exhibited apnea or limb-extension, however, assessment of righting reflex of 5x scTBI to that of 5x SHAM group indicated 5x scTBI had a significantly greater duration of recovery than that of 5x SHAM (Independent samples t-test, $t(28) = 2.953$, $p=0.006$), Table 4.2. Figures 4.5 and 4.6 show the results from ASR. In comparison to 5x SHAM, 5x scTBI sensitivity was not found significant [$F(1,28) = 0.155$, $p=0.697$. There was a main effect of day [$F(1,28) = 15.297$, $p < 0.001$], however no injury X day interaction was found significant [$F(1,28) = 2.263$, $p = 0.144$]. ASR magnitude was significantly reduced after cumulative scTBI [$F(1,28) =$

4.73, p = 0.038], compared to Pre-injury testing of the 5x scTBI and 5x SHAM animals [F(1,28) =0.003, p=0.959]. There was a main effect of stimulus intensity [F(1,28) = 107.375, p < 0.001] on PID1. Neither group was statistically significant at PID 4 or PID7 (p=0.490 and p=0.847, respectively) suggesting that cumulative scTBI resulted in a transient suppression of ASR.

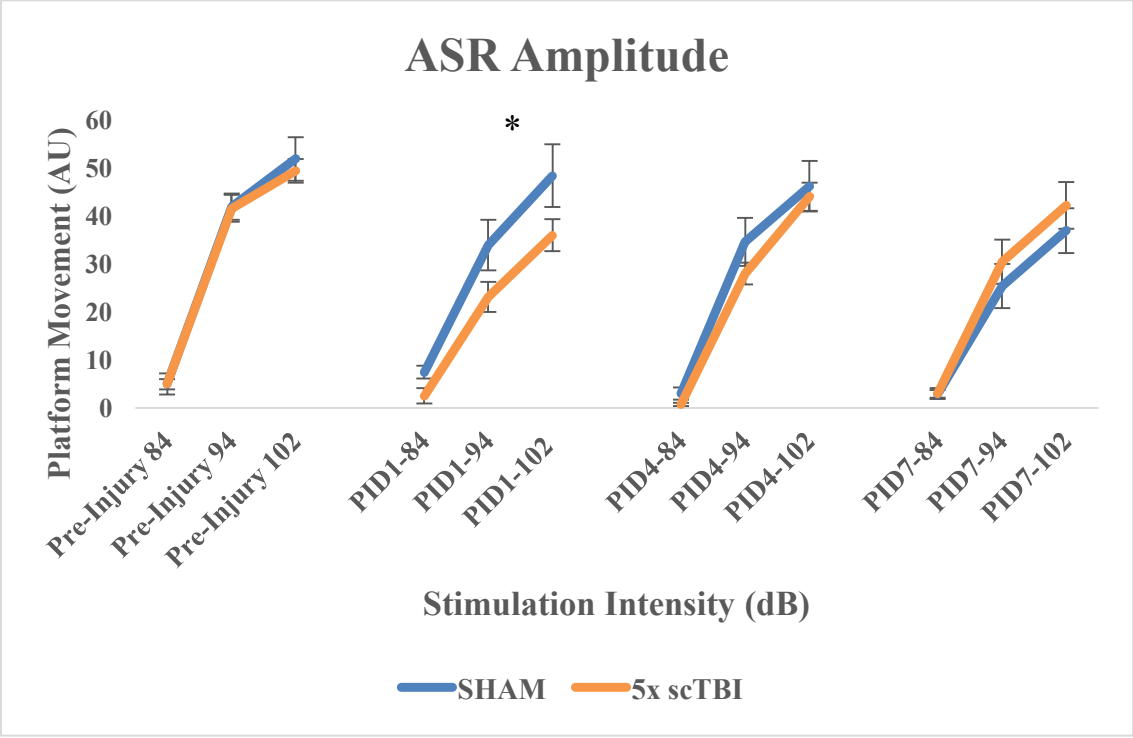

Figure 4.5 ASR magnitude was suppressed on PID1 in 5x scTBI compared to 5x SHAM.

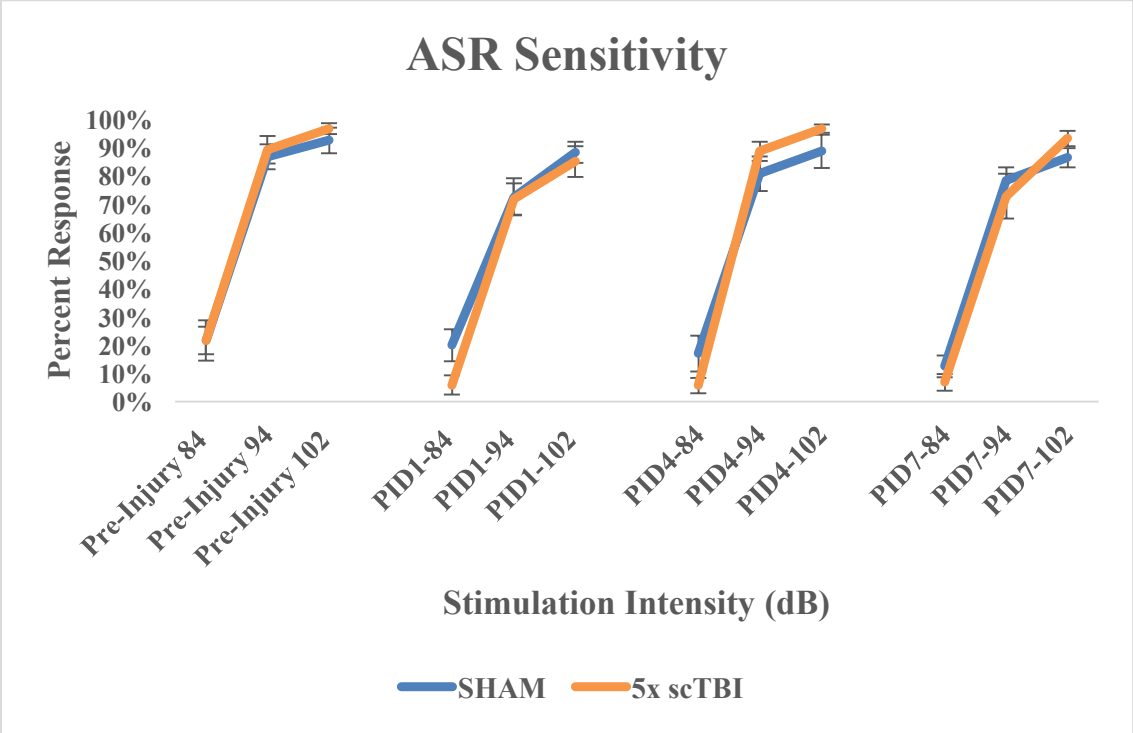

Figure 4.6 Cumulative scTBI had no effect on ASR sensitivity in either groups.

4.4.4 Working Memory Assessment

Figure 4.8 and 4.9 show the results on path efficiency of subjects participating in working 4a significant effect of injury [F(1,28) = 0.144, p = 0.707]. Neither main effect of day nor injury X day interaction were significant [F(2,56) = 0.774, p = 0.466] and [F(2,56) = 0.775, p = 0.466]. Assessment of path efficiency in the choice phase did not result in significant effect of injury [F(1,28) = 0.560, p = 0.461]. Neither main effect of day nor injury X day interaction were found significant [F(2,56) = 2.749, p = 0.073] and [F(2,56) = 2.982, p =0.059].

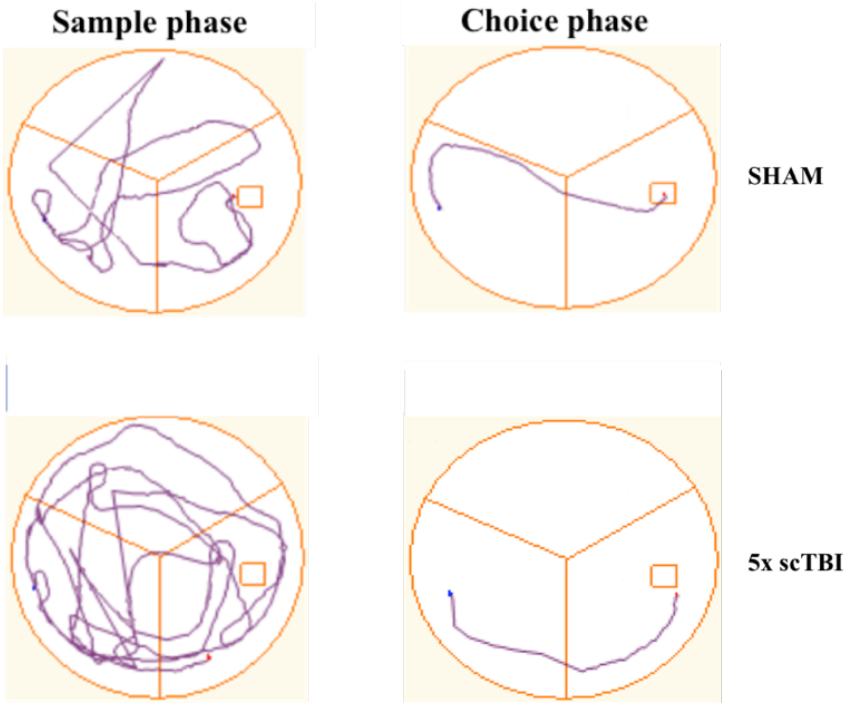

Figure 4.7 Left side, subject swims in the sample phase looking for the platform. Right-side, after rat has located the platform in sample phase, they are put back into the pool to find the same platform location.

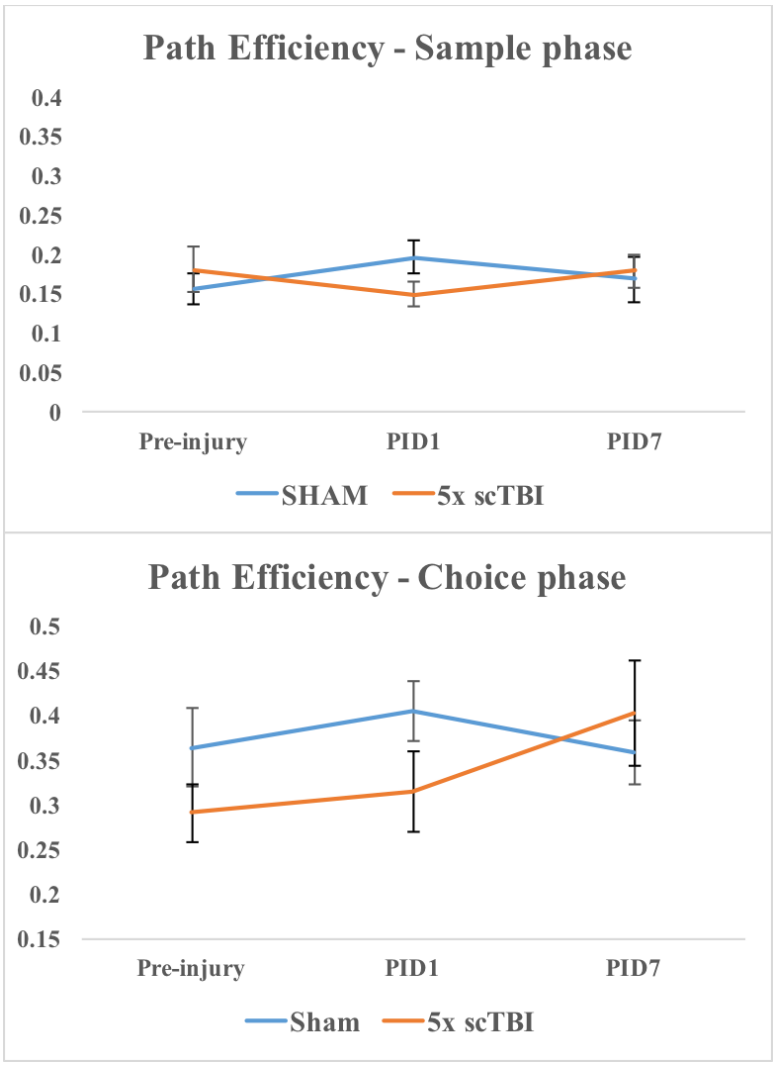

Figure 4.8 Path efficiency of sample nor choice phase was found significant, suggesting no working memory impairment after 5x scTBI.

4.4.5 Latency of Righting Reflex

Examining latency of righting reflex in the three experimental groups (Acute behavior, MWM and ASR) of the cumulative scTBI paradigm led to slight trend of increasing applied pressure that seem to correlate with longer righting times. The first cumulative scTBI experiment, acute behavior and neurodegeneration, there was not statistically significant difference in latency of righting reflex. When examining the remaining

experimental groups, MWM and ASR, a statistically significant increase in latency of righting reflex is observed. Further analysis of individual data points of all groups suggested a trend in increasing mean peak amplitude associated with longer latency of righting reflex, Figure 4.8. Pearson's correlation analysis of the data points shows that latency of righting reflex and mean peak pressure amplitude were significantly correlated (r=0.402, n=34, p =0.020, two-tailed), Figure 4.9. Furthermore, analysis of all animals that received 5x scTBI over the study, had significant increase in latency of righting reflex compared to SHAM animals (independent samples t-test(98) =-2.492, p = 0.031), Figure 4.9.

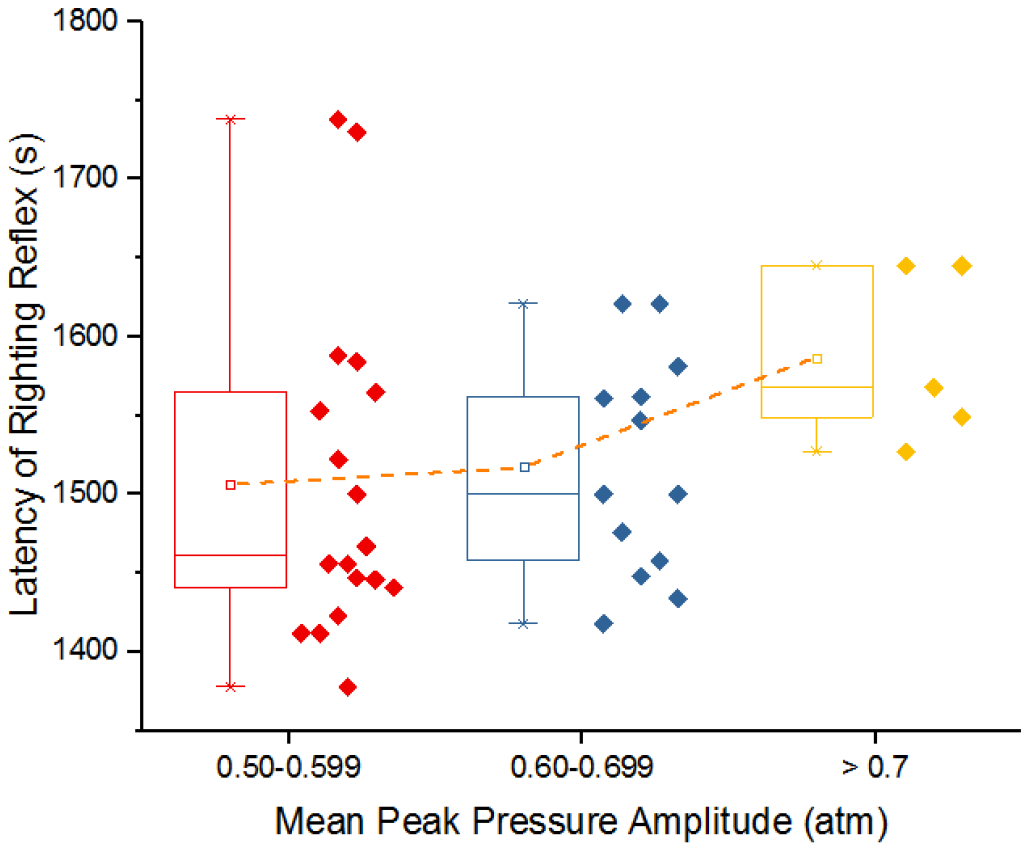

Figure 4.9 Peak pressure-righting reflex response curve.

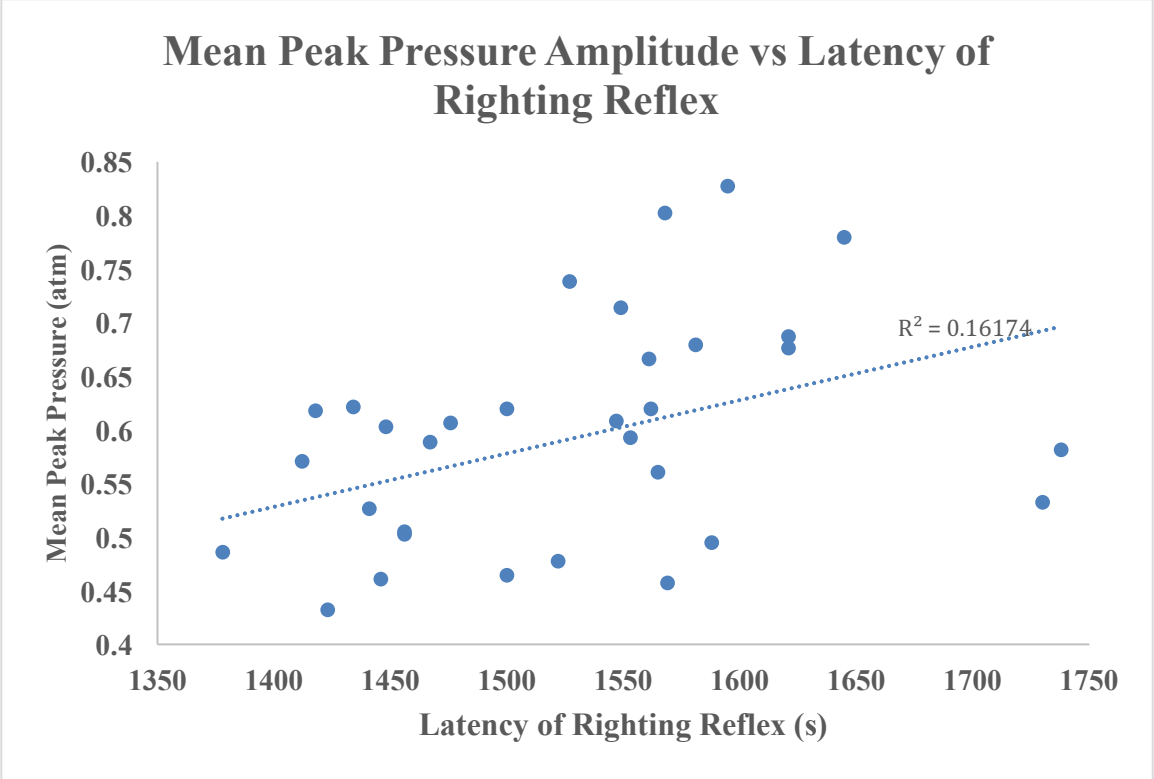

Figure 4.10 Trend in increasing pressure correlates with increasing latency.

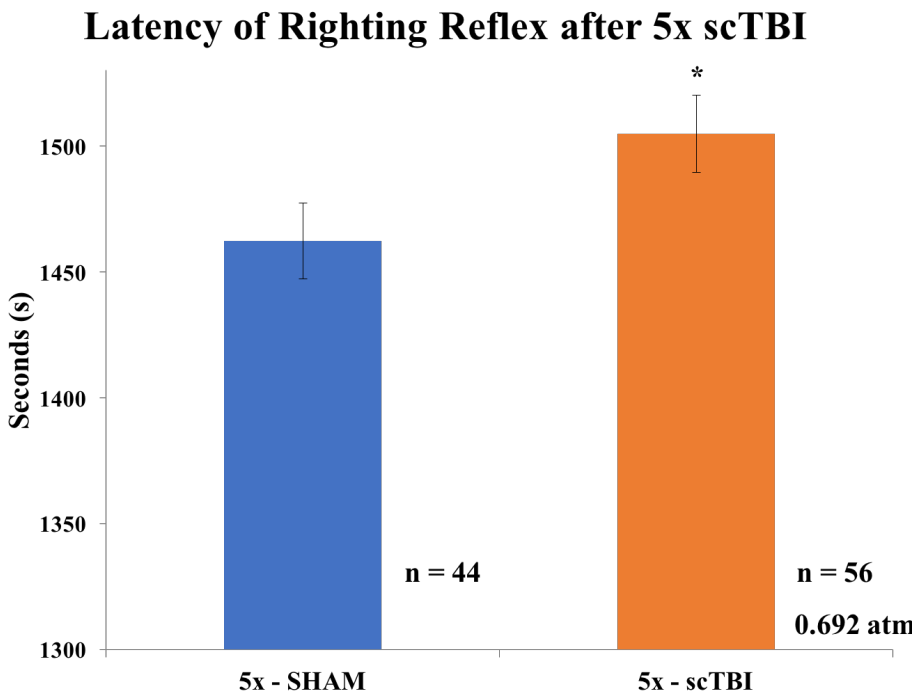

Figure 4.11 Latency of righting reflex of all animals exposed to cumulative scTBI was increased compared to SHAM animals.

4.4.6 Neuroinflammation and Immunoreactivity

4.4.6.1 Ipsilateral Cortex. Figure 4.12 shows cumulative scTBI increased GFAP immunoreactivity and reactive microglia/macrophages at 24 h and 1 week. Figure 4.13 shows image intensity analysis of the ipsilateral cortex. 5x scTBI animals showed a significant increase GFAP and IBA1 immunoreactivity at 24 h ((Independent samples t-test of $\log_{(10)}$ transformed data (43)=9.452, $p < 0.001$) and (Independent samples t-test of $\log_{(10)}$ transformed data t(43)=5.289, $p < 0.001$). One week after cumulative scTBI, a statistical significant increase in GFAP and IBA-1 is present (Independent samples t-test (16) = 9.72, $p < 0.001$ and independent samples t-test (8.831) = 10.726, $p<0.001$).

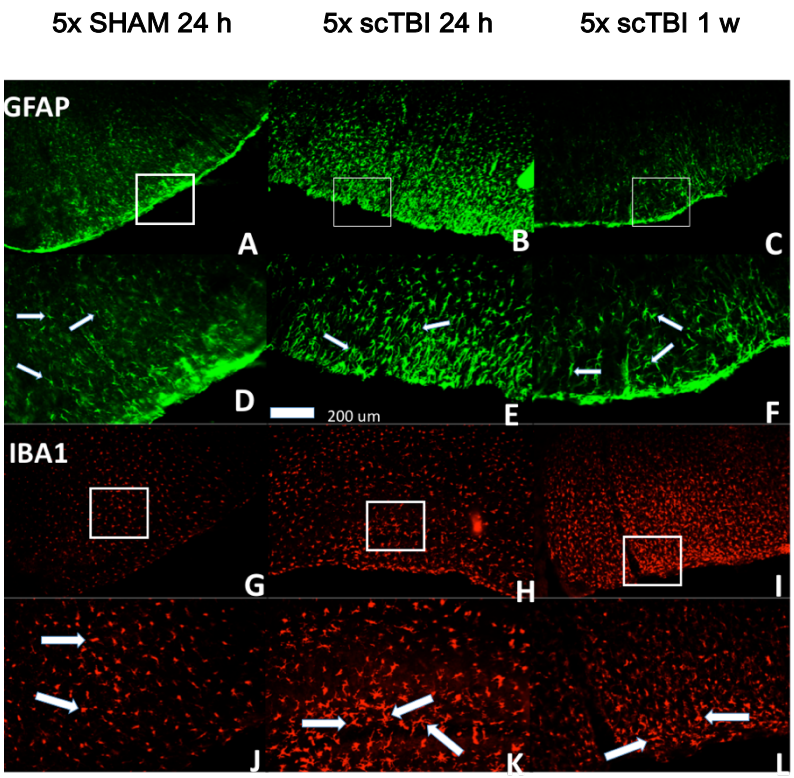

Figure 4.12 Increased GFAP and IBA-1 immunoreactivity in the cortex of 5x scTBI compared SHAM at 24 h. (A-F) Slices were taken from SHAM, 5x scTBI 24 h and 1 week subjects. A-C. GFAP labeled astrocytes ipsilateral cortex (10x). D-F. Insets (20x) of A-C. G-I. IBA1 labeled microglia in the cortex J-L. Insets (20x) of G-I

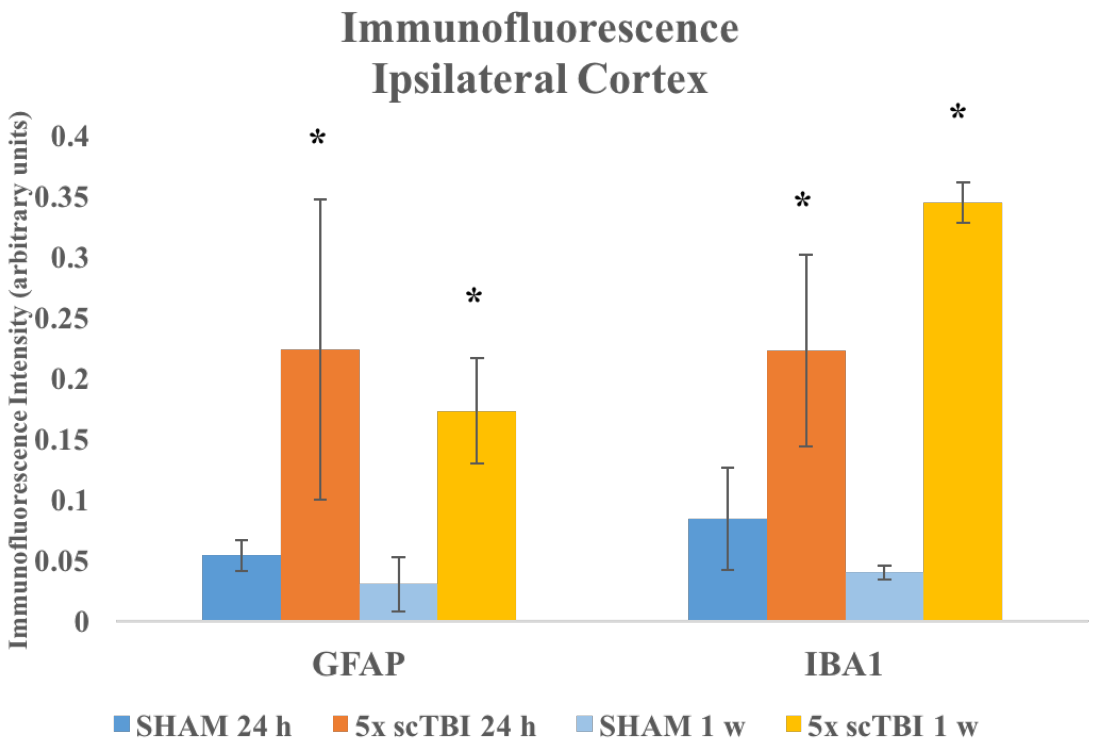

Figure 4.13 Immunocytochemistry Analysis of Ipsilateral Cortex after 5x scTBI at 24 h and 1 w.

4.4.6.2 Ipsilateral Hippocampus. Figure 4.14 shows cumulative scTBI increased GFAP immunoreactivity and reactive microglia/macrophages at 24 h and 1 week. Figure 4.15 shows image intensity analysis of the ipsilateral hippocampus. 5x scTBI animals showed a significant increase GFAP and IBA1 immunoreactivity at 24 h ((Independent samples t-test of $\log_{(10)}$ transformed data (43)=8.491, $p < 0.001$) and (Independent samples t-test t of $\log_{(10)}$ transformed data (43)=7.471, $p < 0.001$), respectively). However, at 1 week after cumulative scTBI, there was not significant increase in GFAP nor IBA-1 ($p = 0.057$ and $p = 0.772$, respectfully).

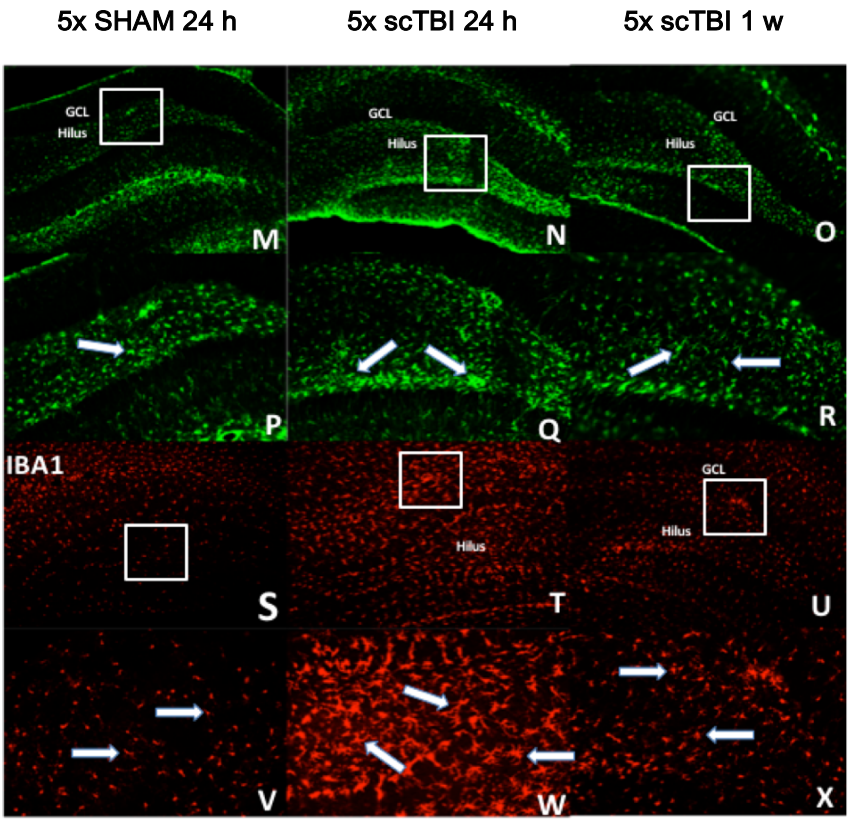

Figure 4.14 Increased IBA-1 immunoreactivity in the hippocampus of 5x scTBI compared SHAM at 24 h and 1 w. M-O. GFAP labeled astrocytes in the hippocampal regions. P-R. Insets (20x) of M-O. S-U. IBA1 labeled microglia. V-X. Insets (20x) T-U. GCL: granule cell layer

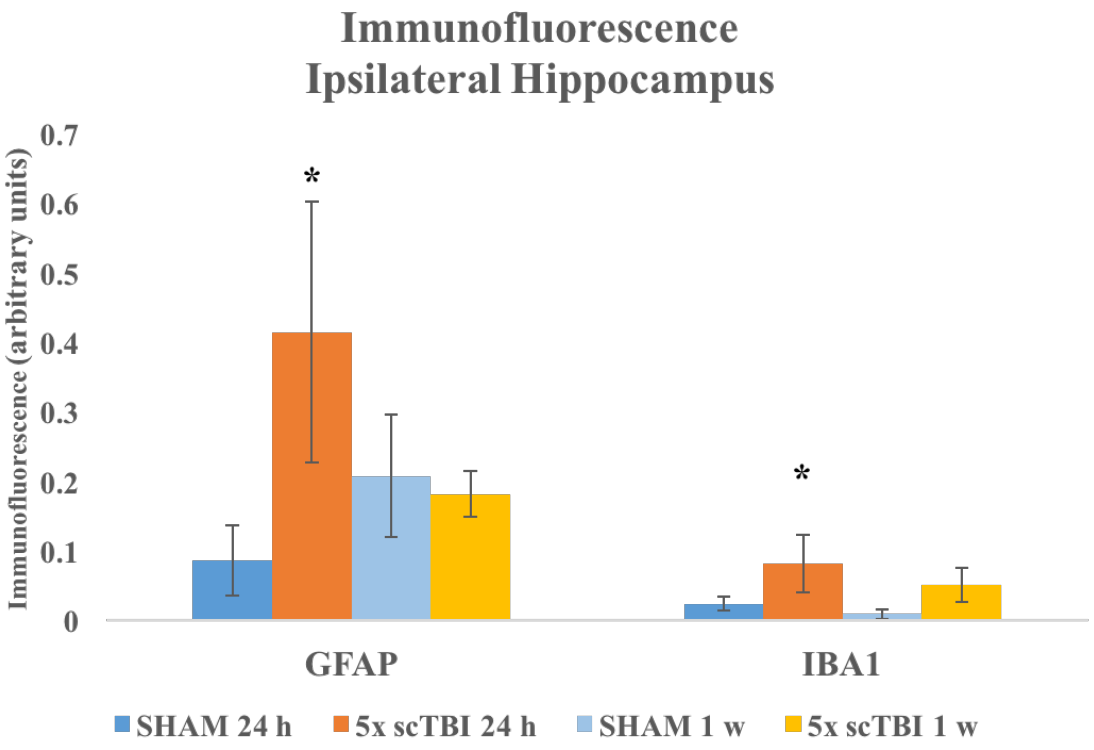

Figure 4.15 Immunocytochemistry analysis of ipsilateral hippocampus after 5x scTBI at 24 h and 1 w.

4.4.6.3 Caudal Pontine Reticular Nucleus (PnC). Figures 4.16 and 4.17 shows cumulative scTBI increased GFAP immunoreactivity and reactive microglia/macrophages at 24 h and 1 week. Figure 4.18 shows image intensity analysis of the PnC. 5x scTBI animals showed a significant increase GFAP and IBA1 immunoreactivity at 24 h ((Independent samples t-test (30.742) = 4.678, $p < 0.001$) and (Independent samples t-test $t(43)=3.22$, $p = 0.003$), respectively). However, at 1 week after cumulative scTBI, there was not significant increase in GFAP nor IBA-1 ($p = 0.317$ and $p = 0.762$, respectfully).

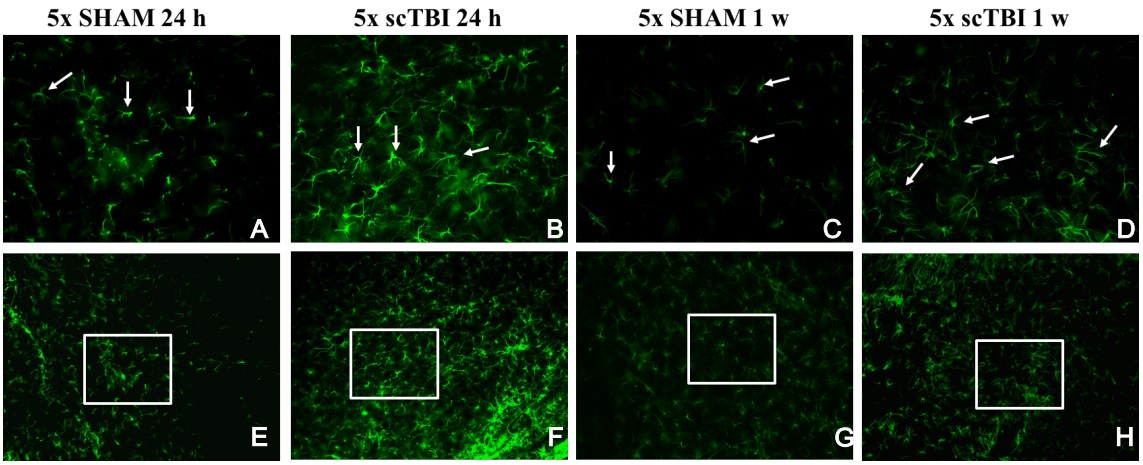

Figure 4.16 (A-D) Increase in GFAP immunofluorescence in PnC of 5x scTBI compared to SHAM at 24 h and 1 w. (E-H) Inset 40x).

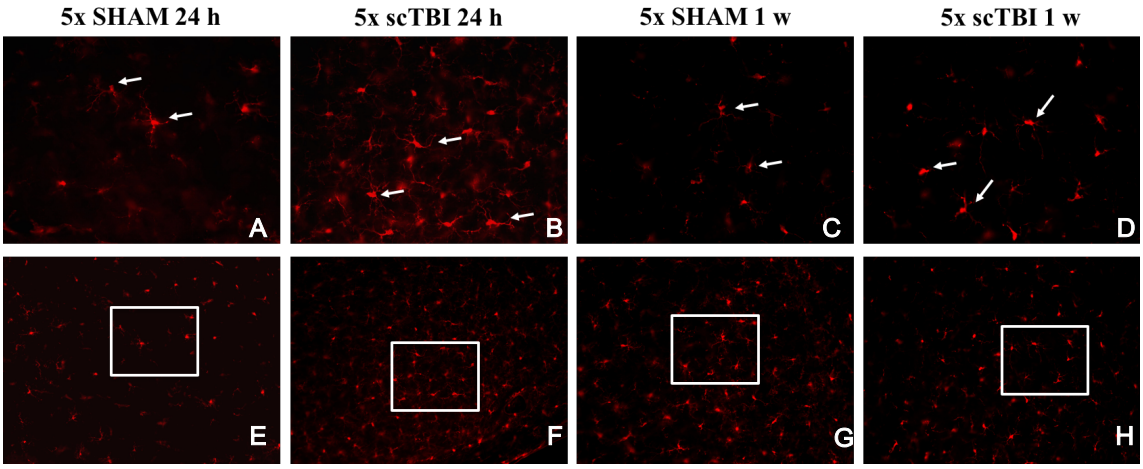

Figure 4.17 (A-D) Increase in IBA-1 immunofluorescence in PnC of 5x scTBI compared to SHAM at 24 h and 1 w. (E-H) Inset 40x.

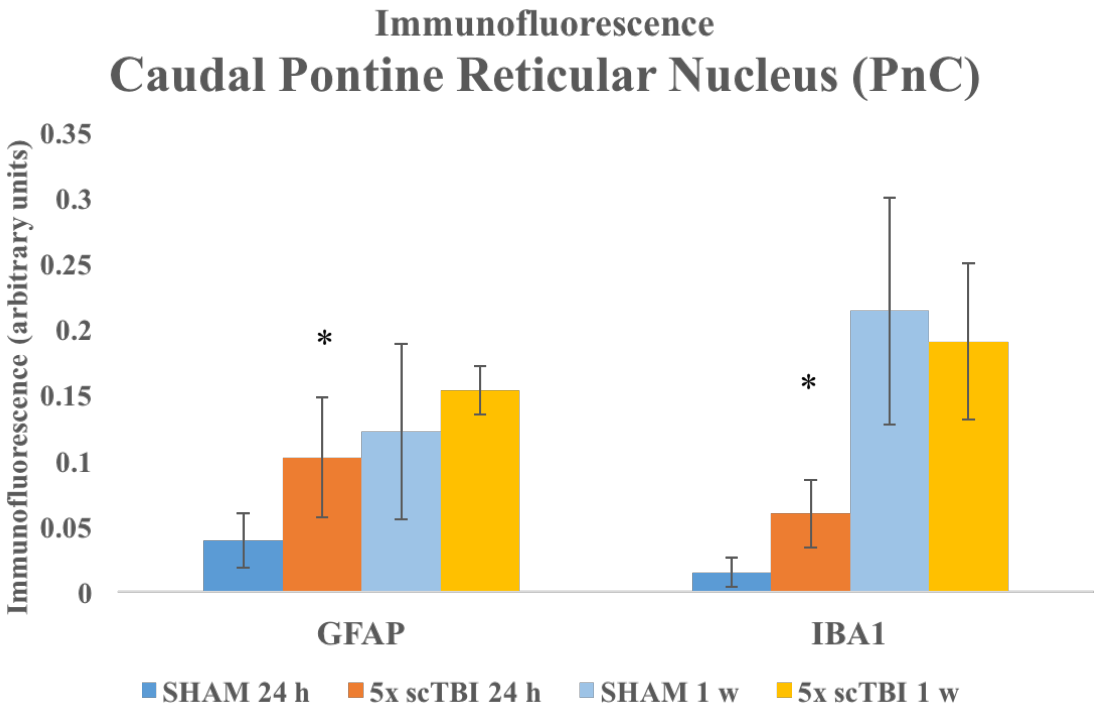

Figure 4.18 Immunocytochemistry analysis of PnC after 5x scTBI at 24 h and 1 w.

4.4.7 Biochemical Analysis

4.4.7.1 Cytokine mRNA Expression in the Ipsilateral Cortex and Hippocampus after Cumulative scTBI. Figure 4.19 represents IL1-α and TNF-α cytokine expression in the ipsilateral cortex, however neither cytokine showed an upregulation on PID1 compared to SHAM. A trend in upregulation for IL1-β was found in the cortex on PID1, however it did not reach significance ($p > 0.05$). Although mRNA expression (at either time-point) did not increase significantly, immunofluorescence analysis early confirmed protein expression of reactive astrocytes and microglia/macrophages.

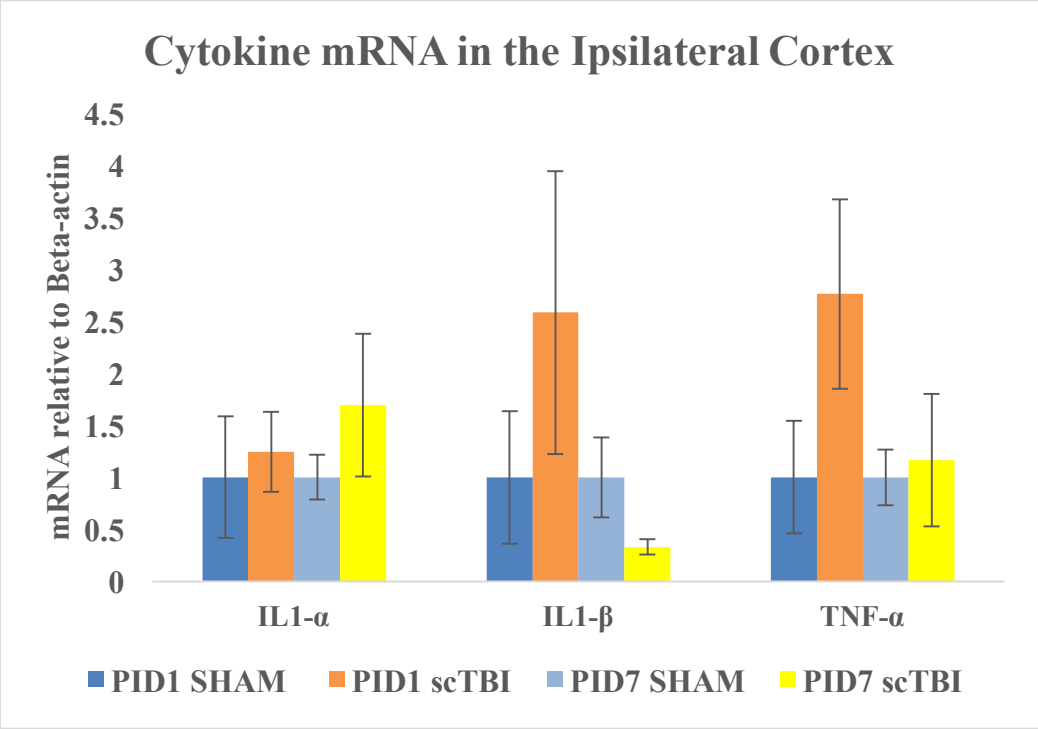

Figure 4.19 Cytokine mRNA expression in ipsilateral cortex.

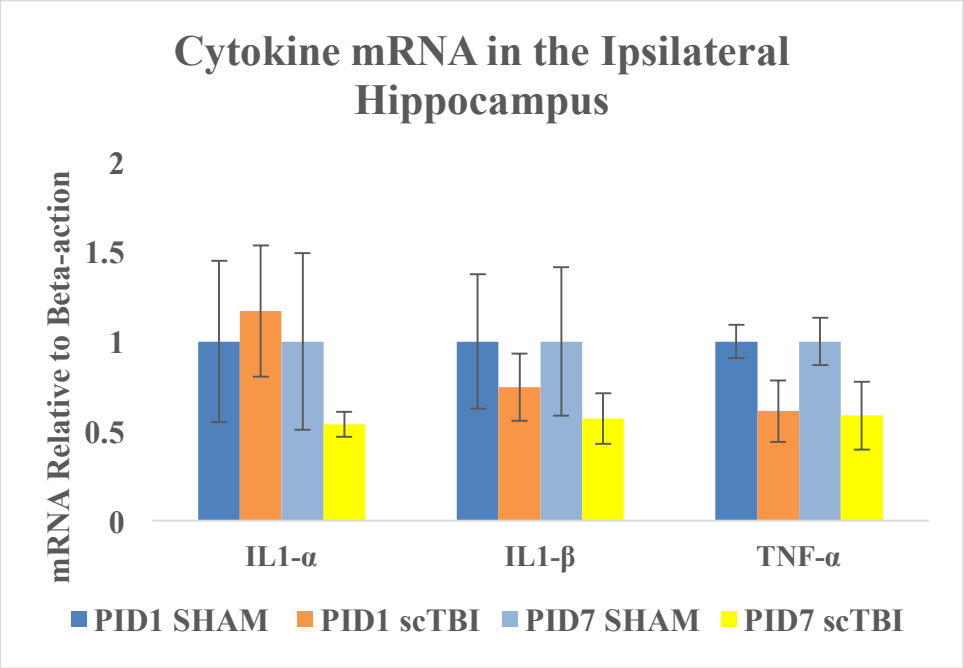

Figure 4.20 Cytokine mRNA expression in ipsilateral hippocampus.

Figure 4.20 exhibits cytokine mRNA expression in the hippocampus region, where no significant increases in IL1-α, IL1-beta or TNF-alpha cytokine expression were found ($p > 0.05$).

4.4.7.2 Cytokine mRNA Expression in the Caudal Pontine Reticular Nucleus after Cumulative scTBI. Overall, cumulative scTBI caused a transient upregulation of pro-inflammatory cytokine IL1-β on PID1 that returned to SHAM levels at PID7. Figure 4.21 shows IL1-β mRNA was significantly increased after 5x scTBI on PID1 [$F(1,12) = 3.078$, $p = 0.046$], although no significant increases were found at PID7. Both IL1-α and TNF-α show a trend increasing on PID1 compared to SHAM and a decrease on PID7, neither time point was statistically significant.

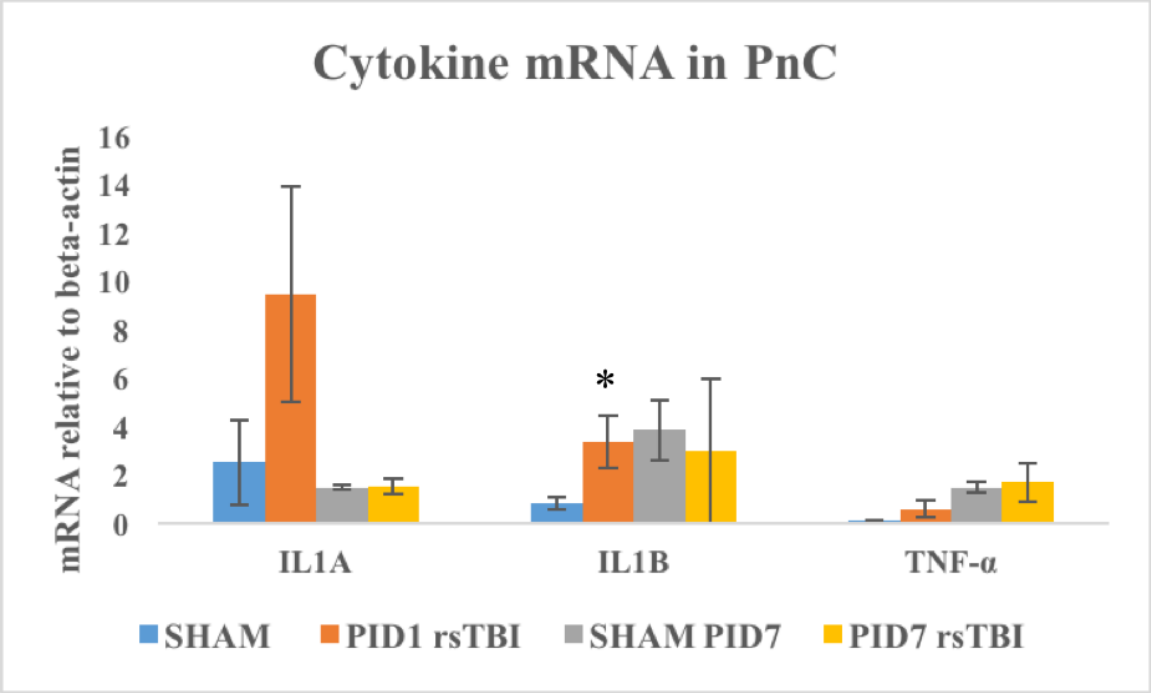

Figure 4.21 Cytokine mRNA expression in the PnC. IL1-β shows a significant increase compared to SHAM PID1.

4.4 Discussion

4.5.1 General

While repetitive TBI is well researched, there is a paucity of information on a pathophysiological and behavioral changes resulting from cumulative subconcussive brain injury. Investigating the pathophysiology of cumulative subconcussive insults clinically is not feasible; however, understanding what interactions exists between cumulative effects of repetitive subconcussive insults and neuropathophysiology in established animal models of subconcussive TBI (scTBI) may benefit the medical and scientific community. This study incorporates a novel animal model of subconcussive brain injury and the effects of cumulative intra-day scTBI utilizing a digitally controlled fluid percussion injury device (dcFPI). Acute behavioral effects of cumulative 5x scTBI`

resulted in longer duration in latency of righting reflex compared to 5x SHAM group. Neuronal degeneration was assessed at 24 h using Fluoro – Jade C, while inconsistent across subjects, half of the 5x scTBI subjects had sparse neuronal degeneration in the granule cell layer of the hippocampus and all 5x subjects exhibit hemorrhage. Neurobehavior assessment revealed no deficits in working memory task, however transient suppression of ASR was observed on PID1, returning to SHAM levels by PID4. The presence of immunoreactive microglia/macrophages and reactive astrocytes was observed in cumulative 5x scTBI at 24 h and to a lesser degree at PID7 when compared to 5x SHAM group. Biochemical analysis of discrete brain regions found a transient upregulation of IL1-β in the PnC at 24 h.

4.5.2 Fluid Percussion Injury Model of Subconcussive Brain Injury

Animal models of TBI have reported effects of repeated brain injury trauma on impairments in cognition and behavior, cellular and molecular dysfunction and neuronal degeneration and death (Schmued, Albertson et al. 1997, DeRoss, Adams et al. 2002, Lovell, Collins et al. 2003, Crisco, Fiore et al. 2010, Blaylock and Maroon 2011, Crisco, Wilcox et al. 2011, McAllister, Flashman et al. 2012). Animal models vary in the mechanism of trauma (e.g. CCI, weight-drop method), while incorporating a range of injury severities, of which, fall under the umbrella of traumatic brain injury. The LFPI model is one of the most frequently used established animal models for TBI. The dcFPI is modified version of the pendulum FPI model, eliminating a few limitations in the original design of pFPI device. Specifically, integrating independent control over different biomechanical parameters of the injury waveforms, apart from peak amplitude alone.

These capabilities allow for individual manipulation in peak amplitude, rise time (also referred to as rate), duration and impulse to model different types of injuries. Traditional pFPI devices, biomechanical parameters rise-time, duration and peak amplitude of the waveform are dependent on each other with limited manipulation via the height of the pendulum. Here, this study was able to replicate subconcussive brain injury in a cumulative paradigm.

4.5.3 Cumulative Subconcussive Brain Injury

The acute behavior group of animals in the cumulative subconcussive paradigm all display evidence of hemorrhage on the ipsilateral side of injury above the hippocampal fissure. In a repetitive closed-head mice model of mTBI, Laurer et al. observed the presence of a small area of immunoreactivity for mouse IgG from a single mild head injury, while a substantial area of immunoreactivity, in the repetitive mild head injuries was noted, suggestive of blood brain barrier (BBB) has been compromised (Laurer, Bareyre et al. 2001). In the 1x scTBI subjects, the presence of hematomas was not apparent, however in our 5x scTBI paradigm, all injured subjects of the acute behavior and neurodegeneration group had evidence of hemorrhage, suggestive that the BBB had been compromised after repeated subconcussive impacts. Interestingly, in the clinical setting, Marchi et al. demonstrated in collegiate football players, an increase in S100B astrocytic protein in serum levels 1 h after participating in game without experiencing a concussion, suggesting a transient BBB disruption from repeated subconcussive impacts (Marchi, Bazarian et al. 2013).

Neuronal degeneration was present in the granular cell layer of the hippocampus in half of the 5x scTBI subjects compared to 5x sham-injured. The inconsistency of all 5x scTBI subjects displaying neuronal degeneration in the granule cell layer could be accounted for from variation in biomechanical parameters of the pressure waveforms and the time course of which neurodegeneration was assessed. Examining the biomechanical parameters of the pressure waveform for the 5x scTBI subjects that resulted in neurodegeneration in granule cell layer reveals a higher mean peak pressure and greater impulse energy of the composite waveforms compared to those that did not result in neurodegeneration (7.79 psi vs 7.10 psi (0.53 vs 0.48 atm) and 559.1 pa.s vs 443.7 pa.s, respectively).

The 24 h assessment time was initially based on previous TBI studies examining neurodegeneration from 30 min. to 7 days' post injury suggesting maximal degeneration at 24 h time-point (Zhao, Ahram et al. 2003, Anderson, Miller et al. 2005, Feng, Van et al. 2011). In an impact acceleration model of repetitive brain injury, Lu et al. showed no significant cell loss after a single mild injury, however in the repetitive regime, significant cell loss in retinal ganglion cells 7 days out was observed. Another impact study by Huh et al. investigated repetitive mild impact spaced 5 minutes apart, where a single impact did not exhibit overt damage, three impacts to the brain led to cortical atrophy at 3 days' post injury (Huh, Widing et al. 2007). Both of these studies examined higher severity of injury than the current study, however the pathophysiological cascades from cumulative subconcussive phenomena may have a different time course then previous studies and warrant additional studies at different time points.

Morris water maze (MWM) tests determine cognitive dysfunction after brain injury. Previous studies have demonstrated cognitive deficits from repetitive mTBI (DeFord, Wilson et al. 2002, Creeley 2004), however assessment of cumulative subconcussions has not been examined. Shultz et al. performed a battery of behavioral tests after one subconcussive brain injury using mLPF, of which they examined spatial cognition, sensorimotor, anxiety-like behavior, locomotor and social behaviors and found no impairment after 24 h. Similar to Shultz et al., this current study did not observe cognition impairments after 5x scTBI at 24 h or a week later from the MWM task. Many subconcussions reported do not produce overt signs or behavioral differences (Bailes, Petraglia et al. 2013), while it is possible that neural substrates the MWM task assess, may not be a the ideal neural substrates to detect brain injury from repeated intra-day subconcussive blows.

Acoustic startle response (ASR) is an evolutionary defense mechanism in response to sudden auditory stimuli. This study found a statistically significant transient suppression of ASR in cumulative 5x scTBI group compared to 5x SHAM group on PID1 that returned to SHAM levels by PID4. Several studies have implicated lasting suppression of ASR after a single mTBI (Pang et al. 2015, Lu et al. 2003, Wiley et al. 1996(Sinha, Avcu et al. 2017)). This finding is of importance in that the ASR task could be used as a potential acute behavioral biomarker on the assessment of brainstem dysfunction following cumulative subconcussion brain injury. ASR neural circuitry is well defined (Davis, Gendelman et al. 1982) and evolutionary conserved between rodents and humans. The brainstem is the fundamental backbone of the ASR circuit, of which it hosts a myriad of body functions, including the relay of all sensory information (minus

visual and smell) to the cerebellum and thalamus, such as respiration, baroreceptors, emesis, and monitoring blood oxygenation. It is the locus of key neuromodulatory systems generating norepinephrine, serotonin and acetylcholine of which have important functions in cognition and mood. Dysfunction of the brainstem can lead to dizziness, balance issues, fatigue, sleep disturbances, headaches, nausea and problems concentrating. Symptoms as just described above may delay the processing of real-time information for ASR and other sensory and motor modalities. This delay in information processing may greatly affect individuals that participate in contact sports or active duty, as it may predispose individuals to subsequent injury and deficits if reaction times are compromised. Interestingly, literature suggests 20-30% of mTBI population report persistent somatic symptoms (e.g. headaches, fatigue) months after mTBI. In addition to ASR paradigm's beneficial use to assess brain injury from repeated subconcussive impacts, the ASR neural circuit may be a promising conduit to investigate changes in brainstem neurobiology and behavior such as somatic symptoms mentioned above.

Trauma to the brain can result in acute neuroinflammation and activation of innate immune system within the central nervous system (CNS) while repetitive trauma may exacerbate that response (Allen, Gerami et al. 2000, Longhi, Saatman et al. 2005, Frank-Cannon, Alto et al. 2009, Fidan, Lewis et al. 2016). Microglia are considered to be the resident mediators in neuroinflammation. These dynamic cells continually survey the landscape of the central nervous system for perturbation in homeostasis. Traumatic brain injury may result in damaged neurons, disruption in blood brain barrier, secondary hemorrhage, mitochondrial dysfunction, shifts in ionic fluctuations or other extracellular changes that are detected and activate microglia. Activated microglia undergo a dramatic

change in cell morphology, contracting their processes, transforming from a ramified state to an amoeboid state, while in the acute stage producing and releasing pro-inflammatory cytokines, chemokines and free radicals (Loane and Byrnes 2010). Astrocytes are another constituent in neuroinflammation and vital regulators of innate and adaptive immune responses. Similar to microglia, astrocytic morphology undergoes hypertrophy and lengthen processes known as reactive astrocytosis. Reactive astrocytosis involves increased expression of GFAP, production and release of pro-inflammatory chemokines and growth factors.

In this study, the inflammatory response was observed at 24 h and remained present 1 week out compared to SHAM-injured subjects. In a single subconcussive brain injury study, Schultz et al., identified the presence of GFAP immunoreactivity and CD68 labeled microglia/macrophage at 4 days post injury. Image intensity analysis in this current study observed GFAP immunoreactivity and IBA1 labeled microglia/macrophage at 24 h and at 1 week out compared to sham-injured rats. A study by Sinha et al., that investigated inflammation and immunoreactivity in the PnC after a mTBI, found persistent reactive astrocytic activation and activated microglia/macrophages at 1 and 7 days after injury and out to 21 days after injury. This study showed activated astrocytes and microglia/macrophage at 1 day after injury, however subsided at 1 week.

The complex process of neuroinflammation involves the release of pro and anti-inflammatory mediators via immunoreactive microglia and reactive astrocytosis. Upregulation of pro-inflammatory cytokines after TBI have been reported (Ciallella, Ikonomovic et al. 2002, Zhao, Su et al. 2003, Lu, Wang et al. 2005, Kamm, VanderKolk et al. 2006, Maegele, Sauerland et al. 2007, Redell, Moore et al. 2013, Gao, Han et al.

2017, Sinha, Avcu et al. 2017). however sparse information exists on cytokine expression from a repetitive TBI paradigm. Here, cytokine mRNA expression of IL1-α, IL1-β and TNF-α were examined for in the ipsilateral cortex and hippocampus and caudal pontine reticular nucleus (PnC) demonstrating a significant upregulation of IL1-β in the PnC at 24 h returning to SHAM levels at 7 days post injury. Although statistically not significant for IL1-α, or TNF-α, there is a trend towards an increase of cytokine expression in the PnC at PID1, which decrease at PID7 in the PnC. This trend is also evident when examining the ipsilateral cortex and hippocampus regions, with the exception of IL1-α mRNA expression increasing in the cortex on PID7. Due to the nature of location and fluid percussion injury model, it is interesting that cytokine mRNA expression was not significant in the ipsilateral cortex and hippocampus at either time-point.

Cytokine expression and their temporal profile after TBI are contingent on several factors, including method of injury, severity of injury, location of injury, brain areas examined and cytokine assay used. For example, controlled cortical impact (CCI) studies have reported acute increase in TNF-α and IL-6 at PID1 and PID3, peaking at PID7, while others have reported TNF-α peaking at 24 h. IL1-α and IL1-β peak mRNA expression has been observed at 3, 6 and 12 h – 24 h (Ciallella, Ikonomovic et al. 2002, Lu, Wang et al. 2005, Kamm, VanderKolk et al. 2006, Maegele, Sauerland et al. 2007, Redell, Moore et al. 2013, Gao, Han et al. 2017). Conversely, The fluid percussion injury model of mTBI has reported acute upregulation of IL1-α in the cortex within hours of injury (Perez-Polo, Rea et al. 2013), while other studies reported later peak expression levels at PID21(Sinha, Avcu et al. 2017).

Injury severity is an important parameter to include when performing cytokine analysis, as a study by Knoblach et al. demonstrated TNF-α protein expression in a severe pFPI model at 1 and 4 h, but not mTBI, suggesting severity of injury plays an importantly role in protein expression (Knoblach, Fan et al. 1999). Conversely, Singh et al. demonstrated significant upregulation of TNF-α mRNA expression at PID1 from a mTBI. A repetitive mild closed head injury (rmCHI) assessed mRNA expression in two-month old mice at 24 h and 1 week after the last rmCHI. Changes in iNOS, IL1-β, nor CD86 mRNA expression levels were detected at 24 h or 1 week. Furthermore, this study did not see any changes in TNF-α in either the cortex or hippocampus regions from repetitive insults(Robinson, Berglass et al. 2017). Indeed, due to the subtle nature of subconcussive phenomena it is possible that our 24 h and 7-day assessment window may have been too long to cap significant changes with the cumulative paradigm. Examining at 1, 6 and 12 h time-points may provide a better assessment of the cellular and molecular cascades taking place. Evidence, like the studies mentioned above and others in literature, suggest a prevailing agreement on an acute increased inflammatory response ensuing after TBI, albeit the specifics seem to vary from experiment to experiment.

RT-PCR assay used in this study reported on mRNA expression. mRNA is a good indicator of gene regulation; however, it can not be directly correlated with protein expression (Greenbaum, Colangelo et al. 2003). Post-transcriptional processes are key to the final native protein, while mature mRNA may never make it out of the nucleus do to internal degradation processes. Protein measures of cytokines should be the preferred method.

This study examined only a few biomarkers that are involved in neuroinflammation cascade. Additional cytokine biomarkers have constitutive involvement in the acute and chronic neural inflammatory cascades, such as IL-10, IL-8, IL-6, IL-4, IL-1, IFN-y cytokines, oxidative stress markers, such as nitric oxide (NO), inducible nitric oxide synthase (iNOS), Sodium diamutase (SOD). The neuroinflammatory cascade involves both neuro-protective and neuro-destructive mechanisms, of which evolve on different temporal course, in an attempt to regain homeostasis of the central nervous system a brain injury. Future studies on subconcussive and cumulative subconcussive brain injury should consider these and other biomarkers in assessing subconcussive phenomena.

CHAPTER 5

SUMMARY AND CONCLUSIONS

We proposed the notion of exploring subconcussive phenomena. In order to accomplish this, a system that could deliver short temporal durations and low peak amplitudes needed to be designed. The redesign of an earlier prototype vFPI resulted in a streamlined dcFPI model that resulted in optimal performance. Experiments were completed on a rigid closed system, an elastic membrane, surrogate model and rodent brain demonstrating dampening effect of compliant materials and diminished control of the pressure waveform when compared to rigid closed system. The system showed the ability to accurately produce pressure pulse amplitude and duration of subconcussive brain injury.

Identifying where the location of the pressure sensor was an important finding in that the location effects the accuracy of the measurement. These findings highlighted ~10% decrease in peak pressure amplitude between distal and proximal sensor within the chamber. Furthermore, based on the results of the intracranial probe measurements, that showed ~10% decrease in peak pressure amplitude inside the brain, that proximal sensor location on the dcFPI device is a valid estimate of the peak pressure amplitude the animal receives.

Next, this study examined acute behavioral and cellular characteristics measured in animal models of TBI, applied to subconcussive brain injury paradigm. Latency of righting reflex is used as an indicator of severity of injury in animal models. Studies done on injury severity have shown longer latency of righting reflex relative to higher peak

pressure amplitudes. Supporting our subconcussive injury paradigm we demonstrated one scTBI did not result in longer latency of righting reflex compared to SHAM animals. Neuronal degeneration is cellular characteristic often reported in literature on intensity of injury. Similar to latency of righting reflex concept, higher counts of neuronal degeneration are injury severity-dependent. Here, we demonstrated absence of degenerating cells from one scTBI supporting our working definition of a subconcussion.

Applying our subconcussive brain injury to a cumulative paradigm lead to interesting finding on result of positive Fluoro – Jade labeled cells in the granule cell layer in only half the population of animals. While the 24 h assessment was based on earlier studies showing maximum neuronal degeneration at that time point, other studies have demonstrated neuronal degeneration as early as 4 h. As subconcussive phenomena is relatively new, it is possible the window of assessment was not optimal. A supplemental study could be done to see if a different assessment window is suited for subconcussive brain injury. Cumulative scTBI would be applied and neurodegenerative assessment window of 4, 12 and 36 h should be applied. Under these conditions, it could be elucidated if there exists an assessment window specific to subconcussive brain injury. Alternatively, a supplemental study could be done to see if five hits is may not be enough. Increasing the frequency of hits to 10 or 15 hits may prove to demonstrate positive Fluoro – jade labeling across all cumulative scTBI.

mRNA cytokine analysis resulted in significant result from IL-1β in the PnC. These results were slightly discouraging as the immunofluorescence analysis was indicative of immunoreactive microglia/macrophages and astrocytosis evident in the ipsilateral cortex and hippocampus and the PnC. IL-1α, IL-1β and TNF-α are pro-

inflammatory cytokines expressed from immunoreactive microglia/macrophages that did not reach significant levels compared to SHAM animals at the 24 h time point. Referenced in chapter 4, mRNA cytokine expression of different severity levels of TBI have varied in their temporal profile. Similar to neurodegeneration supplemental study, a study could be done to determine if different assessment window of mRNA expression from cumulative subconcussive phenomena occurs at 1, 6, 12 or 48 h. However, mRNA expression does not correlate to protein expression. Moving forward, I would take a different approach. mRNA encodes for proteins; however, it is the proteins themselves that perform cellular functions that is of importance. Performing a Western-blot technique to quantify protein expression in brain regions of interest would be more informative.

Lasting suppression of ASR has been implicated in TBI models after one insult, here transient suppression of ASR is a novel finding of cumulative subconcussive brain injury. The neural circuitry is well defined in ASR model involving the brainstem. In addition to ASR's nuclei in the brainstem, rostral to the PnC is the locus coeruleus nuclei. The locus coeruleus is the main norepinephrine production center of the brain with influence on major functions, such as activity, alertness, arousal, attention and memory, emotion and behavior. The locus coeruleus has also been implicated in the earliest stages of CTE with deposits of phosphorylated tau and neurofibrillary tangles (Stein, Alvarez et al. 2014). This study showed the presence of reactive microglia/macrophages and increase in IL-1β after cumulative scTBI. Chronic levels of microglia/macrophages and IL-1β have been shown to lead to the accumulation of neurofibrillary tangles. It would be interesting to apply a multi-day cumulative intra-day subconcussive study where animals

would be subjected to cumulative scTBI over 20 day period and examine for acute neuroinflammation response, chronic response and accumulation of phosphorylated tau in the locus coeruleus. As a result, dysfunction of locus coeruleus nuclei could explain disturbance in attention, memory and learning, sleep and mood issues reported from individuals with CTE.

Previous literature on animal studies has reported on single and repetitive TBI, however this study is the first of its kind to implement a cumulative intra-day subconcussive brain injury model. It has been shown that cumulative subconcussive brain injury results in acute inflammation and transient suppression of acoustic startle response. While the importance of this first step can not be underestimated, the next steps in understanding the effects of repetitive subconcussive brain injury over multiple days need to be addressed. In a particular, MWM data during the choice phase missed reaching statistical significance on main effect of day nor injury X day interaction ($p = 0.073$ and $p = 0.059$, respectfully). One could speculate that a repetitive subconcussive paradigm over five days would result in spatial memory deficits, ASR suppression lasting longer than 24 h and increased immunoreactivity of microglia/macrophages and astrocytosis.

REFERENCES

Abdul-Wahab, R., B. Swietek, S. Mina, S. Sampath, V. Santhakumar and B. Pfister (2011). Precisely controllable traumatic brain injury devices for rodent models. Bioengineering Conference (NEBEC), 2011 IEEE 37th Annual Northeast, IEEE.

Alder, J., W. Fujioka, J. Lifshitz, D. P. Crockett and S. Thakker-Varia (2011). "Lateral fluid percussion: model of traumatic brain injury in mice." Journal of visualized experiments: JoVE(54).

Allen, G., D. Gerami and M. Esser (2000). "Conditioning effects of repetitive mild neurotrauma on motor function in an animal model of focal brain injury." Neuroscience **99**(1): 93-105.

Allsop, D., S. Haga, C. Bruton, T. Ishii and G. Roberts (1990). "Neurofibrillary tangles in some cases of dementia pugilistica share antigens with amyloid beta-protein of Alzheimer's disease." The American journal of pathology **136**(2): 255.

Anderson, K. J., K. M. Miller, I. Fugaccia and S. W. Scheff (2005). "Regional distribution of fluoro-jade B staining in the hippocampus following traumatic brain injury." Experimental neurology **193**(1): 125-130.

Anderson, T., M. Heitger and A. Macleod (2006). "Concussion and mild head injury." Practical Neurology **6**(6): 342-357.

Areza-Fegyveres, R., S. Rosemberg, R. M. R. Castro, C. S. Porto, V. r. S. Bahia, P. Caramelli and R. Nitrini (2007). "Dementia pugilistica with clinical features of Alzheimer's disease." Arquivos de neuro-psiquiatria **65**(3B): 830-833.

Bailes, J. E., A. L. Petraglia, B. I. Omalu, E. Nauman and T. Talavage (2013). "Role of subconcussion in repetitive mild traumatic brain injury: a review." Journal of neurosurgery **119**(5): 1235-1245.

Bergersen, K., J. Ø. Halvorsen, E. A. Tryti, S. I. Taylor and A. Olsen (2017). "A systematic literature review of psychotherapeutic treatment of prolonged symptoms after mild traumatic brain injury." Brain injury **31**(3): 279-289.

Blaylock, R. L. and J. Maroon (2011). "Immunoexcitotoxicity as a central mechanism in chronic traumatic encephalopathy,ÄîA unifying hypothesis." Surgical neurology international **2**.

Blennow, K., J. Hardy and H. Zetterberg (2012). "The neuropathology and neurobiology of traumatic brain injury." Neuron **76**(5): 886-899.

Brody, D. L., C. Mac Donald, C. C. Kessens, C. Yuede, M. Parsadanian, M. Spinner, E. Kim, K. E. Schwetye, D. M. Holtzman and P. V. Bayly (2007). "Electromagnetic Controlled

Cortical Impact Device for Precise, Graded Experimental Traumatic Brain Injury." Journal of Neurotrauma **24**(4): 657-673.

Broglio, S. P., J. J. Sosnoff, S. Shin, X. He, C. Alcaraz and J. Zimmerman (2009). "Head impacts during high school football: a biomechanical assessment." Journal of athletic training **44**(4): 342-349.

Cernak, I. (2005). "Animal models of head trauma." NeuroRx **2**(3): 410-422.

Cernak, I., R. Vink, D. N. Zapple, M. I. Cruz, F. Ahmed, T. Chang, S. T. Fricke and A. I. Faden (2004). "The pathobiology of moderate diffuse traumatic brain injury as identified using a new experimental model of injury in rats." Neurobiology of disease **17**(1): 29-43.

Ciallella, J. R., M. D. Ikonomovic, W. R. Paljug, Y. I. Wilbur, C. E. Dixon, P. M. Kochanek, D. W. Marion and S. T. DeKosky (2002). "Changes in expression of amyloid precursor protein and interleukin-1β after experimental traumatic brain injury in rats." Journal of neurotrauma **19**(12): 1555-1567.

Clausen, F. and L. Hillered (2005). "Intracranial pressure changes during fluid percussion, controlled cortical impact and weight drop injury in rats." Acta neurochirurgica **147**(7): 775-780.

Cole, J. T., A. Yarnell, W. S. Kean, E. Gold, B. Lewis, M. Ren, D. C. McMullen, D. M. Jacobowitz, H. B. Pollard and J. T. O'Neill (2011). "Craniotomy: true sham for traumatic brain injury, or a sham of a sham?" Journal of neurotrauma **28**(3): 359-369.

Creeley, C. E. (2004). "Multiple Episodes of Mild Traumatic Brain Injury Result in Impaired Cognitive Performance in Mice." Academic Emergency Medicine **11**(8): 809-819.

Crisco, J. J., R. Fiore, J. G. Beckwith, J. J. Chu, P. G. Brolinson, S. Duma, T. W. McAllister, A.-C. Duhaime and R. M. Greenwald (2010). "Frequency and location of head impact exposures in individual collegiate football players." Journal of athletic training **45**(6): 549-559.

Crisco, J. J., B. J. Wilcox, J. G. Beckwith, J. J. Chu, A.-C. Duhaime, S. Rowson, S. M. Duma, A. C. Maerlender, T. W. McAllister and R. M. Greenwald (2011). "Head impact exposure in collegiate football players." Journal of biomechanics **44**(15): 2673-2678.

D'Ambrosio, R., J. P. Fairbanks, J. S. Fender, D. E. Born, D. L. Doyle and J. W. Miller (2004). "Post-traumatic epilepsy following fluid percussion injury in the rat." Brain **127**(2): 304-314.

Das, M., S. Mohapatra and S. S. Mohapatra (2012). "New perspectives on central and peripheral immune responses to acute traumatic brain injury." Journal of neuroinflammation **9**(1): 236.

Davis, M., D. S. Gendelman, M. D. Tischler and P. M. Gendelman (1982). "A primary acoustic startle circuit: lesion and stimulation studies." Journal of Neuroscience **2**(6): 791-805.

Davis, M., D. S. Gendelman, M. D. Tischler and P. M. Gendelman (1982). "A primary acoustic startle circuit: lesion and stimulation studies." The Journal of neuroscience **2**(6): 791-805.

DeFord, S. M., M. S. Wilson, A. C. Rice, T. Clausen, L. K. Rice, A. Barabnova, R. Bullock and R. J. Hamm (2002). "Repeated mild brain injuries result in cognitive impairment in B6C3F1 mice." Journal of neurotrauma **19**(4): 427-438.

DeRoss, A. L., J. E. Adams, D. W. Vane, S. J. Russell, A. M. Terella and S. L. Wald (2002). "Multiple head injuries in rats: effects on behavior." Journal of Trauma and Acute Care Surgery **52**(4): 708-714.

Feng, J.-F., K. C. Van, G. G. Gurkoff, C. Kopriva, R. T. Olszewski, M. Song, S. Sun, M. Xu, J. H. Neale and P.-W. Yuen (2011). "Post-injury administration of NAAG peptidase inhibitor prodrug, PGI-02776, in experimental TBI." Brain research **1395**: 62-73.

Fidan, E., J. Lewis, A. E. Kline, R. H. Garman, H. Alexander, J. P. Cheng, C. O. Bondi, R. S. Clark, C. Dezfulian and P. M. Kochanek (2016). "Repetitive mild traumatic brain injury in the developing brain: effects on long-term functional outcome and neuropathology." Journal of neurotrauma **33**(7): 641-651.

Frank-Cannon, T. C., L. T. Alto, F. E. McAlpine and M. G. Tansey (2009). "Does neuroinflammation fan the flame in neurodegenerative diseases?" Molecular neurodegeneration **4**: 47.

Friess, S. H., R. N. Ichord, J. Ralston, K. Ryall, M. A. Helfaer, C. Smith and S. S. Margulies (2009). "Repeated traumatic brain injury affects composite cognitive function in piglets." J Neurotrauma.

Fujita, M., E. P. Wei and J. T. Povlishock (2012). "Intensity- and Interval-Specific Repetitive Traumatic Brain Injury Can Evoke Both Axonal and Microvascular Damage." Journal of Neurotrauma **29**(12): 2172-2180.

Fujita, M., E. P. Wei and J. T. Povlishock (2012). "Intensity- and interval-specific repetitive traumatic brain injury can evoke both axonal and microvascular damage." Journal of neurotrauma **29**(12): 2172-2180.

Gao, H., Z. Han, R. Bai, S. Huang, X. Ge, F. Chen and P. Lei (2017). "The accumulation of brain injury leads to severe neuropathological and neurobehavioral changes after repetitive mild traumatic brain injury." Brain research **1657**: 1-8.

Gavett, B. E., R. A. Stern and A. C. McKee (2011). "Chronic traumatic encephalopathy: a potential late effect of sport-related concussive and subconcussive head trauma." Clinics in sports medicine **30**(1): 179-188, xi.

Giza, C. C. and D. A. Hovda (2001). "The neurometabolic cascade of concussion." Journal of athletic training **36**(3): 228.

Greenbaum, D., C. Colangelo, K. Williams and M. Gerstein (2003). "Comparing protein abundance and mRNA expression levels on a genomic scale." Genome biology **4**(9): 117.

Gurkoff, G. G., C. C. Giza and D. A. Hovda (2006). "Lateral fluid percussion injury in the developing rat causes an acute, mild behavioral dysfunction in the absence of significant cell death." Brain research **1077**(1): 24-36.

Guterman, A. and R. W. Smith (1987). "Neurological sequelae of boxing." Sports Medicine **4**(3): 194-210.

Hallam, T. M., C. L. Floyd, M. M. Folkerts, L. L. Lee, Q.-Z. Gong, B. G. Lyeth, J. P. Muizelaar and R. F. Berman (2004). "Comparison of behavioral deficits and acute neuronal degeneration in rat lateral fluid percussion and weight-drop brain injury models." Journal of neurotrauma **21**(5): 521-539.

Harmon, K. G., J. A. Drezner, M. Gammons, K. M. Guskiewicz, M. Halstead, S. A. Herring, J. S. Kutcher, A. Pana, M. Putukian and W. O. Roberts (2013). "American Medical Society for Sports Medicine position statement: concussion in sport." British journal of sports medicine **47**(1): 15-26.

Hawkins, B. E., S. Krishnamurthy, D. L. Castillo-Carranza, U. Sengupta, D. S. Prough, G. R. Jackson, D. S. DeWitt and R. Kayed (2013). "Rapid Accumulation of Endogenous Tau Oligomers in a Rat Model of Traumatic Brain Injury Possible Link Between Traumatic Brain Injury and Sporadic Tauopathies." Journal of Biological Chemistry **288**(23): 17042-17050.

Hawkins, B. E., S. Krishnamurthy, D. L. Castillo-Carranza, U. Sengupta, D. S. Prough, G. R. Jackson, D. S. DeWitt and R. Kayed (2013). "Rapid accumulation of endogenous tau oligomers in a rat model of traumatic brain injury: possible link between traumatic brain injury and sporadic tauopathies." J Biol Chem **288**(23): 17042-17050.

Hof, P., C. Bouras, L. Buee, A. Delacourte, D. Perl and J. Morrison (1992). "Differential distribution of neurofibrillary tangles in the cerebral cortex of dementia pugilistica and Alzheimer's disease cases." Acta neuropathologica **85**(1): 23-30.

Hoshino, S., A. Tamaoka, M. Takahashi, S. Kobayashi, T. Furukawa, Y. Oaki, O. Mori, S. Matsuno, S. I. Shoji and M. Inomata (1998). "Emergence of immunoreactivities for phosphorylated tau and amyloid‚ÄêŒ≤ protein in chronic stage of fluid percussion injury in rat brain." Neuroreport **9**(8): 1879-1883.

Huh, J. W., A. G. Widing and R. Raghupathi (2007). "Repetitive mild non-contusive brain trauma in immature rats exacerbates traumatic axonal injury and axonal calpain activation: a preliminary report." Journal of neurotrauma **24**(1): 15-27.

Iwata, A., P. K. Stys, J. A. Wolf, X.-H. Chen, A. G. Taylor, D. F. Meaney and D. H. Smith (2004). "Traumatic axonal injury induces proteolytic cleavage of the voltage-gated sodium channels modulated by tetrodotoxin and protease inhibitors." The Journal of neuroscience **24**(19): 4605-4613.

Janda, D. H., C. A. Bir and A. L. Cheney (2002). "An evaluation of the cumulative concussive effect of soccer heading in the youth population." Injury control and safety promotion **9**(1): 25-31.

Kamins, J. and C. C. Giza (2016). "Concussion—Mild Traumatic Brain Injury: Recoverable Injury with Potential for Serious Sequelae." Neurosurgery clinics of North America **27**(4): 441-452.

Kamm, K., W. VanderKolk, C. Lawrence, M. Jonker and A. T. Davis (2006). "The effect of traumatic brain injury upon the concentration and expression of interleukin-1β and interleukin-10 in the rat." Journal of Trauma and Acute Care Surgery **60**(1): 152-157.

Khurana, V. G. and A. H. Kaye (2012). "An overview of concussion in sport." Journal of Clinical Neuroscience **19**(1): 1-11.

Kim, Y., A. H. Fu, L. B. Tucker, J. Liu and J. T. McCabe (2017). "Characterization of controlled cortical impact devices by high-speed image analysis." Journal of Neuroscience Research.

Knoblach, S. M., L. Fan and A. I. Faden (1999). "Early neuronal expression of tumor necrosis factor-α after experimental brain injury contributes to neurological impairment." Journal of neuroimmunology **95**(1): 115-125.

Langlois, J. A., W. Rutland-Brown and K. E. Thomas (2006). "Traumatic brain injury in the United States; emergency department visits, hospitalizations, and deaths."

Laurer, H. L., F. M. Bareyre, V. M. Lee, J. Q. Trojanowski, L. Longhi, R. Hoover, K. E. Saatman, R. Raghupathi, S. Hoshino and M. S. Grady (2001). "Mild head injury increasing the brain's vulnerability to a second concussive impact." Journal of neurosurgery **95**(5): 859-870.

Lee, Y., D. E. L√≥pez, E. G. Meloni and M. Davis (1996). "A primary acoustic startle pathway: obligatory role of cochlear root neurons and the nucleus reticularis pontis caudalis." The Journal of neuroscience **16**(11): 3775-3789.

Li, Y., A. A. Korgaonkar, B. Swietek, J. Wang, F. S. Elgammal, S. Elkabes and V. Santhakumar (2015). "Toll-like receptor 4 enhancement of non-NMDA synaptic currents increases dentate excitability after brain injury." Neurobiology of disease **74**: 240-253.

Lipton, M. L., N. Kim, M. E. Zimmerman, M. Kim, W. F. Stewart, C. A. Branch and R. B. Lipton (2013). "Soccer heading is associated with white matter microstructural and cognitive abnormalities." Radiology.

Loane, D. J. and K. R. Byrnes (2010). "Role of microglia in neurotrauma." Neurotherapeutics **7**(4): 366-377.

Longhi, L., K. E. Saatman, S. Fujimoto, R. Raghupathi, D. F. Meaney, J. Davis, A. McMillan, V. Conte, H. L. Laurer and S. Stein (2005). "Temporal window of vulnerability to repetitive experimental concussive brain injury." Neurosurgery **56**(2): 364-374.

Lovell, M. R., M. W. Collins, G. L. Iverson, M. Field, J. C. Maroon, R. Cantu, K. Podell, J. W. Powell, M. Belza and F. H. Fu (2003). "Recovery from mild concussion in high school athletes." Journal of neurosurgery **98**(2): 296-301.

Lu, K.-T., Y.-W. Wang, J.-T. Yang, Y.-L. Yang and H.-I. Chen (2005). "Effect of interleukin-1 on traumatic brain injury–induced damage to hippocampal neurons." Journal of neurotrauma **22**(8): 885-895.

Maegele, M., S. Sauerland, B. Bouillon, U. Schäfer, H. Trübel, P. Riess and E. Neugebauer (2007). "Differential immunoresponses following experimental traumatic brain injury, bone fracture and “two-hit”-combined neurotrauma." Inflammation Research **56**(8): 318-323.

Magou, G. C., Y. Guo, M. Choudhury, L. Chen, N. Hususan, S. Masotti and B. J. Pfister (2011). "Engineering a high throughput axon injury system." Journal of neurotrauma **28**(11): 2203-2218.

Marchi, N., J. J. Bazarian, V. Puvenna, M. Janigro, C. Ghosh, J. Zhong, T. Zhu, E. Blackman, D. Stewart, J. Ellis, R. Butler and D. Janigro (2013). "Consequences of repeated blood-brain barrier disruption in football players." PLoS One **8**(3): e56805.

McAllister, T., L. Flashman, A. Maerlender, R. Greenwald, J. Beckwith, T. Tosteson, J. Crisco, P. Brolinson, S. Duma and A.-C. Duhaime (2012). "Cognitive effects of one season of head impacts in a cohort of collegiate contact sport athletes." Neurology **78**(22): 1777-1784.

McCrory, P., W. Meeuwisse, K. Johnston, J. Dvorak, M. Aubry, M. Molloy and R. Cantu (2009). "Consensus statement on Concussion in Sport,Äìthe 3rd International Conference on Concussion in Sport held in Zurich, November 2008." South African Journal of Sports Medicine **21**(2).

McKee, A. C., R. C. Cantu, C. J. Nowinski, E. T. Hedley-Whyte, B. E. Gavett, A. E. Budson, V. E. Santini, H. S. Lee, C. A. Kubilus and R. A. Stern (2009). "Chronic traumatic encephalopathy in athletes: progressive tauopathy after repetitive head injury." Journal of neuropathology and experimental neurology **68**(7): 709-735.

Meehan III, W. P., J. Zhang, R. Mannix and M. J. Whalen (2012). "Increasing recovery time between injuries improves cognitive outcome after repetitive mild concussive brain injuries in mice." Neurosurgery **71**(4): 885-892.

Millspaugh, J. (1937). "Dementia pugilistica." US Naval Med Bull **35**: 297Y303.

Montenigro, P. H., C. Bernick and R. C. Cantu (2015). "Clinical features of repetitive traumatic brain injury and chronic traumatic encephalopathy." Brain pathology **25**(3): 304-317.

Morrison III, B., H. L. Cater, C. C. Wang and F. C. Thomas (2003). "A tissue level tolerance criterion for living brain developed with an in vitro model of traumatic mechanical loading." Stapp Car Crash Journal **47**: 93.

Mouzon, B., H. Chaytow, G. Crynen, C. Bachmeier, J. Stewart, M. Mullan, W. Stewart and F. Crawford (2012). "Repetitive mild traumatic brain injury in a mouse model produces learning and memory deficits accompanied by histological changes." Journal of neurotrauma **29**(18): 2761-2773.

Nakadate, H., K. Inuzuka, S. Akanuma, A. Kakuta and S. Aomura (2014). "Effect of amplitude and duration of impulsive pressure on endothelial permeability in in vitro fluid percussion trauma." Biomedical engineering online **13**(1): 44.

Neuberger, E. J., R. Abdul Wahab, A. Jayakumar, B. J. Pfister and V. Santhakumar (2014). "Distinct effect of impact rise times on immediate and early neuropathology after brain injury in juvenile rats." Journal of neuroscience research **92**(10): 1350-1361.

Pang, K. C., X. Jiao, S. Sinha, K. D. Beck and R. J. Servatius (2011). "Damage of GABAergic neurons in the medial septum impairs spatial working memory and extinction of active avoidance: effects on proactive interference." Hippocampus **21**(8): 835-846.

Pang, K. C., S. Sinha, P. Avcu, J. J. Roland, N. Nadpara, B. Pfister, M. Long, V. Santhakumar and R. J. Servatius (2015). "Long-lasting suppression of acoustic startle response after mild traumatic brain injury." Journal of neurotrauma **32**(11): 801-810.

Perez-Polo, J. R., H. C. Rea, K. M. Johnson, M. A. Parsley, G. C. Unabia, G. Xu, S. K. Infante, D. S. DeWitt and C. E. Hulsebosch (2013). "Inflammatory consequences in a rodent model of mild traumatic brain injury." Journal of neurotrauma **30**(9): 727-740.

Pfister, B. and G. Bao "Displacement-controlled stretch injury of neural cells." Summer Bioengng. confer: 25-29.

Povlishock, J. T. (1992). "Traumatically induced axonal injury: pathogenesis and pathobiological implications." Brain pathology (Zurich, Switzerland) **2**(1): 1-12.

Prins, M., A. Hales, M. Reger, C. Giza and D. Hovda (2010). "Repeat traumatic brain injury in the juvenile rat is associated with increased axonal injury and cognitive impairments." Developmental neuroscience **32**(5-6): 510-518.

Redell, J. B., A. N. Moore, R. J. Grill, D. Johnson, J. Zhao, Y. Liu and P. K. Dash (2013). "Analysis of functional pathways altered after mild traumatic brain injury." Journal of neurotrauma **30**(9): 752-764.

Robinson, S., J. B. Berglass, J. L. Denson, J. Berkner, C. V. Anstine, J. L. Winer, J. R. Maxwell, J. Qiu, Y. Yang and L. O. Sillerud (2017). "Microstructural and microglial changes after repetitive mild traumatic brain injury in mice." Journal of neuroscience research **95**(4): 1025-1035.

Santhakumar, V., A. D. H. Ratzliff, J. Jeng, Z. Toth and I. Soltesz (2001). "Long-term hyperexcitability in the hippocampus after experimental head trauma." Annals of Neurology **50**(6): 708-717.

Schmued, L. C., C. Albertson and W. Slikker (1997). "Fluoro-Jade: a novel fluorochrome for the sensitive and reliable histochemical localization of neuronal degeneration." Brain research **751**(1): 37-46.

Servatius, R. J., K. D. Beck, R. L. Moldow, G. Salameh, T. P. Tumminello and K. R. Short (2005). "A stress-induced anxious state in male rats: corticotropin-releasing hormone induces persistent changes in associative learning and startle reactivity." Biological psychiatry **57**(8): 865-872.

Shitaka, Y., H. T. Tran, R. E. Bennett, L. Sanchez, M. A. Levy, K. Dikranian and D. L. Brody (2011). "Repetitive closed-skull traumatic brain injury in mice causes persistent multifocal axonal injury and microglial reactivity." Journal of Neuropathology & Experimental Neurology **70**(7): 551-567.

Shultz, S. R., D. F. MacFabe, K. A. Foley, R. Taylor and D. P. Cain (2011). "A single mild fluid percussion injury induces short-term behavioral and neuropathological changes in the Long-Evans rat: support for an animal model of concussion." Behavioural brain research **224**(2): 326-335.

Shultz, S. R., D. F. MacFabe, K. A. Foley, R. Taylor and D. P. Cain (2012). "Sub-concussive brain injury in the Long-Evans rat induces acute neuroinflammation in the absence of behavioral impairments." Behav Brain Res **229**(1): 145-152.

Sinha, S. P., P. Avcu, K. M. Spiegler, S. Komaravolu, K. Kim, T. Cominski, R. J. Servatius and K. C. Pang (2017). "Startle suppression after mild traumatic brain injury is associated

with an increase in pro-inflammatory cytokines, reactive gliosis and neuronal loss in the caudal pontine reticular nucleus." Brain, behavior, and immunity **61**: 353-364.

Smith, D. H., D. F. Meaney and W. H. Shull (2003). "Diffuse axonal injury in head trauma." The Journal of head trauma rehabilitation **18**(4): 307-316.

Spain, A., S. Daumas, J. Lifshitz, J. Rhodes, P. J. Andrews, K. Horsburgh and J. H. Fowler (2010). "Mild fluid percussion injury in mice produces evolving selective axonal pathology and cognitive deficits relevant to human brain injury." Journal of neurotrauma **27**(8): 1429-1438.

Spiotta, A. M., A. J. Bartsch and E. C. Benzel (2012). "Heading in soccer: dangerous play?" Neurosurgery **70**(1): 1-11; discussion 11.

Stein, T. D., V. E. Alvarez and A. C. McKee (2014). "Chronic traumatic encephalopathy: a spectrum of neuropathological changes following repetitive brain trauma in athletes and military personnel." Alzheimer's research & therapy **6**(1): 4.

Stern, R. A., D. O. Riley, D. H. Daneshvar, C. J. Nowinski, R. C. Cantu and A. C. McKee (2011). "Long-term consequences of repetitive brain trauma: chronic traumatic encephalopathy." PM & R : the journal of injury, function, and rehabilitation **3**(10 Suppl 2): S460-467.

Talavage, T. M., E. A. Nauman, E. L. Breedlove, U. Yoruk, A. E. Dye, K. E. Morigaki, H. Feuer and L. J. Leverenz (2013). "Functionally-Detected Cognitive Impairment in High School Football Players Without Clinically-Diagnosed Concussion." Journal of neurotrauma.

Thompson, H. J., J. Lifshitz, N. Marklund, M. S. Grady, D. I. Graham, D. A. Hovda and T. K. McIntosh (2005). "Lateral fluid percussion brain injury: a 15-year review and evaluation." Journal of neurotrauma **22**(1): 42-75.

Wahab, R. A. (2009). Rate Alterable Traumatic Brain Injury Device for Rodent Models, New Jersey Institute of Technology.

Weber, J. T. (2007). "Experimental models of repetitive brain injuries." Progress in brain research **161**: 253-261.

West, M. J., L. Slomianka and H. J. G. Gundersen (1991). "Unbiased Stereological Estimation of the Total Number of Neurons in the Subdivisions of the Rat Hippocampus Using the Optical Fractionator." Anatomical Record **231**(4): 482-497.

Yu, J., A. Proddutur, F. S. Elgammal, T. Ito and V. Santhakumar (2013). "Status epilepticus enhances tonic GABA currents and depolarizes GABA reversal potential in dentate fast-spiking basket cells." J Neurophysiol **109**(7): 1746-1763.

Zhang, L., K. H. Yang and A. I. King (2004). "A proposed injury threshold for mild traumatic brain injury." Transaction-America Society of Mechanical Engineers Journal of iomedical Engineering **126**(2): 226-236.

Zhao, M., J. Su, E. Head and C. W. Cotman (2003). "Accumulation of caspase cleaved amyloid precursor protein represents an early neurodegenerative event in aging and in Alzheimer's disease." Neurobiology of disease **14**(3): 391-403.

Zhao, X., A. Ahram, R. F. Berman, J. P. Muizelaar and B. G. Lyeth (2003). "Early loss of astrocytes after experimental traumatic brain injury." Glia **44**(2): 140-152.